Testing the competition hypothesis: How niche overlap between carnivoramorphans and creodonts changed from the start to the end of the Eocene

by

Brigid Emily Christison

A thesis submitted to the Faculty of Graduate and Postdoctoral Affairs in partial fulfillment of the requirements for the degree of

Master of Science

in

Biology

Carleton University Ottawa, Ontario

2020

Abstract

Carnivoramorphans and creodonts are two groups of ancestrally carnivorous mammals that both emerged in the Paleocene (66–56 Ma) of North America. During the Eocene (56–33.9 Ma), carnivoramorphans radiated into some of the taxonomic groups we still see today, while creodont diversity declined until the group went extinct in North America during the Oligocene (33.9–23 Ma) and worldwide during the Miocene (23–5.3 Ma). In this thesis, I test the hypothesis that competition with carnivoramorphans may have led to the extinction of the creodonts in North America by examining changes in niche overlap between the two groups from the start to the end of the Eocene. My results do not support the competition hypothesis, but instead suggest that creodonts were hyperspecialized and un-equipped for the dramatically different environments of the late Eocene and early Oligocene.

Acknowledgements

Land acknowledgement

The fossils examined in this study were collected predominantly on Cession 517, 632, and 700 land. These are the territories of the Oglala Sioux Tribe of the Pine Ridge Reservation, Assiniboine and Sioux Tribes of the Fort Peck Indian Reservation, Cheyenne River Sioux Tribe of the Cheyenne River Reservation, Crow Creek Sioux Tribe of the Crow Creek Reservation, Flandreau Santee Sioux Tribe of South Dakota, Lower Brule Sioux Tribe of the Lower Brule Reservation, Lower Sioux Indian Community in the State of Minnesota, Oglala Sioux Tribe of the Pine Ridge Reservation, Prairie Island Indian Community in the State of Minnesota, Rosebud Sioux Tribe of the Rosebud Indian Reservation, Santee Sioux Nation, Shakopee Mdewakanton Sioux Community of Minnesota, Sisseton-Wahpeton Oyate of the Lake Traverse Reservation, Spirit Lake Tribe, Standing Rock Sioux Tribe of North & South Dakota, Upper Sioux Community, Yankton Sioux Tribe of South Dakota, and the Crow Tribe of Montana. This land acknowledgment was made possible through the use of Native-Land.ca and subsequent research.

During the creation of this manuscript, seven natural history museums in Canada and the United States were visited for data collection. I recognize that natural history museums are colonial institutions that were created to lay claim over stolen land and resources, and that the buildings themselves displace the traditional inhabitants of the land they are on. The research and work that went into this manuscript took place predominantly on the unceded territories of the Algonquin Anishinabeg People.

Personal acknowledgements

I would like to sincerely thank my supervisors, Dr. Danielle Fraser and Dr. Jeff Dawson. Dani has supported me since my undergraduate degree and has been a valued mentor and friend, and I am grateful for her guidance. I would also like to thank the members of my thesis committee, Dr. Roslyn Dakin, Dr. Tom Sherratt, and Dr. Emily Standen, for their suggestions and encouragement during the development of my thesis, and Dr. Sue Bertram for acting as my defense chair. Thanks goes to NSERC for funding my research assistantship, the Jackson Travel Award through SVP, and to the Donald R. Wiles Prize (Carleton University biology department) for additional funding. Special thanks to the administration staff, collections managers, and lab technicians who assisted me during the data collection that went into this thesis, namely: Dan Brinkman, Marilyn Fox, Judy Galkin, Verne Lee, Amanda Millhouse, Adam Rountry, and Kevin Seymour. Thanks goes to members of the Fraser and Maddin Labs for their insightful comments during weekly lab meetings. I would like to thank Dr. Hillary Maddin for her guidance and support during my academic career. Thanks to Dr. Jordan Mallon and Margaret Currie, for supervising my early experiences at the Canadian Museum of Nature, and for teaching me the fundamentals of navigating museum collections.

Most importantly I am grateful to my parents for their confidence in my abilities, and to my close friends for cheering me on. Their endless support is the reason I was able to write this thesis while not allowing my job to consume my personal life. Finally, I am grateful to all of the pet carnivorans in my life who continue to inspire my research and fascination with science.

Table of Contents

List of tables

List of illustrations

Chapter 1: Introduction

Modern biodiversity is the result of billions of years of evolution and extinction. It is estimated that up to four billion species of plants and animals have existed on the Earth, yet only a few million remain (Raup 1986). Some clades survive for millions or tens of millions of years (even longer in exceptional cases such as multituberculates (Grossnickle et al. 2019)), while others live for only a snapshot in geological time. One of the biggest questions in evolutionary biology is: why are some taxa more vulnerable to extinction than others? Thanks to the existence of the fossil record, extinct clades are not necessarily lost to science. Preserved remains allow us to learn about the morphology of life forms that are not alive today. By examining their preserved remains in the context of other coexisting clades and in relation to their palaeoenvironments, we can learn about how and why these taxa lived and became extinct.

1.1 Extinction

A species is extinct if it no longer contains living members able to reproduce and propagate member populations (Raup 1986). Extinction can occur gradually or suddenly, and a mass extinction is when a high percentage of species go extinct within a geologically short amount of time (i.e. anywhere between several months or a few million years) (Raup 1986). The most deadly mass extinction in the Earth's history was the end-Permian mass extinction (~251 Ma), during which as much as 95% of species went extinct over a 5-8 million year period (Purvis et al. 2000). Mass extinctions can be driven by rapid, widespread environmental changes (e.g. changes in marine carbon cycling) and, rarer events, such as the impact of

extraterrestrial objects (Alvarez et al. 1980; Gould and Calloway 1980; Pimm et al. 1988; Mayhew et al. 2012; Condamine et al. 2019; Fraser et al. 2020). The majority of extinctions do not occur during mass extinctions however (Raup 1986; De Vos et al. 2015), but occur as "background extinctions," and are estimated to occur at a rate of roughly 0.1 extinction per million species per year (De Vos et al. 2015). Drivers of background extinctions include, but are not limited to, environmental change, habitat loss, and interspecific competition (Fraser et al. 2020) . One of the most often implicated drivers is climate change, including global changes in temperature, oxygen levels, and tectonic activity (Badgley and Fox 2000; Zachos et al. 2001, 2008; McInerney and Wing 2011; Mayhew et al. 2012; Fraser et al. 2020). Species vary in their evolutionary response to such changes and thus vary in their survivability (Raup 1986; Pimm et al. 1988; Alroy et al. 2000; Van Valkenburgh et al. 2004). Species' responses to environmental perturbation are difficult to predict and vary broadly among taxonomic groups (De Vos et al. 2015).

Some species are at a higher risk of extinction than others (Pimm et al. 1988; De Vos et al. 2015; Smits 2015). Many extinctions are highly biologically selective and tend to affect closely related species due to phylogenetic inheritance of environmental tolerances and ecological characteristics (e.g. diets) (Raup 1986; Liow and Stenseth 2007). Factors that may be conserved among closely-related species and increase extinction risk are dietary or habitat specialization, small geographic ranges, low population densities, and slow reproductive rates (Bekoff et al. 1981; Pagel 1999; Van Valkenburgh 2007). Interspecific interactions, such as niche overlap and resource competition, can also lead to extinction of one or several of the involved species (Moen and Morlon 2014; Liow et al. 2015). The fossil record contains many instances of

extinction, providing us the opportunity to understand the processes and the traits that influence the "life spans" of species (Gould and Calloway 1980; Mckinney 1987; Smits 2015).

1.2 Resource competition

Competition among organisms is a broad descriptor for any kind of interaction, direct (e.g. *Panthera leo* stealing a carcass from *Panthera pardus*) or indirect (e.g. *Canis latrans* preying on small mammals within the territory of a *Lynx canadensis*), which benefits one organism at the expense of another's ability to survive and reproduce (Elton 1946). Competition between two or more organisms can arise when they exhibit niche overlap (i.e. share resources) and if resources are limited, such as in ecosystems with comparatively low energy availability (i.e. primary productivity) (Levins 1968). Competition can occur among individuals from different species and can have impacts on entire species (Elton 1946).

Over time, resource competition can lead to the extinction of species through depressed rates of speciation, increased mortality rates, or both (Stanley 1973; Liow and Stenseth 2007; Moen and Morlon 2014). Competition can have a direct influence on the maximum geographic range a species can occupy, in cases where competitive exclusion prevents the less-equipped species from occupying certain areas (Armstrong and McGehee 1980), which can reduce the population and genetic diversity of the species overall (Liow and Stenseth 2007; Castiglione et al. 2017; Žliobaitė et al. 2017). The most common examples are the introduction of foreign species to areas whose populations are unequipped to deal with resource competition. This has been proposed for the influx of placental mammals to South America, when it became connected by land to North America during the Pliocene 5.33–2.58 (Webb 2006; Woodburne et

al. 2009), and for the introduction of invasive species like *Rattus norvegicus* (brown rat) by humans all over the world (Stanley 1973). Species can also become more vulnerable to extinction via competition during intervals of climate change, when resource availability can rapidly fluctuate and established means of avoiding resource competition fail (Jankowski et al. 2010; Sinervo et al. 2010; Urban et al. 2012). These effects are amplified when species share resources. For example, similarity in prey preference can increase the frequency of competitive interactions, particularly if resources are declining, which can increase the risk of extinction if one species is competitively dominant over the other (Urban et al. 2012). For this reason, I investigate the niches of extinct species in order to test for competition and its consequences.

1.3 The ecological niche

The niche is defined as the combination of abiotic and biotic conditions in which an organism can exist (Hutchinson 1957; Wiens 2011). Abiotic factors are the external conditions of where species live and what they can tolerate (i.e. climate), and biotic factors are interactions species have with other species in that environment (e.g. predator-prey pairs) (Hutchinson 1957). A species must occupy a niche that provides for all its essential needs if it is to thrive and remain established. The fundamental niche is combination of abiotic and biotic factors in which it is possible for a species to survive, while the realized niche is the observed conditions in which a species is found at a particular point in time (Hutchinson 1957; Wiens and Graham 2005; Pearman et al. 2008). The realized niche is smaller than the fundamental niche, usually due to interspecific interactions (e.g. competitive exclusion) or dispersal limitations (Hutchinson 1957; Ashby et al. 2017). The fundamental niche cannot typically be observed, so the realized niche is determined by observing the abiotic (e.g. climate, landscape) and biotic

(e.g. primary producers, prey populations, competitors) factors associated with the geographic locations where species is maintains viable populations (Hutchinson 1957; Pearman et al. 2008; Ashby et al. 2017).

There are a number of ways to quantify the niche of a species, including direct observation of behaviour (typically not possible in the fossil record), comparison of species occurrence observations with climate and landscape data, co-existence patterns (e.g. the relationships between predator and prey), and comparison of body form among species (Hutchinson 1957; Colwell and Futuyma 1971; Gould and Calloway 1980; Fraser et al. 2015; Liow et al. 2015; Ashby et al. 2017). Species engage in different lifestyles (e.g. climbing, digging) and dietary behaviours (e.g. meat and plant eating) that are typically inherited from their ancestors (Price 1997; Lyons et al. 2016; Fraser et al. 2018a; b). These differences are reflected in the form and function of some of their various body parts (e.g. teeth and limb bones) (Reilly et al. 2001; McGill et al. 2006; Van Valkenburgh 2007; Meachen and Van Valkenburgh 2009). For example, different foods have different physical properties (e.g. soft meat vs tough plants), which require a species to possess different suites of traits (Sacco and Van Valkenburgh 2004; Ungar 2010; Pineda-Munoz et al. 2017). By examining the ecologically relevant traits, we can infer the lifestyles and diets of different species (Sacco and Van Valkenburgh 2004; Van Valkenburgh 2007; Smits and Evans 2012; Pineda-Munoz et al. 2017). It is impossible to obtain the same amount of information from a fossil as from a living specimen, but by comparing the morphology of extinct species to extant, closely-related species with known lifestyles, we can make reasonable inferences about the lifestyles of extinct forms (McGill et al. 2006; Polly 2010; Smits and Evans 2012; Pineda-Munoz et al. 2017). Herein, I specifically consider dental, cranial,

and post-cranial linear metrics plus body size to approximate the niches of extinct carnivorous mammals.

1.4 Inferring niche overlap from morphology

Among mammals from ancestrally carnivorous clades, the shape of the teeth, skull, and post-crania are highly indicative of a species' ecology. Dental measurements correspond closely with preferred diet (i.e. meat, bones, insects, plants), while cranial and post-cranial measurements correspond with feeding strategy (Friscia et al. 2007; Van Valkenburgh 2007; Meachen and Van Valkenburgh 2009; Smith 2019). Mammalian teeth vary greatly in form and function, depending on diet and phylogeny (Reilly et al. 2001; Wall and Smith 2001; Lucas 2004; Ungar 2010; Fraser et al. 2018a). Carnivorous mammals, including carnivoramorphans, marsupials, and "creodonts," possess a set of blade-like teeth for slicing meat, carnassialized teeth (Ungar 2010). Carnivorans and their extinct relatives each developed carnassialized teeth independently, and thus carnassial tooth pairs are formed by different teeth in the jaw (Flynn 1998; Gunnell 1998; Van Valkenburgh and Jenkins 2002). Note that in this thesis, I use the notation "m" for molar and "p" for premolar, with lowercase letters indicating a lower tooth and uppercase indicating an upper tooth, followed by the number indicating the position in the mouth. Carnivoramorphans possess carnassials m1 and P4, oxyaenids possess carnassials m2 and M1, and hyaenodontids possess multiple carnassial teeth with the cutting function being most concentrated on the m3/M2 pair (Fig. 1.1) (Gunnell 1998).

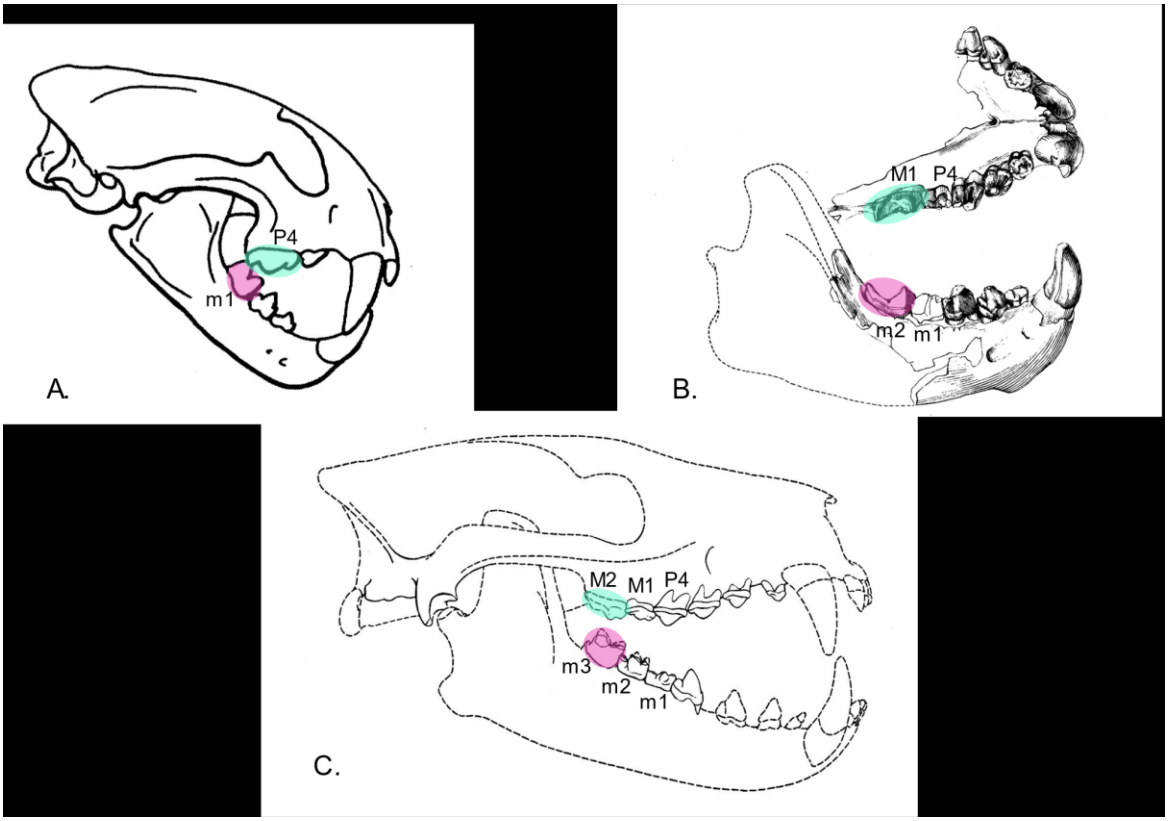

Figure 1.1. Carnassial teeth of carnivorous mammals. Upper carnassials are circled in teal and lower carnassials are circled in pink. A. Carnivoramorpha (e.g. *Neofelix nebulosa*, pictured) possess carnassials on the P4 and m1. B. Oxyaenida (e.g. *Sarkastodon mongoliensis*, pictured) possess carnassials M1 and m2. C. Hyaenodontida (e.g. *Dissalidictis carnifex*, pictured) possess carnassials M2 and m3, with the exception of the genus *Prolimnocyon* which possess M1 and m2 carnassials. Images altered from (Colbert 1933; Granger 1938; Van Valkenburgh and Jenkins 2002).

When combined, linear metrics of tooth shape, as well as metrics of bite force and rigidity of the jaw, can be analyzed to determine the amount of meat or vegetation that was consumed (Friscia et al. 2007; Van Valkenburgh 2007; Smith 2019). These metrics also correspond to hunting style and prey size preference (Friscia et al. 2007; Van Valkenburgh 2007; Meachen and Van Valkenburgh 2009; Smith 2019). For example, a long, narrow snout is indicative of an insectivorous diet, while a short, broad snout is needed to hold onto and kill

struggling prey (Friscia et al. 2007; Van Valkenburgh 2007; Meachen and Van Valkenburgh 2009; Smith 2019).

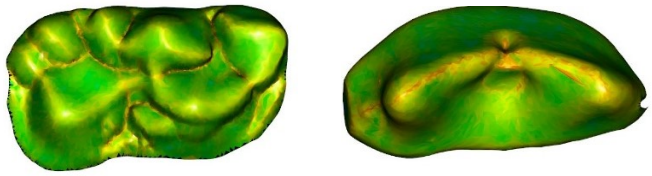

Figure 1.2. Surface relief images of the lower first molars of a giant panda (*Ailuropoda melanoleuca*; left) and a cheetah (*Acionyx jubatus*; right).

Three-Dimensional morphometrics can be used to quantify tooth shape to infer diet (Smits and Evans 2012; Pineda-Munoz et al. 2017). Orientation Patch Count (OPC) is a 3D metric, which takes a digital tooth mesh and calculates the total number of "patches" (2 or more faces which are connected and oriented in the same direction). OPC increases with increased tooth complexity and is associated with less carnivorous diets, for example the herbivorous giant panda (*Ailuropoda melanoluca*) possesses molars that have highly complex surfaces, as opposed to the hypercarnivorous cheetah (*Acionyx jubatus*) which possesses simple lower molars (Fig 1.2; Smits and Evans 2012; Pineda-Munoz et al. 2017; Christison et al. 2020). Relief Index (RI) is the quantification of the "steepness" of the tooth's surface; RI is higher in sharper teeth and is correlated with increased carnivory (Fig. 1.3; Bunn et al. 2011; Pineda-Munoz et al. 2017; Spradley et al. 2017; Pampush et al. 2018; Christison et al. 2020).

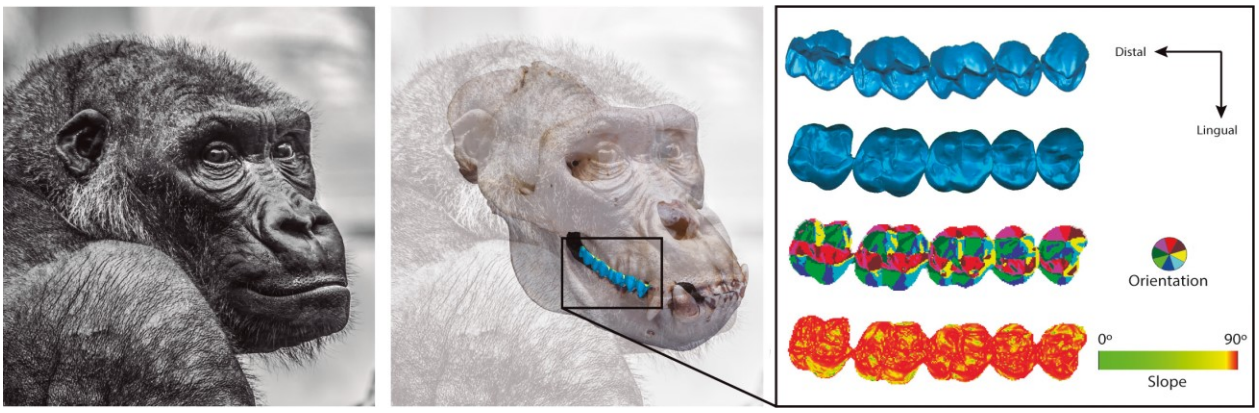

Figure 1.3. Three-dimensional occlusal reconstruction of western gorilla (*Gorilla gorilla*). Orientation patch count (OPC; each differently-oriented patch is represented by a different colour as shown in the colour wheel) and surface relief (RI; green-yellow-red gradient from 0 to 90° as in slope chart) are two of the variables obtained for each specimen in the study. Upper right tooth row, anterior towards the right. Figure from Pineda-Munoz et al. (2017).

Other metrics can also enable inference of the dietary niche of extinct animals. The body mass of a mammal is informative because it determines the types of food individuals can or cannot access (Alroy 1998; Van Valkenburgh et al. 2004). For example, *Lynx canadensis* and *Puma concolor* have similar dental shapes and dietary preferences (i.e. meat), but *L. canadensis* has a much lower body mass (Ivan and Shenk 2016; Lavoie et al. 2019). *L. canadensis* therefore cannot exploit the same kinds of prey as *P. concolor* (e.g. large bodied mule deer) and feeds primarily on small mammals, such as hares (Di Bitetti et al. 2010; Ivan and Shenk 2016; Lowrey et al. 2016). Similarly, the large body size of *P. concolor* means that it cannot fulfill its daily caloric needs by exclusively hunting the same small prey as *L. canadensis*, though *P.concolor* is not precluded from occasionally feeding on small prey (Hemmer 2004). Calculating Prey-Focus Mass (PFM), which is based on the predator's body mass and the body masses of the prey species within the same geographic area, can be used infer the potential sizes of prey species a carnivore is able to access (Hemmer 2004; Volmer et al. 2016; Christison et al. 2020).

Locomotor posture can also be inferred from post-cranial anatomy and is correlated with the dietary niche (Polly 2010; Lovegrove and Mowoe 2013). The three postures that are observed among carnivorans are digitigrady, protodigitigrady, and plantigrady (Polly 2010; Lovegrove and Mowoe 2013). A digitigrade posture is when the carpus and tarsus are held high above the substrate and the animal's body weight is supported by the ends of the metapodials. A plantigrade posture is when the carpus and tarsus are positioned on the substrate and support the animal's weight along with the metapodials, while a protodigitigrade posture intermediate to digitigrady and platigrady (Polly 2010; Lovegrove and Mowoe 2013). Digitigrady is associated with a more cursorial lifestyle and with open environments, while plantigrady is associated with an arboreal or generalized lifestyle in heavily vegetated environments (Polly 2010). The locomotory mode of an animal therefore provides insight into the behaviour of an extinct animal, such as differentiating between arboreal or terrestrial lifestyles, or between pursuit or ambush predators (Polly 2010). For example, wolves are digitigrade pursuit predators while bears are plantigrade opportunists and scavengers (Polly 2010).

1.5 Niche overlap and competition

Niche overlap occurs when one or more species in the same ecosystem occupy all or part of the same niche. The degree to which different species in a community exhibit niche overlap (if they do at all) can provide information on the intensity of species-species interactions (Wiens 2011). For example, if two species within the same community rely on the same food source as a major part of their diet, they are more likely to interact with each other than species that rely on differing food sources (Sale 1974). The competitive exclusion principle states that no two species, which subsist entirely off the same resources can co-exist and is

typically used to refer to situations in which species with the same or similar niches have spatially distinct geographic ranges (Hardin 1960). This is because species that are vulnerable to the effects of resource competition may either adapt to subsist off of alternative food sources or relocate to a geographic area without other competitors (Hardin 1960; Stanley 1973). Competitive exclusion can also lead to extinction of the least competitive species (Brown and Wilson 1956). Character displacement is a way that species can adapt to competitive pressures in the absence of extinction and competitive exclusion (Brown and Wilson 1956; Strong et al. 1979; Dayan and Simberloff 2005; Di Bitetti et al. 2010). When two or more species exhibit niche overlap within a community, character displacement is the process by which they adapt to occupy new niches or smaller parts of their niche in order to reduce resource competition (Brown and Wilson 1956; Strong et al. 1979; Futuyma and Moreno 1988; Dayan and Simberloff 2005; Di Bitetti et al. 2010).

Behavioural shifts are a form of character displacement that can allow multiple species of morphologically similar carnivoran to coexist in the same community (Brown and Wilson 1956; Strong et al. 1979; Dayan and Simberloff 1998; Volmer et al. 2016). One example are the neotropical felids: jaguar (*Panthera onca*), cougar (*Puma concolor*), ocelot (*Leopardus pardalis*), jaguarundi (*Herpailurus yagouaroundi*), margay (*Leopardus wiedii*), and oncilla (*Leopardus tigrinus*) exhibit geographic overlap and morphological similarity (Di Bitetti et al. 2010; Silva-Pereira et al. 2011; Sánchez-Barradas and Villalobos 2020). These felids are hypothesized to coexist due to their opportunistic feeding behaviours and dietary flexibility in the presence of an abundance of resources (Sánchez-Barradas and Villalobos 2020). Hunting patterns also facilitate co-existence between species, for example the margay and ocelot are nocturnal, while

the jaguarundi is diurnal (Di Bitetti et al. 2010). The puma and oncilla can be active during the day or night (Di Bitetti et al. 2010). Ocelots and pumas are also known to hunt on old roads or paths (Di Bitetti et al. 2006), while margays are adapted to highly arboreal lifestyles, and oncillas are more terrestrial (Di Bitetti et al. 2010). These species are also not morphologically identical: the jaguar and cougar have higher body masses than the other species listed here (Wilman et al. 2014) allowing them to exploit larger prey types (Pineda-Munoz et al. 2016). In combination, these forms of character displacement can allow multiple species with similar morphologies to coexist without necessarily leading to competition.

Specialization is another form of character displacement. For example, all taxa within the family Felidae have lost their post-carnassial molars through evolution (Meachen and Van Valkenburgh 2009). This loss of the grinding functionality of their dentition means that all felids rely on their carnassial teeth for processing food; in other words, all felids are hypercarnivores (diet consists of >70% vertebrate flesh) because their teeth can no longer process tough materials (Holliday and Steppan 2004; Van Valkenburgh 2007; Meachen and Van Valkenburgh 2009). This reduces competition with other carnivores that have retained the grinding functionality of their molars and can feed on a wider variety of food items (i.e. bones, vegetation). Some felids (e.g. *Panthera*) have further specialized to feed on large-bodied prey, which reduces competition with smaller felids. Though extreme specialization may be beneficial in the short term, it can lead to the taxon becoming more vulnerable to environmental changes, particularly those that impact the resources on which they specialize (Futuyma and Moreno 1988; Holliday and Steppan 2004; Van Valkenburgh et al. 2004; Van Valkenburgh 2007; Smits 2015).

1.6 Carnivoramorpha and "Creodonta" during the Eocene

Carnivoramorpha is the taxonomic clade encompassing the extinct families Viverravidae and Miacidae, and the extant family Carnivora (Fig. 1.4). Carnivora encompasses at least 286 extant species, including all modern carnivorous placental mammals (Fig. 1.4), though some have secondarily adapted to omnivorous and even herbivorous diets (Janis et al. 1998a). Fossils of the Carnivoramorpha are first found in the early Paleocene (~60 Ma). Though miacids and viverravids went extinct by the end of the Eocene (~40 Ma) (Fig. 1.5), Carnivora persisted and began to diversify toward the end of the Eocene (~33 Ma) (Fig. 1.5).

Figure 1.4. Compilation phylogeny of carnivorous mammals based on Janis 1998 and Goswami 2010.

Concurrent with early carnivoramorphans were the creodonts, a polyphyletic group of carnivorous mammals hypothesized to be a sister group to Carnivora (Fig. 1.4) (Flynn 1998; Gunnell 1998; Janis et al. 1998a). "Creodonta" is made up of two groups, which emerged in the

early Paleocene (~60 Ma), the Oxyaenida and Hyaenodontida (Figs. 1.4, 1.5). The oxyaenids went extinct in the late Eocene (~40 Ma) (Fig. 1.5), while the hyaenodontids went regionally extinct in North America in the late Oligocene (~10 Ma) and globally extinct by the late Miocene (~6 Ma) (Figs. 1.5, 1.6; Gunnell 1998).

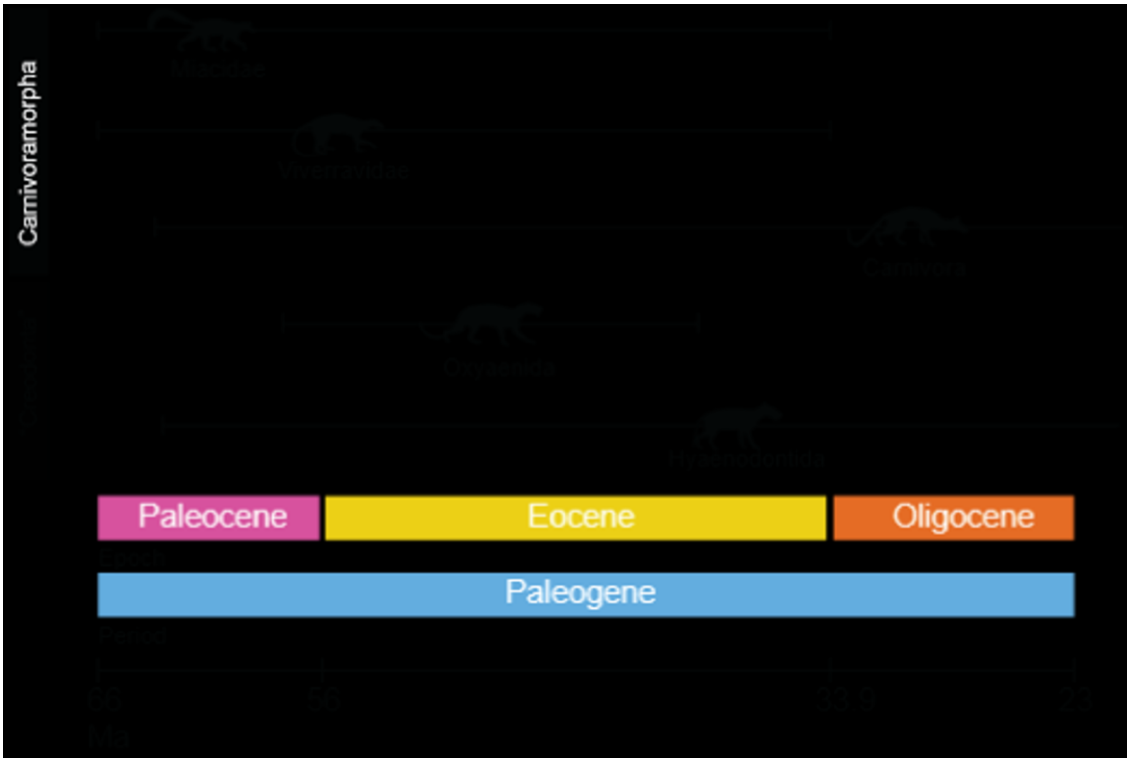

Figure 1.5. Paleogene carnivorous mammals. Global first and last appearances are based on the maximum age of the oldest known fossil and minimum age of the youngest known fossil within each group (Paleobiology Database). FAD = Fist Appearance Date; LAD = Last Appearance Date.

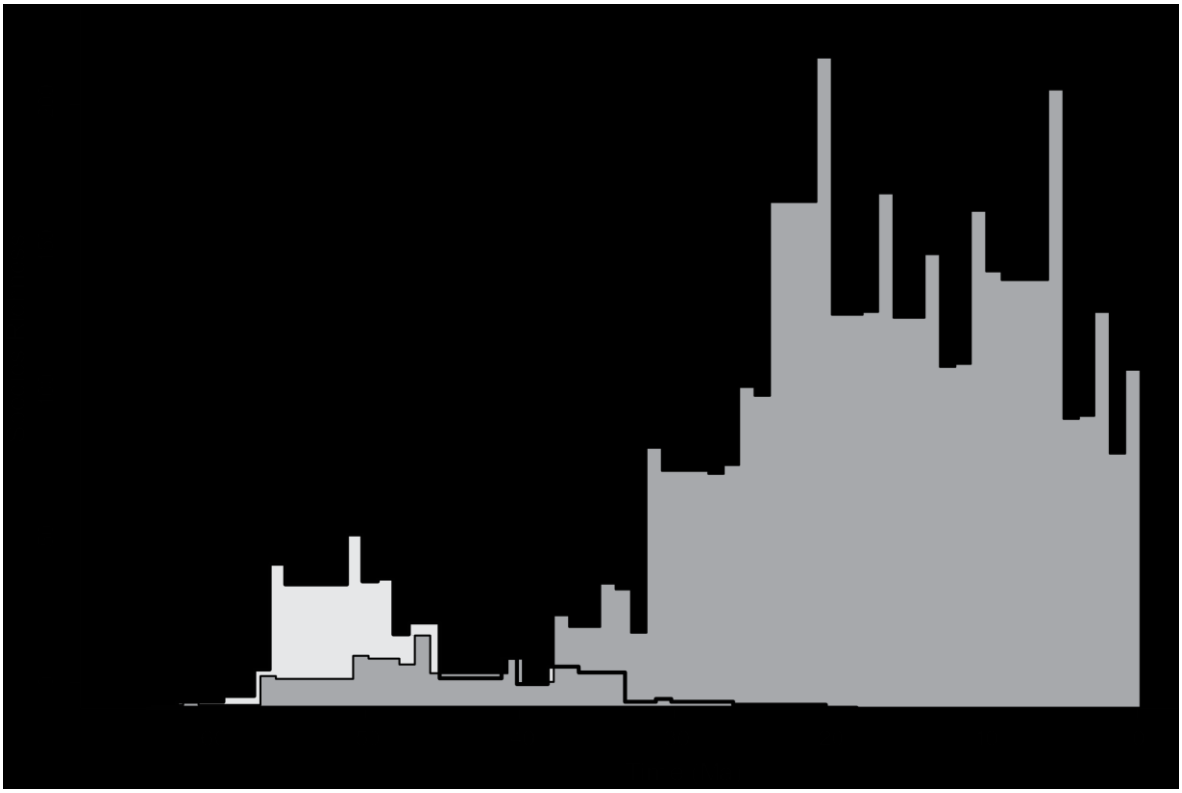

Figure 1.6. Creodont species richness declined while carnivoran richness increased during the late Eocene. Time is millions of years ago (Ma). Figure altered from Christison et al. (2020). The data were downloaded from the Paleobiology Database in March 2018, using the group name 'Mammalia' and the following parameters: time intervals = Cenozoic, region = North America, paleoenvironment = terrestrial.

Both carnivoramorphans and creodonts emerged in North America during the Paleocene, a period with a relatively steady climate (Fig. 1.7), however the groups did not begin to diversify until the Eocene (Fig. 1.6). The Eocene epoch lasted from the 56 Ma to 33.9 Ma, and began with some of the highest temperatures of the Cenozoic, the Paleocene-Eocene thermal maximum (PETM; ~55.8 Ma), the early Eocene climatic optimum (EECO; ~53-50 Ma), and the middle Eocene climatic optimum (MECO; ~44-41.5 Ma) (Fig 1.7; Prothero 1998a; Woodburne et al. 2009; Figueirido et al. 2011). Early Eocene North America was made up of tropical and sub-tropical landscapes, which coincided with an influx of mammalian immigration to North America, including hyaenodontids, primates, artiodactyls, and perissodactyls (Stucky 1992;

Maas et al. 1995; Woodburne et al. 2009). North America was able to support many large mammalian herbivores during this period, thanks to the lush vegetation that grew in the warm, productive climate (Prothero 1998a; Wing 1998; Figueirido et al. 2011; Secord et al. 2012).

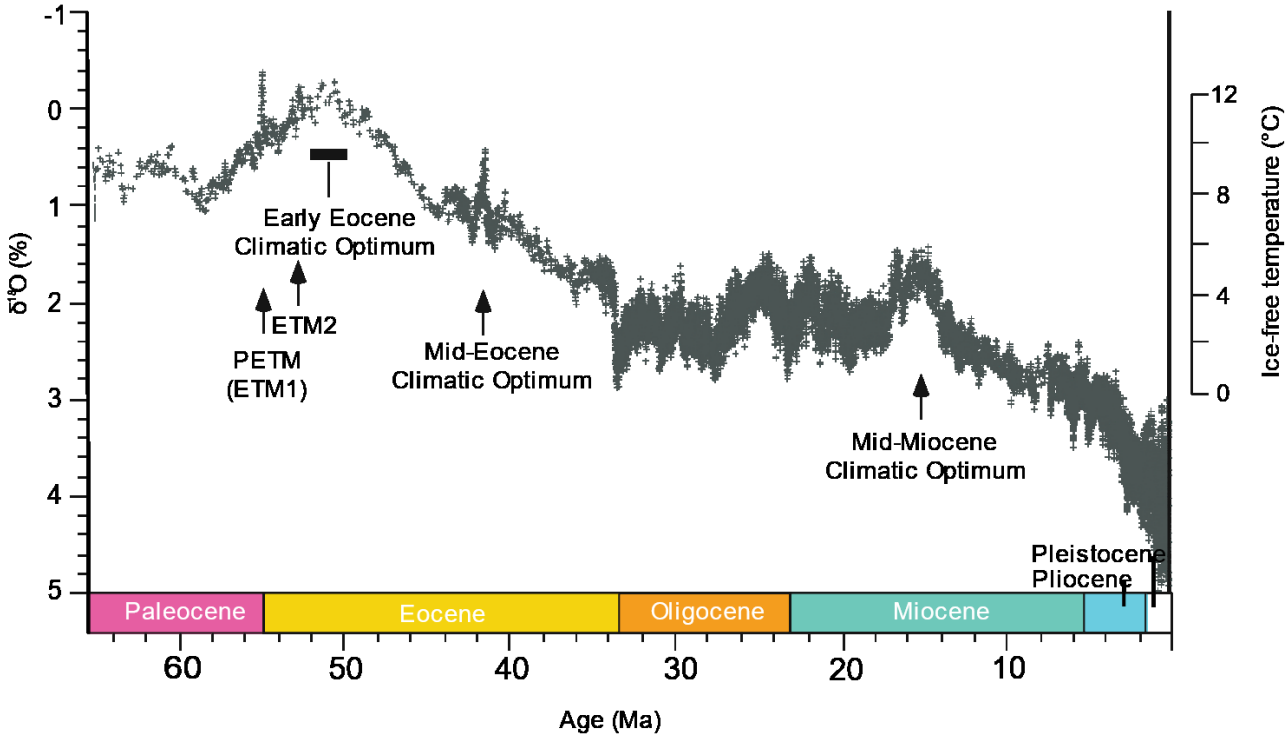

Figure 1.7. Evolution of global climate over the past 65 million years. Figure modified from Zachos et al. (2008). $\delta^{18}O$ values are from benthic forams collected at deep sea drilling sites and are a proxy for global temperatures. Higher values of $\delta^{18}O$ indicate higher global temperatures.

After the EECO, the climate began to cool (with a brief period of warming at the MECO) (Fig. 1.7), and tropical landscapes and lush forests gave way to woodland savannah over the 17 Ma year period between the EECO and the end of the Eocene (Fig 1.7; Prothero 1998a; Wing 1998). As the landscape and vegetation changed, so did the herbivores that occupied these areas (Russell 1973; Prothero 1998a). Many of the large browsers such as brontotheres were able to persist in the limited woodland areas until the late Eocene (Russell 1973; Strömberg 2004), while smaller herbivores, such as horses and small rhinoceroses, were better-suited to

the new landscape and more open vegetation (Stucky 1992; Prothero 1998a; b). This relatively long period of gradual global cooling preceded the rapid cooling event of the early Oligocene, which coincided with a turnover of North American mammals at the Eocene-Oligocene boundary (Alroy et al. 2000; Figueirido et al. 2011; Fraser 2015). By the early Oligocene, creodonts were nearly extinct in North America, save for four species of the genus *Hyaenodon* (Van Valkenburgh 1994). These holdovers did not last long, however; *Hyaenodon* went extinct during the Oligocene and creodonts went extinct globally during the Miocene (Gunnell 1998).

1.7 Competition hypothesis

During the Eocene in North America, creodont diversity declined simultaneously with an increase in carnivoramorphan diversity (Fig. 1.6). It has been suggested that this was a result of increasing competition between the two groups, resulting directly in the extinction of all creodonts in North America (Friscia and Van Valkenburgh 2010), and later the world. A previous study of dental morphologies by Friscia and Van Valkenburgh (2010) found that, at the start of the Eocene, carnivoramorphans and creodonts both possessed generalized dentition, with some hypercarnivorous creodont outliers. Near the end of the epoch, after the extinction of non-carnivoran carnivoramorphans and oxyaenids, there was a trend toward increasing carnivory in both Carnivora and Hyaenodontida. However, carnivorans retained their more generalized forms, while hyaenodontids continued to evolve into more hypercarnivorous forms (Friscia and Van Valkenburgh 2010). These results are consistent with those of Christison et al. (2020), which found that the carnivorans and hyaenodontids at Calf Creek, a Late Eocene (Chadronian North American Land Mammal Age (NALMA)) locality on Treaty 4 land in southwestern Saskatchewan, were meso- to hypercarnivorous, but that the creodonts were

more specialized due to their relatively large body masses and corresponding dietary requirements (i.e. their focus on large prey). Previous studies, however, have either found support for the competition hypothesis at the genus level without consideration of whether taxa are found together (Friscia and Van Valkenburgh 2010) or have found little niche overlap between carnivoran and creodont species at the same locality (Christison et al. 2020). Competition occurs among individuals and can have effects on species as a whole (Dayan and Simberloff 2005), so any support for the Competition Hypothesis must come from comparing species. We also must have reason to believe that the species in question coexisted at the same time with overlapping geographic ranges. Temporal and geographic overlap between species can be assumed if their fossils have been found at the same locality; a loose term which encompasses any sedimentary deposits at specific geographic sites containing fossils from the same stratigraphic horizon (Rey and Galeotti 2008).

In our previous study on carnivoran and hyaenodontid species from the Calf Creek locality, which is situated on Treaty 4 land in southwestern Saskatchewan, my coauthors and I found that there was little to no niche overlap among creodont and hyaenodontid species (Christison et al. 2020). Our study used carnassial tooth shape and body mass to approximate dietary niche, and placed the fossil species in a Principal Component Analysis (PCA) space with modern carnivorans as a comparison with species whose diets are well-known (Christison et al. 2020). The fossil carnivoran and hyaenodontid species exhibited no overlap with each other, largely due to body mass differences between the groups (Christison et al. 2020). Our study, however, only examined the Chadronian Calf Creek locality, a time when creodont diversity had declined significantly (Christison et al. 2020). We proposed that the lack of niche overlap at the

site did not necessarily refute the competition hypothesis; it is possible that carnivorans and creodonts were competing earlier in the epoch, indirectly leading to the eventual extinction of creodonts by driving them to highly specialized niches (Christison et al. 2020).

1.8 Study objective

The objective of this study is to determine if and how dietary niche overlap between North American carnivorans and creodonts changed during the Eocene. Specifically, to determine if the competition hypothesis for the extinction of the creodonts is supported under rigorous examination. We interpret dietary niche overlap between two taxa as evidence for competition if it precedes a decrease in diversity of one of the taxa. There are four potential outcomes this study: two which support the hypothesis that competition was the ultimate driver of the creodont extinction, and two which do not. The first outcome, which would support the competition hypothesis, would be that I find evidence for niche overlap in both the beginning and the end of the Eocene (Fig. 1.8). This would indicate that niche overlap was an ongoing phenomenon between carnivorans and creodonts throughout the epoch, which could indicate that they were competing. If this was the case, it would stand to reason that competition may have been a factor in the ultimate extinction of the creodonts.

The second outcome, which would support the competition hypothesis, is if I found little to no evidence of niche overlap during the beginning of the Eocene, and strong evidence of niche overlap at the end of the Eocene (Fig. 1.9). This would indicate that carnivorans diversified and eventually shared niche with the creodonts, possibly driving their extinction through competition.

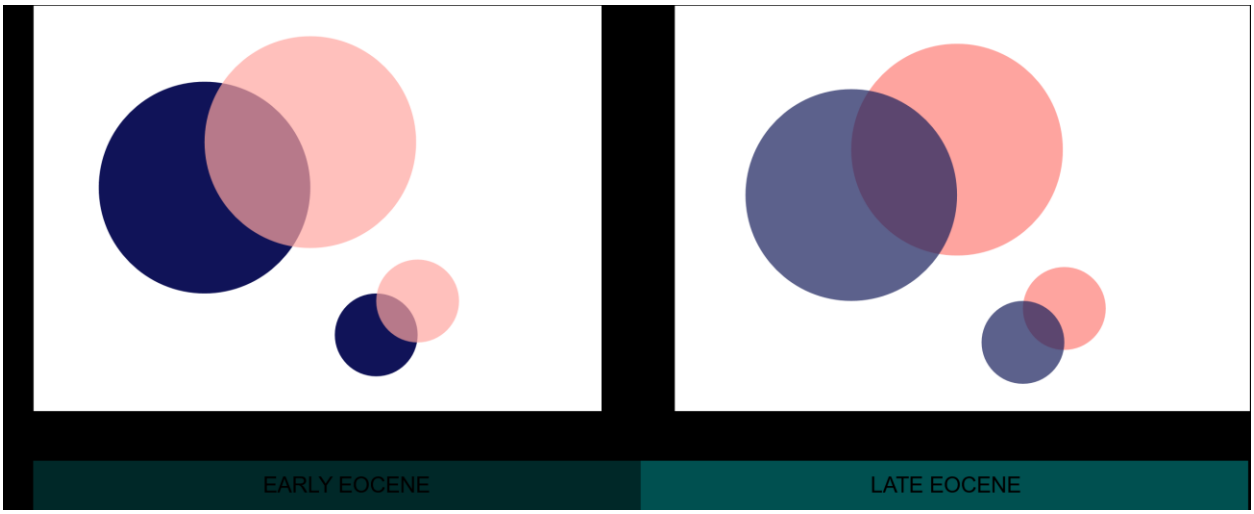

Figure 1.8. A hypothetical distribution of niche space occupied by carnivorans and creodonts. The axis titles represent different elements that comprise imaginary niche elements. In both the early Eocene (left) and late Eocene (right), there is niche overlap between the two groups. Therefore, competition was existent throughout the Eocene and may have been a factor contributing to the creodont extinction. The dark purple circles represent hypothetical carnivoran niches and the pink circles represent hypothetical creodont niches.

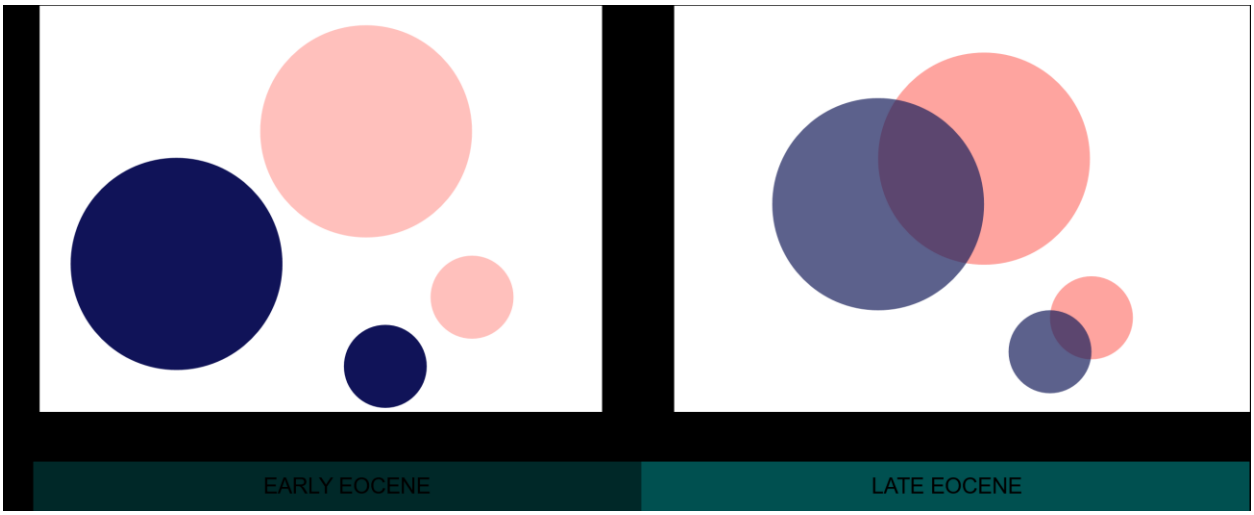

Figure 1.9. A hypothetical distribution of niche space occupied by carnivorans and creodonts. The axis titles represent different elements that comprise imaginary niche elements. In the early Eocene (left), there is no overlap between the niches of carnivorans and creodonts. In the late Eocene (right), there is niche overlap between the two groups. In this scenario, competition increased during the epoch and may have finalized the extinction of the creodonts as carnivorans proved to be superior competitors. The dark purple circles represent hypothetical carnivoran niches and the pink circles represent hypothetical creodont niches.

Potential results that would not support the competition hypothesis include if no niche overlap was found at either the start or the end of the Eocene (Fig. 1.10). This would mean that niche overlap was not a factor in the extinction of the creodonts, and that some other factor, such as the elimination of the niches occupied by creodonts, was the cause.

The final potential result that could arise from this study would be if niche overlap, and thus potentially competition, between carnivorans and creodonts at was present at the start of the Eocene epoch, but not at the end of the epoch (Fig. 1.11). This would suggest that competition between the two groups at the start of the Eocene may have driven creodonts to specialize their diets to occupy smaller niches (and ironically feed on larger prey). This could indicate that competition with carnivoramorphans drove the creodonts to highly specialized niches and thus made them more vulnerable to extinction from external factors in the long run, Competition would not have been present in the late Eocene and thus could not have been the proximate cause of the ultimate extinction of the creodonts.

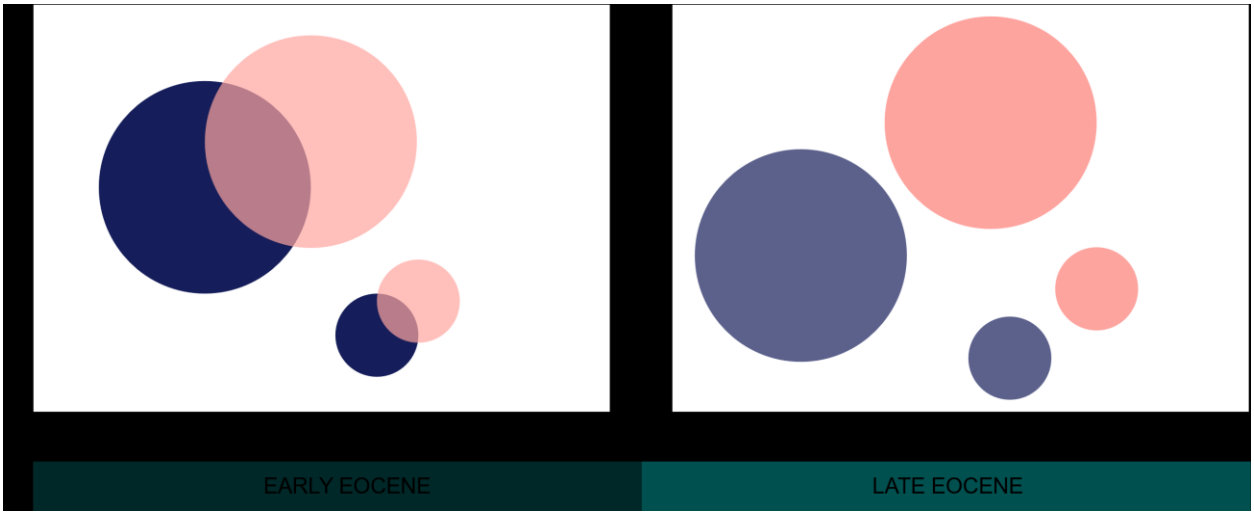

Figure 1.10. A hypothetical distribution of niche space occupied by carnivorans and creodonts. The axis titles represent different elements that comprise imaginary niche elements. In the early Eocene (left), there is overlap between the niches of carnivorans and creodonts. In the late Eocene (right), there is no niche overlap between the two groups, and the size of the creodont niches has been reduced. Competitive pressures have eliminated the generalist morphs that existed within the niche overlap. The dark purple circles represent hypothetical carnivoran niches and the pink circles represent hypothetical creodont niches.

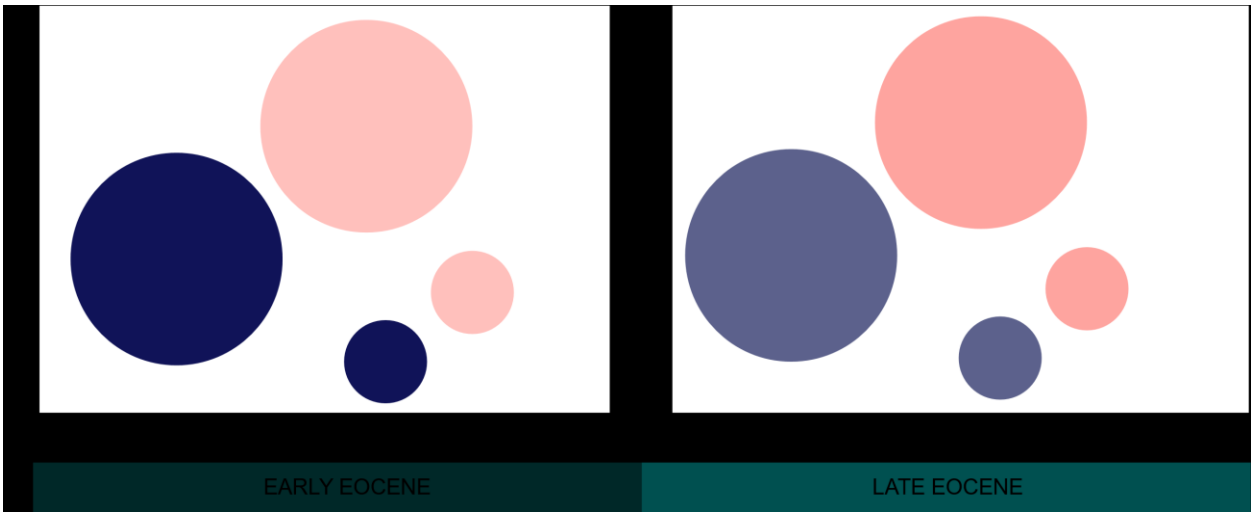

Figure 1.11. A hypothetical distribution of niche space occupied by carnivorans and creodonts. The axis titles represent different elements that comprise imaginary niche elements. In both the early Eocene (left) and late Eocene (right), there is no niche overlap between the two groups. Therefore, competition was nonexistent throughout the Eocene and therefore not a factor in the creodont extinction. The dark purple circles represent hypothetical carnivoran niches and the pink circles represent hypothetical creodont niches.

1.9 Hypotheses and predictions

I hypothesize that overspecialization, not competition, was the ultimate driver of creodont extinction at the end of the Eocene. I predict that we will find support for the overspecialization hypothesis; that niche overlap between carnivorans and creodonts existed at the beginning of the Eocene, but that by the end of the Eocene, creodonts had specialized to a hypercarnivorous diet, thus minimizing competition with carnivorans.

1.10 Structure of this thesis

This thesis is organized into two main chapters; the first is a comparative analysis investigating the efficacy of two methods of determining carnivoran diet, and the second incorporates those results to determine the dietary niche overlap of carnivoramorphans and creodonts during the start and the end of the Eocene. Introduction and conclusion chapters are also present to provide context to the research conducted in this thesis, and to synthesize the results of my research.

Chapter 2: Comparison of the efficacy of 2D and 3D tooth shape morphometrics for predicting the diets of carnivorous mammals

2.1 Introduction

As new technology becomes available, so do new ways of studying the evolution and ecology of extinct organisms (e.g. Evans and Fortelius 2008; Pineda-Munoz et al. 2017; Spradley et al. 2017; López-Torres et al. 2018). An example is digital scanning and the construction of 3D models, which has revolutionized the study of morphological evolution (Goswami 2006; Evans and Fortelius 2008; Meachen et al. 2014; Pineda-Munoz et al. 2017; Spradley et al. 2017). Digital scanning has continued to become more accessible and less costly to researchers in recent years due to the implementation of light-based scanning, photogrammetry, and high-resolution Computed Tomography (CT) scanning (Goswami 2006; Evans and Fortelius 2008; Meachen et al. 2014; Pineda-Munoz et al. 2017; Spradley et al. 2017). 3D methods have thus become a relatively standard way of studying animal form and function. CT scans, for example, are used to examine fossils that cannot be removed from the matrix they are embedded in, enabling materials of different densities to be differentiated and thus allowing the isolation of bone elements (Maddin et al. 2013; Adams 2020; Atkins et al. 2020). It can also be used to view the internal anatomy of fossil or zoological specimens that cannot be dissected or destroyed (Fernandez et al. 2013; Maddin et al. 2013; Adams 2020; Atkins et al. 2020). Digital scans can be used to observe the external anatomy of a specimen as well, particularly, when access to physical specimens is limited or when scientists desire to make complex comparisons of shape and topography. Given the wealth of data provided by digital scans, studies utilizing 3D data have, in some fields, nearly supplanted more traditional studies based on 2D linear

measurements (Evans and Fortelius 2008; Fernandez et al. 2013; Pineda-Munoz et al. 2017; López-Torres et al. 2018; Christison et al. 2020). Though 3D scanning continues to become easier and less time consuming, it still incurs a relatively high cost in terms of time and money; it can take hours to scan a single specimen and the equipment needed to perform 3D scanning is a financial barrier for many labs. Use of equipment at external labs, while more affordable, is still often a financial burden. Therefore, the objective of the present study is to make direct comparisons of 3D and 2D methods.

One example for which a comparison of 2D and 3D methods is important is tooth shape analysis, which traditionally included the use of 2D metrics (e.g. measurements of length, width, height) but has since grown to include a variety of 3D approximations of shape (e.g. Orientation Patch Count and Relief Index) (Evans and Fortelius 2008; Pineda-Munoz et al. 2017; Evans and Pineda-Munoz 2018). 2D and 3D metrics for tooth shape have been demonstrated to reflect the diets of modern mammals (Van Valkenburgh and Koepfli 1993; Friscia et al. 2007; Evans and Fortelius 2008; Meachen and Van Valkenburgh 2009; Pineda-Munoz et al. 2017; Evans and Pineda-Munoz 2018). Subsequently, the same methods have been applied to close relatives for the purpose of inferring the diets of long extinct species but, to date, no one has directly compared the 2D and 3D metrics in terms of how accurately they reflect diet (Allen et al. 2015; López-Torres et al. 2018; Christison et al. 2020).

Orientation Patch Count (OPC) and Relief Index (RI) are two 3D metrics that have been demonstrated to correspond with the average diets (those that they have evolved to eat) of modern mammals, including those of the taxonomic family Carnivora (e.g. bears, cats, dogs) (Pineda-Munoz et al. 2017; Evans and Pineda-Munoz 2018). OPC and RI are quantifications of

dental complexity, which require that tooth surfaces be scanned and converted to 3D meshes. OPC is determined by calculating the total number of polygons comprising the surface of a 3D mesh. Each polygon is oriented in one of eight cardinal directions, and any two or more polygons oriented in the same direction form a "patch." OPC is calculated as the total number of patches on 3D mesh. Lower OPC corresponds to less complex, blade-like teeth, which are typically found among species with hypercarnivorous diets (diets consisting of over 70% vertebrate flesh), such as the cheetah (*Acinonyx jubatus*) (Fig. 2.1; Van Valkenburgh 2007; Pineda-Munoz et al. 2017). Higher OPC corresponds to teeth with more complex shapes and larger surfaces for grinding, which are typically found among herbivorous species (diet consisting mainly of plant material; see methods for diet categories) such as the giant panda (*Ailuropoda melanoleuca*) (Fig. 2.1; Evans and Fortelius 2008; Pineda-Munoz et al. 2017; Christison et al. 2020).

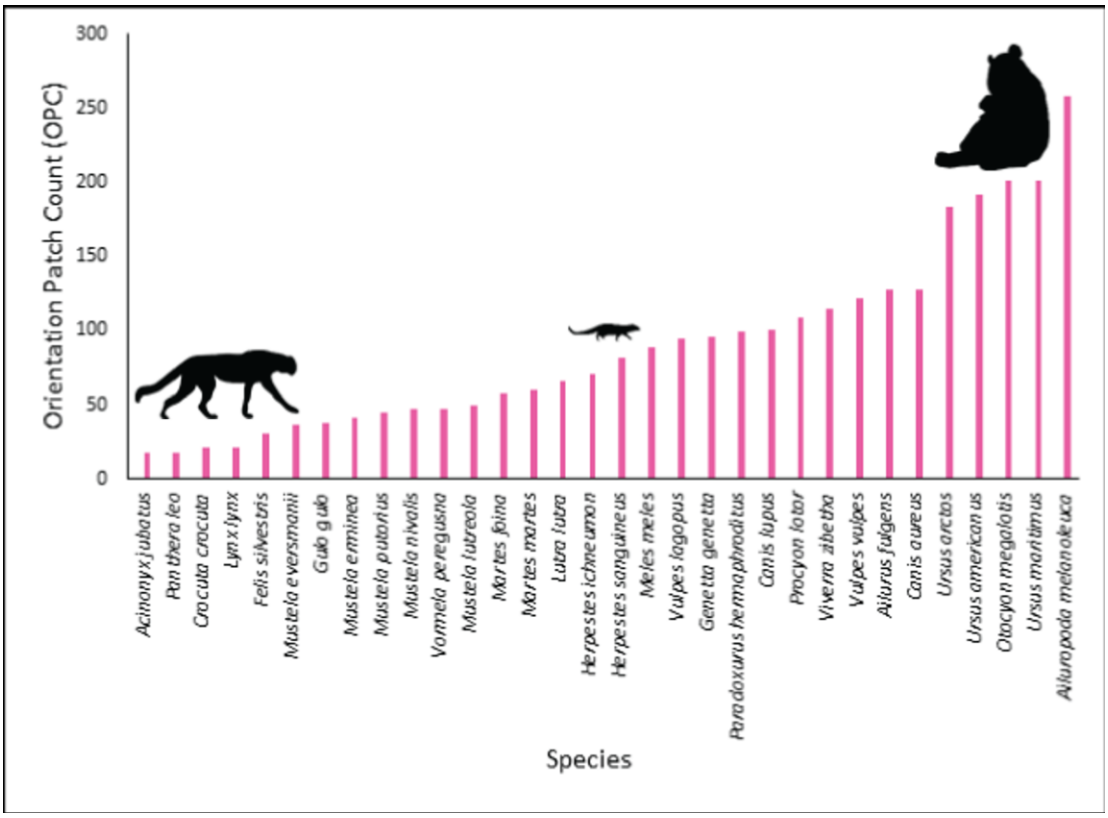

Figure 2.1. Tooth row Orientation Patch Count (OPC) of each species of carnivoran used in Pineda-Munoz et al. (2017). Silhouettes represent species with extremely low (*Acinonyx jubatus*), medium (*Herpestes sanguineus*), and extremely high (*Ailuropoda melanoluca*) OPCs.

RI estimates the "steepness" of a tooth's surface by using the ratio of the 3D surface area of the scan to the 2D area of the base (Pineda-Munoz et al. 2017). Enhanced grinding functionality corresponds with increased total surface area and decreased "steepness" and RI, while enhanced slicing capability, such as is observed in highly carnivorous species, increases "steepness" and RI (Fig. 2.2; Pineda-Munoz et al. 2017). To date these methods have been employed widely and applied to many groups of mammals and non-mammalian taxa (e.g. lizards) (Bunn et al. 2011; Melstrom 2017; Pineda-Munoz et al. 2017; López-Torres et al. 2018).

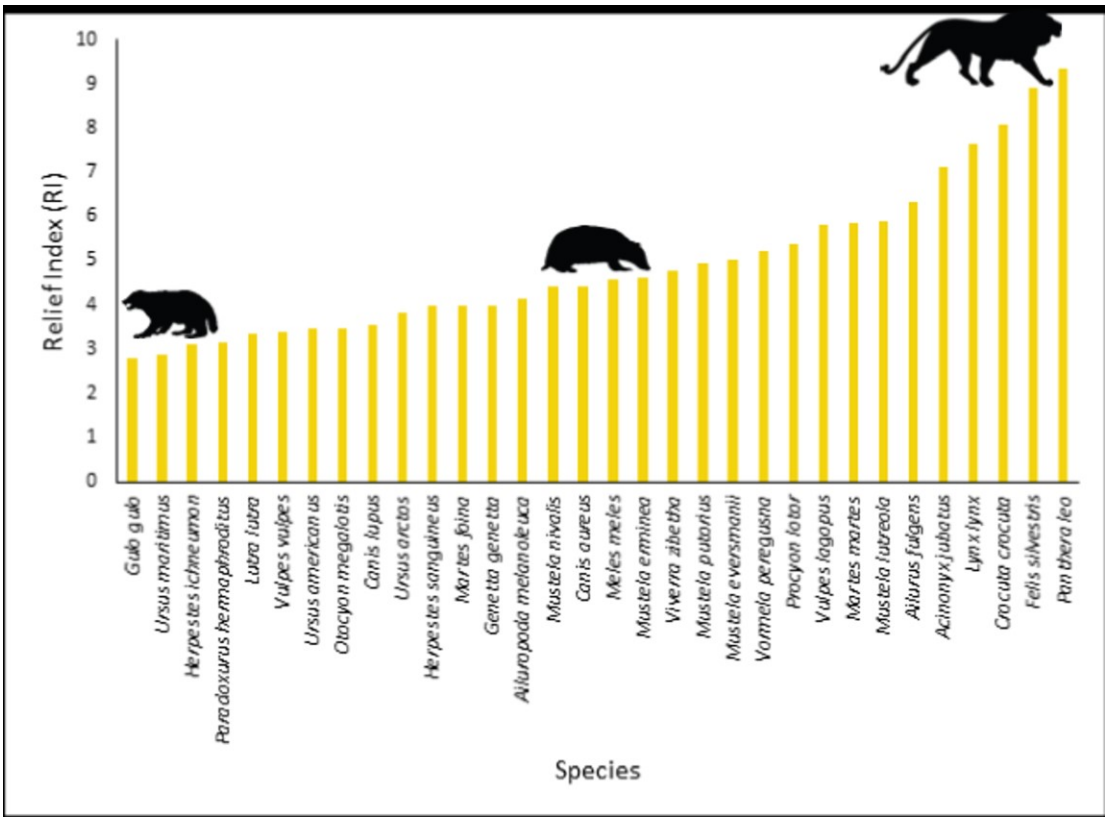

Figure 2.2. Tooth row Relief Index (RI) of each species of carnivoran used in Pineda-Munoz et al. (2017). Silhouettes represent species with extremely low (*Gulo gulo*), medium (*Meles meles*), and extremely high (*Ailuropoda melanoluca*) RIs.

Though digital scanning is now widely used and is increasingly becoming a standard approach in palaeoecology, 2D cranial and dental measurements have also been shown to correspond with everything from preferred foraging style (e.g. scavenging) to preferred prey size among Carnivorans (Van Valkenburgh and Koepfli 1993; Friscia et al. 2007; Meachen and Van Valkenburgh 2009; Slater and Friscia 2019). Van Valkenburgh and Koepfli (1993), for instance, developed a series of measurements of the lower jaw and teeth that are highly correlated with the dietary preferences of canids. The ratios are representative of various morphological traits associated with carnivoran diets: long, slender jaws are associated with rapidly catching small, quick prey (e.g. insects), while wide muzzles and robust canines are

associated with holding onto struggling prey and thus indicative of hypercarnivory (diet consisting of over 70% vertebrate prey) (Van Valkenburgh 2007; Meachen and Van Valkenburgh 2009). High proportions of grinding surfaces on the molars are associated with lower levels of carnivory (e.g. more generalized or herbivorous diets), while the opposite is indicative of more carnivorous diets (Van Valkenburgh and Koepfli 1993; Friscia et al. 2007; Slater and Friscia 2019). These measures have been shown to apply to extinct and extant carnivorans (Friscia et al. 2007; Slater and Friscia 2019), and to consistently correlate with diets (Van Valkenburgh and Koepfli 1993; Friscia et al. 2007; Slater and Friscia 2019).

In this chapter, I compare how well the 2D and 3D dental and jaw measurements differentiate carnivorans by diet using existing data collected by Friscia et al. (2007), Smits and Evans (2012), Pineda-Munoz et al. (2017), and Slater and Friscia (2019). Using various statistical analyses, I determined how different combinations of 2D and 3D metrics perform when attempting to determine dietary category. I also tested the individual metrics for correlation and distribution among dietary categories. The benefit of 2D measurements is that they can be taken from physical specimens in a museum setting, high-quality photographs, and 3D digital scans, while OPC and RI are only quantifiable using digital 3D scans. OPC and RI are therefore more difficult to obtain, since not every institution has access to the scanning machinery or computing power required, nor is it always cost-effective when working with specimens from other institutions. If they perform similarly, researchers may therefore be able to infer the diets of extinct species accurately without the use of expensive, time consuming 3D methods.

2.2 Methods

The jaw and tooth measurements used in this study were downloaded from Friscia et al. (2007) and Slater and Friscia (2019) based on the methods of Van Valkenburgh and Koepfli (1993). The authors took jaw and skull measurements (Fig. 2.3) from a combined total of 206 species of carnivoran. Abbreviations for the various metrics are defined in Table 2.1. I combined the datasets of Friscia et al. (2007) and Slater and Friscia (2019) and updated the taxonomy, taking the average measurements when there were multiple observations for a species. Because I am comparing linear data to lower jaw 3D metrics, I used only the lower jaw linear metrics.

The tooth row Orientation Patch Count (OPC) and Relief Index (RI) values used in this study were collected by Evans (2007) and Pineda-Munoz et al. (2017). Herein I use the OPC and RI values published in Pineda-Munoz et al. (2017) because it is a relatively large dataset of carnivoran tooth row scans. The authors collected 3D morphometric data from 32 species of carnivoran, 31 of which were also present in the combined Friscia et al. (2007) and Slater and Friscia (2019) linear metric dataset (only *Otocyon megalotis* was measured in Pineda-Munoz et al. (2017) but not Friscia et al. (2007) or Slater and Friscia (2019)). The scans used to collect OPC and RI were made with surface laser scanners using a Laser Design DS 2025 3D scanner with an RPS-120 probe (Laser Design Inc., Minneapolis, MN) or Nextec Hawk (Nextec Technologies, Israel). Scanning resolution was set between 10 and 50 µm, depending on the size of the tooth row (Pineda-Munoz et al. 2017).

Table 2.1. Jaw and dental measurements used to determine diet in Van Valkenburgh and Koepfli (1993), Friscia et al. (2007), Slater and Friscia (2019). Referenced measurements appear in bold and are illustrated in Figure 1. Descriptions obtained from Friscia et al. (2007).

Abbreviation	Meaning
P4S	Lower fourth premolar shape, measured as maximum width of p4 **(PMW)** divided by its maximum length **(PML**)
P4Z	Relative length of fourth lower premolar, measured as the maximum length of p4 **(PML)** divided by dentary length **(dL)** (measured as in M1BS)
RBL	Relative blade length of lower first molar **(BL)**, measured as the ratio of trigonid length to total anteroposterior length of m1 **(M1L)**
M1BS	m1 blade size relative to dentary length, measured as the length of the trigonid of m1 **(MTL)** divided by dentary length **(dL)**. Dentary length was measured as the distance between the posterior margin of the mandibular condyle and the anterior margin of the canine
RLGA	Relative lower grinding area, measured as the square root of the summed areas of the m1 talonid and m2 (if present) **(LGA)** divided by the length of the m1 trigonid **(MTL)**. Area was estimated as the product of maximum width and length of the talonid of m1 and m2, respectively
M2S	m2 size relative to dentary length, measured as the square root of m2 area (if present) divided by dentary length **(dL)**. Tooth area measured as in RLGA and dentary length (measured as in M1BS). If no m2 was present in the taxon, M2S was recorded as zero
MAT	Mechanical advantage of the temporalis muscle **(MAT)**, measured as the distance from the mandibular condyle to the apex of the coronoid process divided by dentary length **(dL)** (measured as in M1BS)
MAM	Mechanical advantage of the masseter muscle **(MAM)**, measured as the distance from the mandibular condyle to the ventral border of the mandibular angle (see Fig. 2) divided by dentary length **(dL)** (measured as in M1BS)
IxP4	Second moment of area of the dentary at the interdental gap (Ix) between the third and fourth lower premolars (P4) relative to dentary length. Moment area is used as an estimate of resistance of the dentary to bending. Second moment of area was calculated using the formula $Ix = (\pi D_x D_y^3)/64$, where $\mathbf{D_x}$ is maximum dentary width and $\mathbf{D_y}$ is maximum dentary height at the p3–p4 interdental. IxP4 was then estimated as the fourth root of Ix divided by dL (measured as in M1BS)
IxM2	Estimate of resistance of dentary to bending, as measured by the second moment of area at the interdental gap between the first and second molars (or posterior to the first molar if no second molar was present). Measured as IxP4, except maximum dentary width and height were taken at the m1–m2 interdental gap (or posterior to m1 if m2 was not present in the taxon)

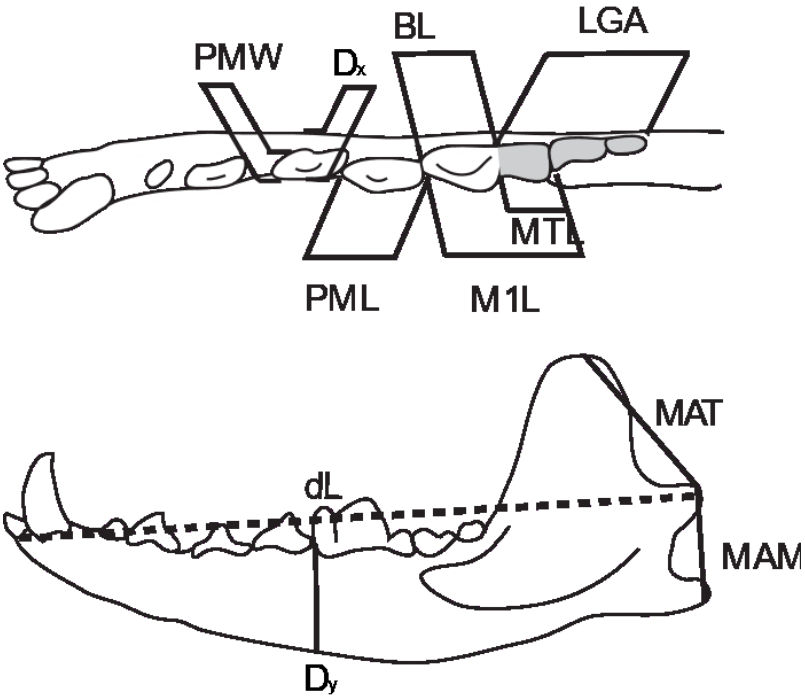

Figure 2.3. Linear measurements used to determine diet in Friscia et al. (2007) and Slater and Friscia (2019). Top: occlusal view of lower jaw. Bottom: Labial view of lower dentition. Descriptions of abbreviations are in Table 2.1. Figure modified from Slater and Friscia (2019).

I used two different methods of categorizing species by diet. The first was the diet categories reported by Pineda-Munoz et al. (2017), which they based on published stomach contents for each species; if any single food source made up over 50% of the animals' diet, it was classified as a specialist. The specialist categories were herbivory, carnivory (flesh eating), granivory (seed eating), insectivory (invertebrate eating), and fungivory (fungus eating), and if no food source made up over 50% of an animal's diet it was labeled as a generalist (Pineda-Munoz et al. 2017). The second set of diet categories was determined using Elton Traits 1.0 (Wilman et al. 2014), a dietary dataset based on global handbooks and monographs, from which I categorized species into the following diet categories: hypercarnivore (diet 100–80% vertebrate flesh), mesocarnivore (diet 80–60% vertebrate flesh), insectivore (diet >60%

invertebrates), herbivore (>80% plants), and omnivore (<80% plants and <60% vertebrate flesh or invertebrates) (Christison et al. 2020). Additional diets for species not included in Elton traits were hypothesized using the average for the genus or were derived from the literature (Appendix I).

I conducted Linear Discriminant Analyses (LDAs) in PAST (Hammer et al. 2001) to determine the rates at which the different tooth row metrics correctly classified species by diet. I first analyzed the 2D and 3D metrics separately: lower jaw OPC and RI for 32 species reported by Pineda-Munoz et al. (2017), and the combined dataset of 2D lower jaw metrics reported by Friscia et al. (2007) and Slater and Friscia (2019). I then combined the 2D and 3D metrics. I conducted LDAs for both methods of categorizing species by diet (described above).

I created box plots using PAST to visualize the differences in the various 2D and 3D metrics among diet for both diet categorization systems. I then conducted ANOVA tests using the R package "stats" (RStudio Team 2020) to determine to what degree the metrics vary or not among dietary categories. I performed Tukey's post hoc significance tests for the metrics which were shown to vary significantly among dietary categories.

I conducted Ordinary Least Squares (OLS) regressions using R (RStudio Team 2020) to determine which, if any, of the dental metrics are correlated (determined using $p < 0.05$ and r^2 values). I regressed OPC and RI against each other and the lower jaw measurements (P4Z, P4S, RBL, M1BS, and RLGA) used by Friscia et al. (2007) or Slater and Friscia (2019). I also regressed the dental metrics (P4Z, P4S, RBL, M1BS, and RLGA) against each other, excluding M2S, MAT, MAM, IxP4, and IxM2, which are related to jaw measurements as opposed to dental

measurements, and are thus not directly comparable with OPC and RI. Biplots of these analyses were created in PAST (Hammer et al. 2001) to visualize the data (Fig. 2.7).

I calculated the phylogenetic signal among the residuals from the OLS regressions (Pagel's λ value) using the R packages "ape" and "phytools" (Revell 2012; Paradis and Schliep 2019) and the phylogeny developed by Faurby and Svenning (2015). I calculated Pagel's λ using the phytools package in R (Pagel 1999; Freckleton et al. 2002; Revell 2012). I used residuals in our tests for a phylogenetic signal because, similar to ordinary least squares regression that assumes normality of residuals, phylogenetic comparative methods assume phylogenetic signal in the residuals (Revell 2010). Values of $\lambda = 0$ are indicative of phylogenetic independence, while high values of λ indicate Brownian evolution of a trait across a given phylogenetic tree or indicate significant phylogenetic signal (Pagel 1999; Freckleton et al. 2002; Fraser et al. 2018b). We used a likelihood ratio test to determine the statistical significance of Pagel's λ for each set of residuals (Revell 2010). When phylogenetic signal was determined to be statistically significant, I conducted Phylogenetic Generalized Least Squares (PGLS) regressions again using the R packages "ape," "phytools," and "nlme" (Revell 2012; Paradis and Schliep 2019; Pinheiro et al. 2020) and the phylogeny developed by Faurby and Svenning (2015).

2.3 Results

The Linear Discriminant Analyses (LDAs) yielded the highest correct classifications for the 2D and 3D metrics combined and for the 2D metrics alone, both with a sample size of 31 species (Table 2.2). The results for these LDAs were the same for both dietary classification systems and were slightly higher for the combined 2D and 3D metrics (93.55%) than for the 2D metrics alone (90.32%). The 2D metrics were less effective when the sample size was increased,

with 64.08% correct classification (Figs. 2.4, 2.5; Table 2.2). The LDAs with the lowest correct classifications were for the 3D metrics alone, and of the 3D metrics the diet categories determined using Elton Traits 1.0 had slightly lower correct classification (43.75%) than the diet categories determined by Pineda-Munoz et al. (2017) (56.25%).

Table 2.2. Linear Discriminant Analysis (LDA) results for different dietary categories. Numbers are percent correct classification. 2D lower metrics are summarized in table 2.1 and are published in Friscia et al. (2007) and Slater and Friscia (2019), and OPC and RI are published in Pineda-Munoz et al. (2017).

Combination	Diets from Pineda-Munoz et al. (2017)	Diets based on Elton Traits 1.0 (Wilman et al. 2014)
OPC and RI (32 species)	56.25	43.75
2D lower metrics (206 species)	-	64.08
2D lower metrics (31 species)	90.32	90.32
OPC, RI, and 2D metrics (31 species)	93.55	93.55

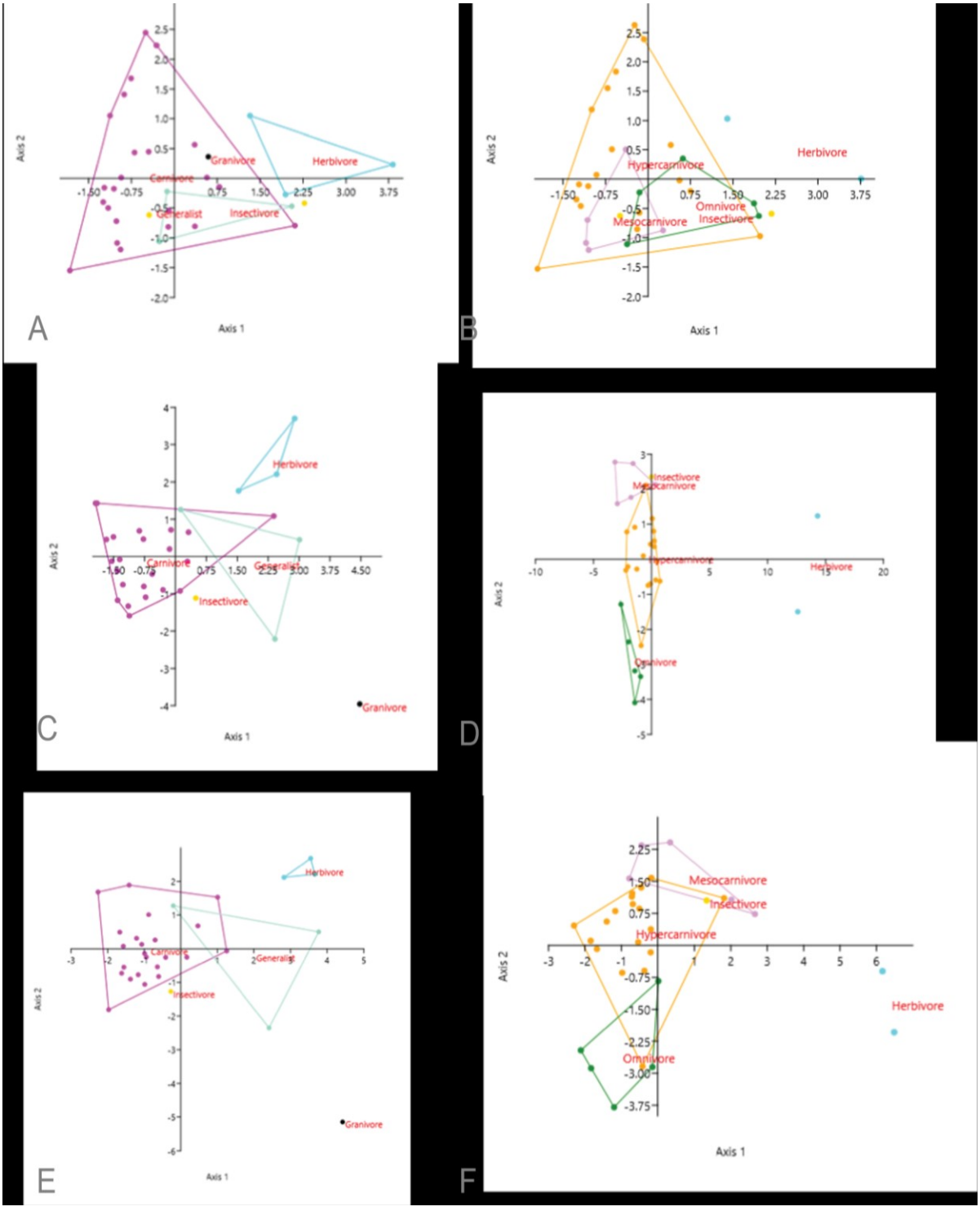

Figure 2.4. Linear discriminant analyses of the diets of extant carnivorans. DC1 = dietary categories from Pineda-Munoz et al. (2017); DC2 = dietary categories created using Elton Traits 1.0 (Wilman et al. 2014); 2D metrics = those listed in Table 2.1; 3D metrics = Orientation Patch Count (OPC) and Relief Index (RI) from Pineda-Munoz et al. (2017). **A**: 3D metrics, DC1, n = 32, **B**: 2D metrics, DC2, n = 32; **C**: 2D metrics, DC1, n = 31; **D**: 2D metrics, DC2, n=31; **E**: 2D and 3D metrics, DC1, n = 31; **F**: 2D and 3D metrics, DC2, n = 31.

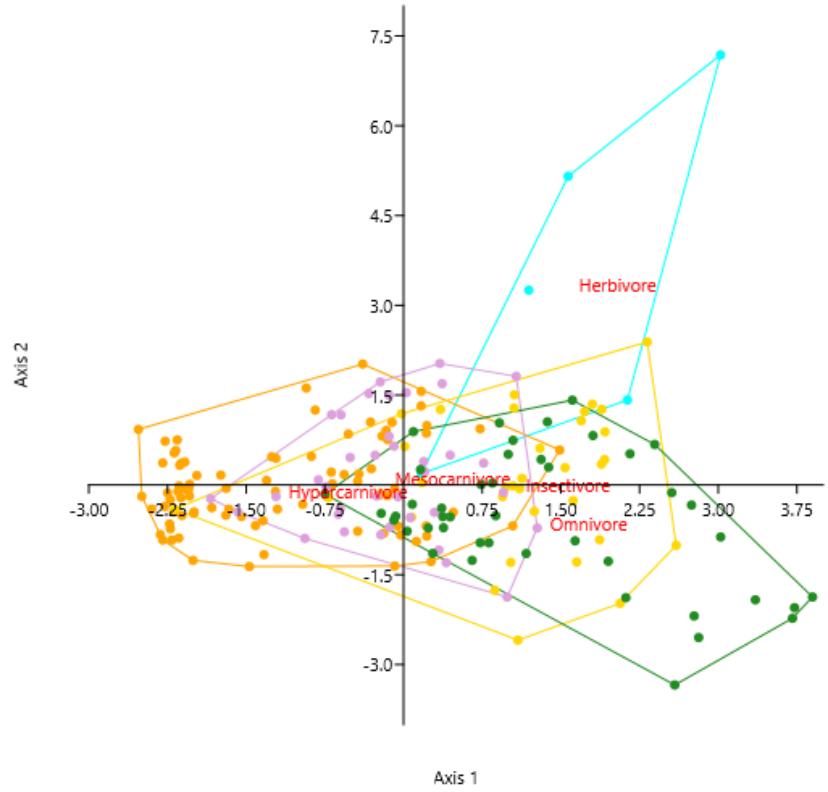

Figure 2.5. Linear discriminant analyses of 206 species of extant carnivoran published in Friscia et al. (2007) and Slater and Friscia (2019) using dietary categories created using Elton Traits 1.0 (Wilman et al. 2014) and 2D dental and jaw metrics listed in Table 2.1.

OPC, P4Z, M1BS, RLGA, and M2S (see Table 2.1 for abbreviations) differed significantly among the Pineda-Munoz et al. (2017) diet categories (Fig. 2.6; Table 2.3) and the diet categories which I based on Elton Traits 1.0 (Fig. 2.6; Table 2.3). P4S also differed significantly among the Pineda-Munoz et al. (2017) diet categories (Fig. 2.6; Table 2.3). Overall, individual metrics are only significantly different among one or two of the dietary categories, whether the Pineda-Munoz et al. (2017) categories or those based on Elton Traits 1.0. Often, significant differences are only found between the extremes on the dietary spectrum (e.g. Hypercarnivore and herbivore) (Fig. 2.6; Table 2.3). These results suggest that individual metrics are largely not sufficient to differentiate carnivorans with different diets.

Table 2.3. Analysis of variance (ANOVA) results comparing the distribution of 2D and 3D metrics for two dietary category systems. Diet is the dependent variable against which metric (independent) is tested. Mean Sq = mean square, i.e. variance; Pr(>f) = p value for the ANOVA test; DC1 = dietary categories from Pineda-Munoz et al. (2017); DC2 = dietary categories created using Elton Traits 1.0 (Wilman et al. 2014); OPC = Orientation Patch Count; RI = Relief Index; all other acronyms are listed and defined in Table 2.1.

Diet	~	metric	Mean Sq	Pr(>f)	Comparison			Tukey's test		
DC1	~	OPC	13118	0.003	Carnivore	~	Insectivore	p	>	0.05
					Carnivore	~	Generalist	p	>	0.05
					Carnivore	~	Granivore	p	>	0.05
					Carnivore	~	Herbivore	p	=	0.003
					Insectivore	~	Generalist	p	>	0.05
					Insectivore	~	Herbivore	p	>	0.05
					Insectivore	~	Granivore	p	>	0.05
					Generalist	~	Granivore	p	>	0.05
					Generalist	~	Herbivore	p	>	0.05
					Granivore	~	Herbivore	p	>	0.05
DC1	~	RI	2	0.6				p	>	0.05
DC1	~	P4S	0.01	0.05	Carnivore	~	Insectivore	p	>	0.05
					Carnivore	~	Generalist	p	>	0.05
					Carnivore	~	Granivore	p	>	0.05
					Carnivore	~	Herbivore	p	>	0.05
					Insectivore	~	Generalist	p	>	0.05
					Insectivore	~	Herbivore	p	>	0.05
					Insectivore	~	Granivore	p	>	0.05
					Generalist	~	Granivore	p	>	0.05
					Generalist	~	Herbivore	p	>	0.05
					Granivore	~	Herbivore	p	>	0.05
DC1	~	P4Z	0.001	0.04	Carnivore	~	Insectivore	p	>	0.05
					Carnivore	~	Generalist	p	<	0.07
					Carnivore	~	Granivore	p	>	0.05
					Carnivore	~	Herbivore	p	>	0.05
					Insectivore	~	Generalist	p	>	0.05
					Insectivore	~	Herbivore	p	>	0.05
					Insectivore	~	Granivore	p	>	0.05
					Generalist	~	Granivore	p	>	0.05
					Generalist	~	Herbivore	p	>	0.05
					Granivore	~	Herbivore	p	>	0.05
DC1	~	RBL	0.03	0.1				p	>	0.05
DC1	~	M1BS	0.003	0.01	Carnivore	~	Insectivore	p	>	0.05
					Carnivore	~	Generalist	p	>	0.07
					Carnivore	~	Granivore	p	>	0.05
					Carnivore	~	Herbivore	p	>	0.07
					Insectivore	~	Generalist	p	>	0.05
					Insectivore	~	Herbivore	p	>	0.05
					Insectivore	~	Granivore	p	>	0.05

					Generalist	~	Granivore	p	>	0.05
					Generalist	~	Herbivore	p	>	0.05
					Granivore	~	Herbivore	p	>	0.05
DC1	~	RLGA	0.9	0.001	Carnivore	~	Insectivore	p	>	0.05
					Carnivore	~	Generalist	p	>	0.01
					Carnivore	~	Granivore	p	>	0.1
					Carnivore	~	Herbivore	p	>	0.01
					Insectivore	~	Generalist	p	>	0.05
					Insectivore	~	Herbivore	p	>	0.05
					Insectivore	~	Granivore	p	>	0.05
					Generalist	~	Granivore	p	>	0.05
					Generalist	~	Herbivore	p	>	0.05
					Granivore	~	Herbivore	p	>	0.05
DC1	~	M2S	0.002	0.02	Carnivore	~	Insectivore	p	>	0.05
					Carnivore	~	Generalist	p	>	0.05
					Carnivore	~	Granivore	p	>	0.05
					Carnivore	~	Herbivore	p	>	0.03
					Insectivore	~	Generalist	p	>	0.05
					Insectivore	~	Herbivore	p	>	0.05
					Insectivore	~	Granivore	p	>	0.05
					Generalist	~	Granivore	p	>	0.05
					Generalist	~	Herbivore	p	>	0.05
					Granivore	~	Herbivore	p	>	0.05
DC1	~	MAT	0.0002	1				p	>	0.05
DC1	~	MAM	0.001	0.4				p	>	0.05
DC1	~	IxP4	0.0001	0.8				p	>	0.05
DC1	~	IxM2	0.00005	0.8				p	>	0.05
DC2	~	OPC	12470	0.004	Herbivore	~	Hypercarnivore	p	<	0.02
					Herbivore	~	Insectivore	p	>	0.05
					Herbivore	~	Mesocarnivore	p	<	0.07
					Herbivore	~	Omnivore	p	>	0.05
					Hypercarnivore	~	Insectivore	p	>	0.05
					Hypercarnivore	~	Mesocarnivore	p	>	0.05
					Hypercarnivore	~	Omnivore	p	>	0.07
					Insectivore	~	Mesocarnivore	p	>	0.05
					Insectivore	~	Omnivore	p	>	0.05
					Mesocarnivore	~	Omnivore	p	>	0.05
DC2	~	RI	4.5	0.2				p	>	0.05
DC2	~	P4S	0.01	0.1				p	>	0.05
DC2	~	P4Z	0.001	0.02	Herbivore	~	Hypercarnivore	p	>	0.05
					Herbivore	~	Insectivore	p	>	0.05
					Herbivore	~	Mesocarnivore	p	>	0.05
					Herbivore	~	Omnivore	p	>	0.05
					Hypercarnivore	~	Insectivore	p	>	0.05
					Hypercarnivore	~	Mesocarnivore	p	>	0.05
					Hypercarnivore	~	Omnivore	p	>	0.01
					Insectivore	~	Mesocarnivore	p	>	0.05
					Insectivore	~	Omnivore	p	>	0.05

					Mesocarnivore	~	Omnivore	p	<	0.05
DC2	~	RBL	0.04	0.06	Herbivore	~	Hypercarnivore	p	>	0.05
					Herbivore	~	Insectivore	p	>	0.05
					Herbivore	~	Mesocarnivore	p	>	0.05
					Herbivore	~	Omnivore	p	>	0.05
					Hypercarnivore	~	Insectivore	p	>	0.05
					Hypercarnivore	~	Mesocarnivore	p	>	0.05
					Hypercarnivore	~	Omnivore	p	=	0.003
					Insectivore	~	Mesocarnivore	p	>	0.05
					Insectivore	~	Omnivore	p	>	0.05
					Mesocarnivore	~	Omnivore	p	>	0.05
DC2	~	M1BS	0.003	0.005	Herbivore	~	Hypercarnivore	p	=	0.03
					Herbivore	~	Insectivore	p	>	0.05
					Herbivore	~	Mesocarnivore	p	>	0.05
					Herbivore	~	Omnivore	p	>	0.05
					Hypercarnivore	~	Insectivore	p	>	0.05
					Hypercarnivore	~	Mesocarnivore	p	>	0.05
					Hypercarnivore	~	Omnivore	p	>	0.05
					Insectivore	~	Mesocarnivore	p	>	0.05
					Insectivore	~	Omnivore	p	>	0.05
					Mesocarnivore	~	Omnivore	p	>	0.06
DC2	~	RLGA	0.9	0.0004	Herbivore	~	Hypercarnivore	p	=	0.003
					Herbivore	~	Insectivore	p	>	0.05
					Herbivore	~	Mesocarnivore	p	>	0.05
					Herbivore	~	Omnivore	p	>	0.05
					Hypercarnivore	~	Insectivore	p	>	0.05
					Hypercarnivore	~	Mesocarnivore	p	>	0.05
					Hypercarnivore	~	Omnivore	p	<	0.04
					Insectivore	~	Mesocarnivore	p	>	0.05
					Insectivore	~	Omnivore	p	>	0.05
					Mesocarnivore	~	Omnivore	p	>	0.05
DC2	~	M2S	0.003	0.002	Herbivore	~	Hypercarnivore	p	=	0.003
					Herbivore	~	Insectivore	p	>	0.05
					Herbivore	~	Mesocarnivore	p	>	0.05
					Herbivore	~	Omnivore	p	>	0.05
					Hypercarnivore	~	Insectivore	p	>	0.05
					Hypercarnivore	~	Mesocarnivore	p	>	0.05
					Hypercarnivore	~	Omnivore	p	<	0.04
					Insectivore	~	Mesocarnivore	p	>	0.05
					Insectivore	~	Omnivore	p	>	0.05
					Mesocarnivore	~	Omnivore	p	>	0.05
DC2	~	MAT	0.003	0.6						
DC2	~	MAM	0.002	0.07						
DC2	~	IxP4	0.0001	0.5						
DC2	~	IxM2	0.0001	0.3						

Figure 2.6. ANOVA distribution of dietary categories for 3D (OPC (Orientation Patch Count) and RI (Relief Index)) and 2D (see Table 2.1 for abbreviation definitions) tooth row metrics. Diet categories are defined by Pineda-Munoz et al. (2017) or are based on Elton traits 1.0 (Wilman et al. 2014). P value and Tukey's test are listed in Table 2.3. Diet category legend: hot pink = carnivore, blue = herbivore, yellow = insectivore, teal = generalist, orange = hypercarnivore, green = omnivore, light pink = mesocarnivore.

Orientation Patch Count (OPC) and Relief Index (RI) were negatively correlated with each other (Fig. 2.7; Table 2.4). RLGA, M1BS, RBL, P4Z, and M2S correlate significantly with both OPC and RI (Fig. 2.7; Table 2.4), with RLGA and M1BS to OPC having the highest r^2 values (Table 2.4). Most 2D metrics were correlated with OPC and RI even when accounting for significant phylogenetic autocorrelation (Table 2.4). However, MAT was the only metric that was not significantly correlated with OPC or RI when accounting for significant phylogenetic autocorrelation (Fig. 2.7; Table 2.4). Nearly all of the residuals from the linear regressions show statistically significant phylogenetic signal (λ value) between 75% and 100% ($p < 0.05$), with the exception of the regression of RBL and RI (Table 2.4). Even when accounting for significant phylogenetic autocorrelation, however, nearly all of the 2D metrics are correlated to each other with the exception of OPC to MAT, and P4S to M1BS and P4Z (Table 2.4).

Table 2.4. Ordinary least squares regressions determining the correlation and phylogenetic signal between different 2D and 3D metrics of determining tooth shape. OPC = Orientation Patch Count; RI = Relief Index; all other abbreviations are listed in Table 2.1.

Model	Ordinary least squares regression				Phylogenetic signal		Generalized least squares regression			
	Slope	t value	p value	r^2	λ value	p value	Slope	t value	p value
OPC ~ RI	-0.01 ± 0.004	-3.41	p < 0.001	0.28	0.75	p = 0.02	-0.05 ± 0.01	-8.01	< 0.001
OPC ~ P4S	0.0001 ± 0.0002	0.43	p = 0.67	0.01	1.00	p = 0.01	0.002 ± 0.0003	4.99	p < 0.001
OPC ~ P4Z	-0.0003 ± 4E-05	-5.81	p < 0.001	0.54	0.96	p = 0.11	-0.0003 ± 0.00003	-11.04	p < 0.001
OPC ~ RBL	-0.001 ± 0.0003	-4.31	p < 0.001	0.39	0.94	p < 0.001	-0.004 ± 0.0004	-9.34	p < 0.001
OPC ~ M1BS	-0.0004 ± 5E-05	-7.99	p < 0.001	0.69	0.97	p = 0.03	-0.0005 ± 0.00005	-11.20	p < 0.001
OPC ~ RLGA	0.007 ± 0.0008	8.20	p < 0.001	0.70	1.00	p < 0.001	0.01 ± 0.001	12.16	p < 0.001
OPC ~ M2S	0.0004 ± 6E-05	5.80	p < 0.001	0.54	0.98	p < 0.001	0.0006 ± 0.0001	10.03	p < 0.001
OPC ~ MAT	-0.0003 ± 0.000199	-1.71	p = 0.10	0.09	0.93	p < 0.001	0.0002 ± 0.0002	0.92	p = 0.36
OPC ~ MAM	-0.00002 ± 0.000103	-0.18	p = 0.86	0.00	0.96	p = 0.01	0.0004 ± 0.0001	4.74	p < 0.001
OPC ~ lxP4	-0.00003 ± 3E-05	-0.79	p = 0.44	0.02	1.00	p < 0.001	-0.0002 ± 0.00004	-4.65	p < 0.001
OPC ~ lxM2	-0.00005 ± 3E-05	-1.59	p = 0.12	0.08	0.95	p < 0.001	-0.0002 ± 0.00003	-5.41	p < 0.001
RI ~ OPC	-18.8 ± 5.5	-3.41	p < 0.001	0.28	1.00	p < 0.001	-13.3 ± 1.66	-8.01	p < 0.001
RI ~ P4S	-0.01 ± 0.008	-1.55	p = 0.13	0.08	0.95	p < 0.001	-0.03 ± 0.003	-10.59	p < 0.001
RI ~ P4Z	0.006 ± 0.002	3.38	p < 0.001	0.28	0.91	p < 0.001	0.004004 ± 0.001	7.53	p < 0.001
RI ~ RBL	0.06 ± 0.01	6.03	p < 0.001	0.56	0.31	-	- -	-	-
RI ~ M1BS	0.008 ± 0.003	2.86	p = 0.01	0.22	0.89	p < 0.001	0.1 ± 0.02	6.71	p < 0.001
RI ~ RLGA	-0.2 ± 0.04	-4.70	p < 0.001	0.43	0.87	p < 0.001	-3.09 ± 0.10	-29.98	p < 0.001
RI ~ M2S	-0.01 ± 0.002	-4.94	p < 0.001	0.46	0.90	p = 0.01	-0.2 ± 0.01	-20.43	p < 0.001
RI ~ MAT	-0.005 ± 0.007	-0.70	p = 0.49	0.02	0.90	p = 0.01	-0.1 ± 0.04	-3.02	p = 0.01
RI ~ MAM	-0.003 ± 0.003	-0.82	p = 0.42	0.02	0.90	p = 0.01	-0.1 ± 0.01	-9.48	p < 0.001
RI ~ lxP4	0.001 ± 0.001	10.05	p = 0.30	0.04	0.99	p < 0.001	0.03 ± 0.01	3.53	p < 0.001
RI ~ lxM2	0.002 ± 0.001	1.86	p = 0.07	0.11	0.99	p < 0.001	0.03 ± 0.01	4.50	p < 0.001
P4S ~ P4Z	-0.05 ± 0.02	-2.8	P < 0.006	0.04	0.92	p < 0.001	-0.02 ± 0.02	-0.66	p = 0.51
P4S ~ RBL	-0.6 ± 0.09	-6.2	p < 0.001	0.16	0.99	p < 0.001	-0.86 ± 0.19	-4.61	p < 0.001
P4S ~ M1BS	-0.06 ± 0.02	-2.8	P < 0.006	0.04	0.96	p < 0.001	-0.02 ± 0.04	-0.49	p = 0.63
P4S ~ RLGA	2.3 ± 0.3	8.04	p < 0.001	0.24	0.99	p < 0.001	2.40 ± 0.60	4.01	p < 0.001
P4Z ~ P4S	-0.8 ± 0.3	-2.8	P < 0.006	0.04	0.35	p < 0.001	-0.36 ± 0.55	-0.66	p = 0.51
P4Z ~ RBL	1.7 ± 0.4	4.5	p < 0.001	0.09	0.99	p < 0.001	4.55 ± 0.84	5.39	p < 0.001
P4Z ~ M1BS	1.04 ± 0.06	17.2	p < 0.001	0.59	0.98	p < 0.001	1.12 ± 0.13	8.42	p < 0.001
P4Z ~ RLGA	-9.1 ± 1.2	-7.5	p < 0.001	0.22	0.99	p < 0.001	15.51 ± 2.55	-6.08	p < 0.001
RBL ~ P4S	-0.3 ± 0.05	-6.2	p < 0.001	0.16	0.96	p < 0.001	-0.26 ± 0.06	-4.61	p < 0.001

RBL	**~**	**P4Z**	0.05	±	0.01	4.5	p < 0.001	0.09	0.84	p < 0.001	0.06	±	0.01	5.39	p < 0.001
RBL	**~**	**M1BS**	0.1	±	0.01	8.7	p < 0.001	0.27	0.92	p < 0.001	0.13	±	0.02	8.25	p < 0.001
RBL	**~**	**RLGA**	-3.01	±	0.1	-26.1	p < 0.001	0.77	0.99	p < 0.001	-2.89	±	0.14	-20.30	p < 0.001
M1BS	**~**	**P4S**	-0.6	±	0.2	-2.8	P < 0.006	0.04	0.96	p < 0.001	-0.17	±	0.34	-0.49	p = 0.63
M1BS	**~**	**P4Z**	0.6	±	0.03	17.2	p < 0.001	0.59	0.90	p < 0.001	0.44	±	0.05	8.42	p < 0.001
M1BS	**~**	**RBL**	2.2	±	0.3	8.7	p < 0.001	0.27	0.98	p < 0.001	3.70	±	0.45	8.25	p < 0.001
M1BS	**~**	**RLGA**	-10.7	±	0.7	-15.7	p < 0.001	0.55	0.96	p < 0.001	-14.29	±	1.02	-14.05	p < 0.001
RLGA	**~**	**P4S**	0.1	±	0.01	8.04	p < 0.001	0.24	0.95	p < 0.001	0.07	±	0.02	4.01	p < 0.001
RLGA	**~**	**P4Z**	-0.02	±	0.003	-7.5	p < 0.001	0.22	0.81	p < 0.001	-0.02	±	0.004	-6.08	p < 0.001
RLGA	**~**	**RBL**	-0.3	±	0.01	-26.1	p < 0.001	0.77	0.99	p < 0.001	-0.29	±	0.01	-20.30	p < 0.001
RLGA	**~**	**M1BS**	-0.05	±	0.003	-15.7	p < 0.001	0.55	0.83	p < 0.001	-0.05	±	0.004	-14.05	p < 0.001

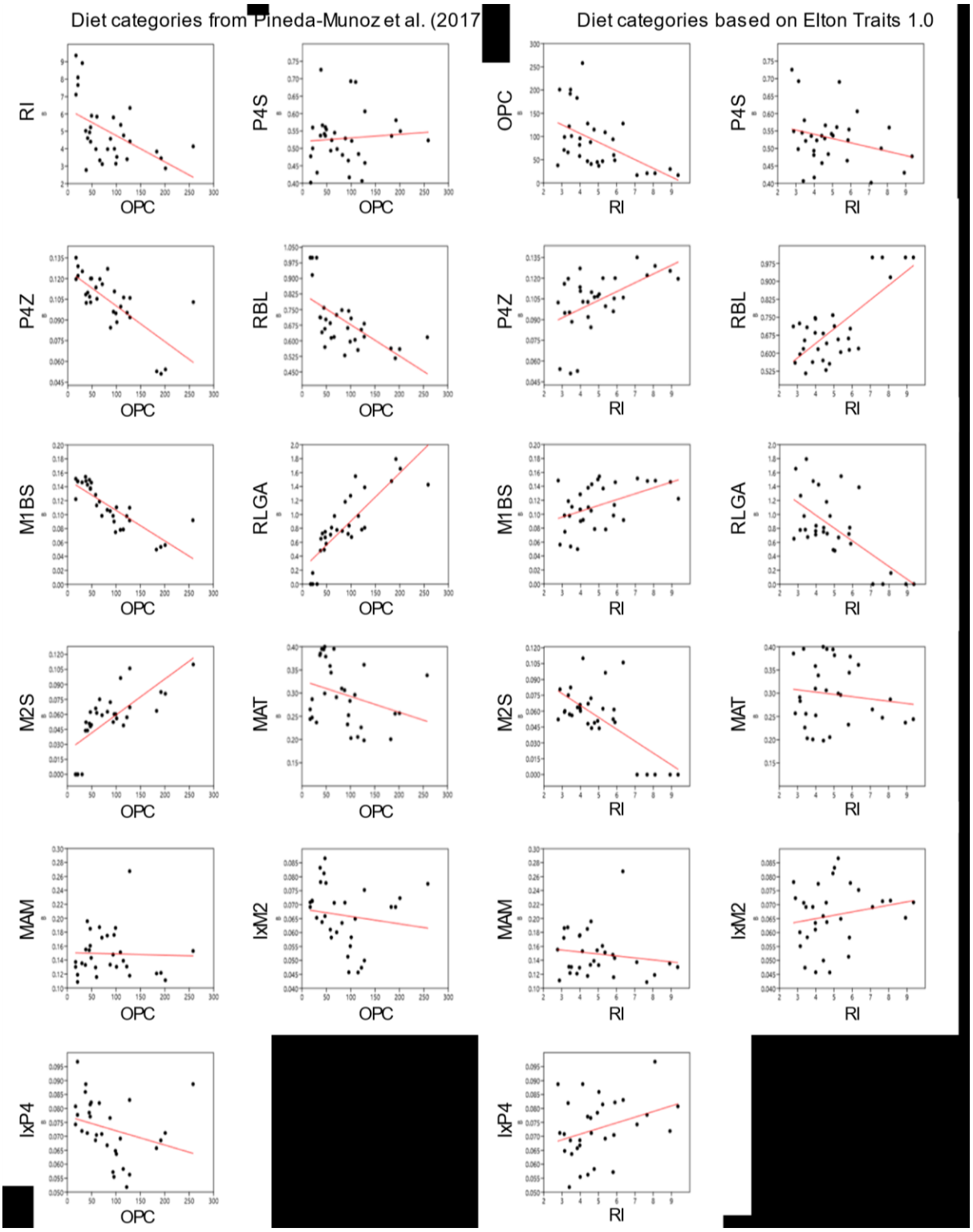

Figure 2.7. Linear regressions of 2D (see Table 2.1 for abbreviation definitions) tooth row metrics against 3D (OPC (Orientation Patch Count) and RI (Relief Index)) metrics. Slope and phylogenetic signal data can be found in Table 2.4.

2.4 Discussion

2D metrics can be obtained directly from specimens as well as from casts or 3D scans with resolutions below the threshold needed to obtain accurate and comparable Orientation Patch Count (OPC) and Relief Index (RI) values. 2D metrics are therefore cheaper and easier to obtain than 3D metrics, which require the purchase of costly equipment or the considerable expense of utilizing equipment in cost-recovery labs. The goal of the present study was therefore to determine whether 2D metrics could be used to infer diets among carnivoran mammals and to compare their performance to the commonly employed 3D metrics of OPC and RI.

The results of the linear discriminant analyses indicate that 2D jaw and tooth metrics correctly classify carnivoran species by diet at a higher rate than OPC and RI (Table 2.2). When combined, 2D and 3D metrics correctly classify species by diet at a slightly higher rate than the 2D metrics alone (Table 2.2), however, by only by a small margin (3.23%). The highest correct classifications occurred with the smallest sample size (31), which reflects the inclusion of more species with similar tooth morphologies but different diets in the analyses with higher sample sizes (Figs. 2.4, 2.5). 3D metrics alone show the lowest correct classification (Table 2.2), likely because OPC and RI were developed to work on a wider range of mammalian taxonomic groups than Carnivora (Pineda-Munoz et al. 2017). The 2D metrics, in contrast, were developed to differentiate among diets within the Carnivora alone and, therefore, provide better clade-specific resolution (Van Valkenburgh and Koepfli 1993; Friscia et al. 2007; Slater and Friscia 2019).

I found that OPC differs only between herbivores and carnivores plus hypercarnivores, while RI does not differ among species with different diets (Table 2.3). OPC is a quantification of tooth row curvature and thus complexity. Therefore, it is unsurprising that OPC easily differentiates herbivores and carnivores, which occupy the extremes of tooth shape spectrum (Fig 2.1; Pineda-Munoz et al. 2017). Herbivory requires extreme modification and specialization of the carnivoran tooth row. Herbivores possess relatively complex teeth with a high surface area and curvature that enables them to break down resistant vegetation through emphasis on grinding (Ungar 2010). In contrast, carnivorous species possess teeth with a simpler, blade-like shape, effectively concentrating pressure on the blade edge enabling slicing through meat (Van Valkenburgh 2007; Ungar 2010).

RI may be a poor predictor of diet relative to OPC due to differences in the number of teeth among taxa with similar diets. Low values of RI tend to correlate with increased grinding area, thus tending to be higher in herbivores (Fig. 2.6), but also correlate with greater numbers of teeth, thus tending to be higher among specific non-herbivorous taxa (Fig. 2.2). Feliforms, including all extant felids (e.g. *Panthera leo* (African lion)) and hyaenids (e.g. *Crocuta crocuta* (spotted hyena)), have lost their post-carnassial molars, whereas all caniforms (e.g. extant bears, dogs, mustelids) have retained them (Martin 1998). As such, feliforms uniformly possess higher values of RI than caniforms (Fig. 2.2). I therefore propose that employing RI to isolated carnassial teeth rather than complete tooth rows may be more informative of diet. This would allow us to measure diet as determined from the carnassial as opposed to quantifying the total number of teeth in the tooth row, which have little to do with diet and more to do with phylogeny. Pineda-Munoz et al. (2013) showed that diet can be effectively predicted using the

OPC of the lower m1 (lower carnassial), if whole tooth rows are not available (the likely case in paleontology), given that the carnassial performs the majority of the chewing function in carnivorans (Mellett 1981; Greaves 1983; Van Valkenburgh 2007; Ungar 2010).

Several of the 2D dental metrics (P4S, P4Z, RBL, M1BS, RLGA, M2S) differed significantly among species with different diets, especially among carnivores, herbivores, and generalists (using the Pineda-Munoz (2017) diet categories) and among hypercarnivores, mesocarnivores, omnivores, and herbivores (dietary categories based on Elton Traits 1.0) (Table 2.3). P4S and P4Z are both quantifications of the shape and size of the lower fourth premolar (full description in Table 2.1). Though the p4 is not as vital for processing food as the m1 (the carnassial), it performs some action during mastication and has clearly been modified (Ungar 2010), whether by adaptation or developmental and functional linkage along the tooth row (Laffont et al. 2009; Smits and Evans 2012; Halliday and Goswami 2013), to suit the dietary needs of carnivoran species.

RBL, M1BS, RLGA, and M2S all relate to the length and total area of the trigonid and talonid of lower molars, those that perform cutting and grinding actions during chewing, respectively (full description in Table 2.1). For carnivorans, grinding area (measured by RLGA) varies widely among species with different diets (Fig. 2.6). For example, members of the family Felidae are all hypercarnivorous and possess no grinding area on their lower molars nor post-carnassial grinding teeth (Martin 1998; Van Valkenburgh 2007; Ungar 2010). In contrast, members of the family Ursidae, whether omnivorous (e.g. black bears) or hypercarnivorous (e.g. polar bears), retain the grinding area on their talonid as well as post-carnassial molars (Sacco and Van Valkenburgh 2004). Within ursids and other caniforms, the dimensions of the

molars still correlate with diet; they are greatly reduced in hypercarnivores and enlarged in herbivores and omnivores (Sacco and Van Valkenburgh 2004). Thus, there are dietary and phylogenetic signals that make these metrics comparatively good dietary indicators.

Linear jaw metrics (MAT, MAM, IxP4, and IxM2) were not significantly different among carnivoran species with different diets (Table 2.3). These jaw metrics correspond to depth and shape of the mandible, which are important variables for determining bite force and jaw rigidity (Van Valkenburgh and Koepfli 1993). MAT and MAM approximate the mechanical advantage of the temporalis and masseter muscles, respectively. The temporalis muscle, which translates the jaw vertically, is important in jaw closing and immobilizing prey (Herring 1993). The masseter muscle, which translates the jaw horizontally, is vital to the chewing functionality required by herbivores to break down vegetation (Herring 1993). IxP4 and IxM2 are taken at the base of the p4 and m1, respectively, and are estimates of the resistance of the lower jaw to bending (Van Valkenburgh and Koepfli 1993). Low bite force and rigidity corresponds to animals that must rapidly catch prey but do not need to employ a lot of force to kill (Meachen and Van Valkenburgh 2009). High bite force, however, may correspond to either hypercarnivory or herbivory because it is needed both to hold on to and kill struggling large prey, but also to process tough vegetation (Sacco and Van Valkenburgh 2004; Van Valkenburgh 2007; Meachen and Van Valkenburgh 2009). Bite force alone is therefore a poor indicator of diet, as it is defined in the present study, but within the context of other dietary indicators, may be highly informative for inferring variables such as prey size preference (Meachen and Van Valkenburgh 2009).

To explore collinearities among the various available 2D and 3D metrics, I employed both ordinary least squares (OLS) and phylogenetic generalized least squares (GLS) regressions. OPC and RI are not highly correlated to each other ($r^2 = 0.28$; Table 2.4), meaning there is little redundancy when the methods are combined. Redundancy in this case would be variables that are so closely correlated that there would be no significant benefit to including them both. The carnivorous or hypercarnivorous wolverine (*Gulo gulo*) possesses the lowest RI, yet one of the lowest OPC values (Tables 2.1, 2.2), possibly due to their wide and robust teeth (Evans et al. 2005). Conversely, the herbivorous red panda (*Ailurus fulgens*) possesses a relatively high RI as well as a high OPC, possibly due to the relatively high tooth cusps that assist it in biting and slicing leaves (Mellett 1981; Greaves 1983). Combining RI and OPC has also been demonstrated to improve the degree to which species with different diets can be differentiated; each variable provides the power to differentiate between dietary categories that could not be differentiated using a univariate approach (Pineda-Munoz et al. 2017). For example, in Pineda-Munoz et al. (2017) the authors found that the standard deviation of OPC for teeth in a row discriminates between gummivores and frugivores, while other variables are better at discriminating between carnivores and gummivores, and between herbivores and insectivores.

Nearly all of the linear measurements are correlated with each other and OPC and RI, with the exception of OPC with MAT, and P4S with M1BS, and P4S and P4Z (Fig 2.7; Table 2.7). MAT measures the mechanical advantage of the temporalis muscle, one of the two primary jaw closing muscles among mammals. It originates on the temporal bone of the skull and inserts on the coronoid process of the dentary (Van Valkenburgh and Koepfli 1993). Though we would expect a correlation between OPC and MAT if both differed between herbivores and carnivores,

MAT does not vary significantly among species with different diets (Fig. 2.6) and is highly variable within the carnivoran clade (Fig. 2.7), explaining the lack of correlation with OPC. High dental complexity (high OPC values) is associated with greater grinding functionality also for breaking down fibrous plant material (Evans et al. 2007; Pineda-Munoz et al. 2017). Thus, the positive correlation of MAM with OPC but not MAT appears to reflect the mechanical requirements of herbivory. MAT is, however, potentially correlated with other dietary variables including prey size that are not considered here (Meachen and Van Valkenburgh 2009). P4S is a measurement of the robustness of the p4, while M1BS and P4Z are the lengths of the m1 and p4, respectively, in proportion to the dentary length (Table 2.1). Though the robustness of the p4 is related to the size of the m1 and p4, it is not correlated with their size in respect to total dentary length.

RI is most highly correlated with m1 blade length, indicating that there is a correlation between the steepness of the teeth in the tooth row and the length of the carnassial tooth (Table 2.3). High relative carnassial blade length is an adaptation to a more carnivorous diet (Van Valkenburgh 2007; Ungar 2010). Enhanced blade length allows the tooth to be taller, while maintaining sufficient mechanical support by the tooth base (Van Valkenburgh 2007; Ungar 2010). Though much of the cutting action occurs at the carnassial, the premolars are also involved. Therefore, they also become steeper and sharper, increasing the total surface available for cutting meat (Van Valkenburgh 2007; Ungar 2010), leading to increased tooth row RI. Whether the shape of the premolars represents an adaptation or some degree of modularity, functional or developmental, is presently unknown for carnivorans (Laffont et al. 2009; Halliday and Goswami 2013).

The remaining 2D metrics are correlated with each other to varying degrees (Table 2.4). P4S, P4Z, RBL, M1BS, RLGA, and M2S are all quantifications of tooth size and shape, which explains their correlation with the 3D tooth shape metrics. For example, a longer relative blade length correlates negatively with OPC, because the larger the blade length, the less grinding functionality and therefore complexity of the tooth (Van Valkenburgh and Koepfli 1993). Similarly, the part of the tooth with the highest relief (RI) is the blade; the higher the blade, the higher the RI, and length of the support base (RBL) (Pineda-Munoz et al. 2017).

2.5 Conclusions

All of the 2D and 3D metrics together attempt to differentiate species on the basis of dietary differences, as inferred from their teeth and lower jaw (Van Valkenburgh and Koepfli 1993; Evans et al. 2007; Friscia et al. 2007; Pineda-Munoz et al. 2017; Slater and Friscia 2019). My analyses have shown that 2D metrics are better predictors of diet than 3D metrics, and that combining 2D and 3D metrics may yield marginally higher results. The sample size and selection of included species also influences how well species with different diets can be separated. Though higher sample sizes in this study correspond with lower percent correct classification, they are likely more accurate in terms of determining the true efficacy of the methods. The metrics I analyzed possess different levels of power to differentiate carnivoran species based on diet and were correlated with each other to varying degrees, but combining metrics appears effective, as it provides higher resolution when it comes to separating species with specialist diets.

Chapter 3: Testing the competition hypothesis: How niche overlap between carnivoramorphans and creodonts changed from the start to the end of the Eocene

3.1 Introduction

Carnivoramorpha and "Creodonta" are two closely related groups of ancestrally carnivorous mammals that emerged in North America during the Paleocene (Flynn 1998; Gunnell 1998; Goswami 2010). Carnivoramorpha consists of the crown group Carnivora, and the extinct families Miacidae and Viverravidae (Fig 3.1; Goswami 2010). Creodonts were likely polyphyletic and were comprised of the extinct groups Oxyaenida and Hyaenodontida (Fig. 3.1; Gunnell 1998). During the Eocene (56–33.9 Ma), creodont diversity declined significantly, and they eventually went extinct in North America during the Oligocene and worldwide during the Miocene (Fig. 3.2; Gunnell 1998). Carnivoramorphans, in contrast, diversified greatly in both ecology and number of species during the Eocene and are still alive today (Fig. 3.2; Goswami 2010).

Figure 3.1. Compilation phylogeny of carnivorous mammals based on Janis et al. (1998) and Goswami (2010).

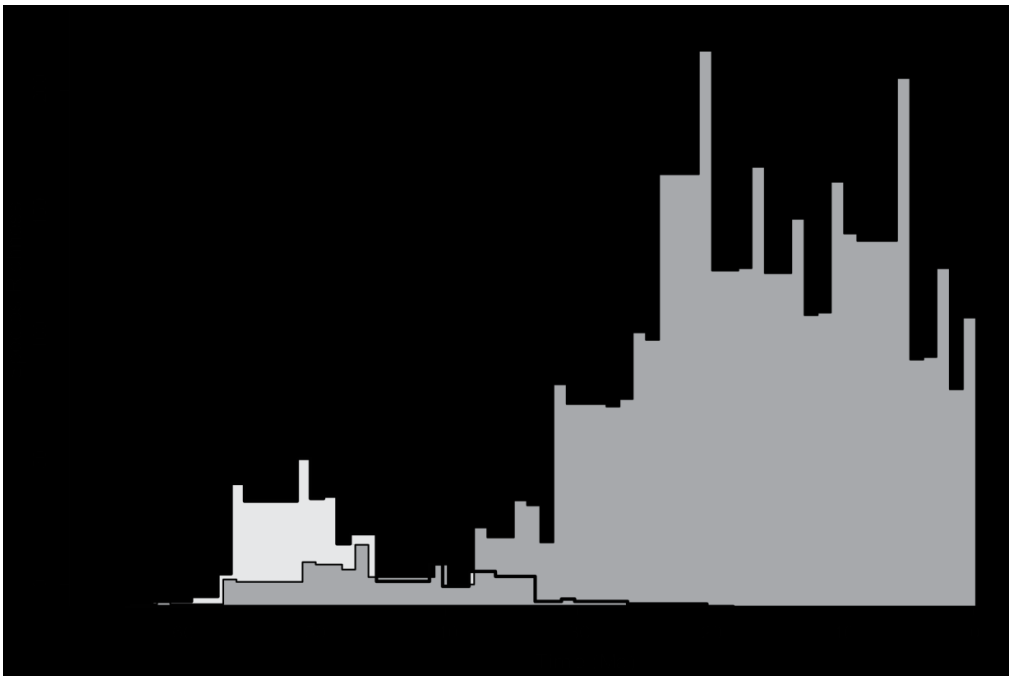

Figure 3.2. Creodont species richness declined while carnivoran richness increased during the late Eocene. Time is millions of years ago (Ma). Vertical dashed line indicates the age of the Calf Creek Local Fauna. Light gray indicates creodont species richness. Figure altered from Christison et al. (2020). The data were downloaded from the Paleobiology Database in March 2018, using the group name 'Mammalia' and the following parameters: time intervals = Cenozoic, region = North America, paleoenvironment = terrestrial.

The Eocene epoch began with some of the highest global temperatures of the Cenozoic and cooled throughout the 22-million-year period with occasional warm spikes (Fig. 3.3; Zachos et al. 2008). The lush, near-tropical forests that covered North America at the beginning of the Eocene (55.4–50.3 Ma; Wasatchian NALMA) began to disappear during this cooling period, and by the end of the epoch (38–33.9 Ma; Chadronian NALMA) the landscape had given way to mixed woodland and savannah habitats (Prothero 1998a; Wing 1998; Figueirido et al. 2011; Secord et al. 2012). As such, the herbivores that lived in North America changed as well. Though maximum mammalian body size increased during the Eocene, maximum body size decreased shortly after the end of the Epoch (Alroy 1998; Smith et al. 2004). Large browsers like brontotheres (relatives of horses, rhinoceroses, and tapirs) went extinct, as their food sources dwindled (Russell 1973; Strömberg 2004). Herbivorous prey species adapted to the new, more open landscapes, and grazing species became more numerous (Jacobs et al. 1999; Fraser et al. 2015; Lyons et al. 2016). The changes in prey lifestyles likely had a considerable impact on the ways in which carnivorous mammals would have sought food.

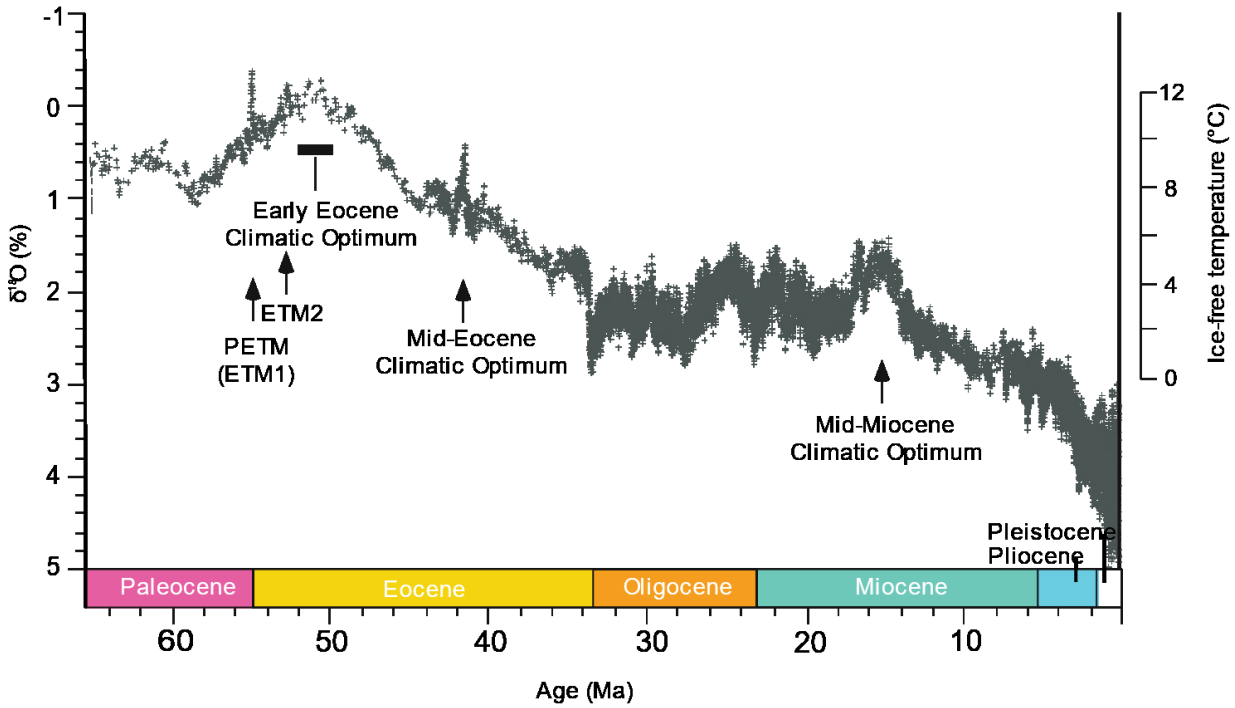

Figure 3.3. Evolution of global climate over the past 65 million years. Figure modified from Zachos et al. (2008).

The "competition hypothesis" poses that carnivoramorphans out-competed creodonts for food resources during the Eocene in North America, leading to their eventual extinction (Polly 1993; Friscia and Van Valkenburgh 2010). Support for the competition hypothesis has been found in the form of morphological similarity of carnivoran and creodont genera in North America (Friscia et al. 2007). However, competition occurs among individuals with consequences that can affect entire species (Liow and Stenseth 2007). Previous studies also do not account for coexistence in specific geographic regions or localities. By comparing all North American taxa that existed during each North American Land Mammal Age (NALMA; a geological timescale based on North American faunal assemblages from the Late Cretaceous to the present), regardless of whether they shared any portion of their geographic range,

carnivorous mammals with dramatically different climate and habitat preferences may have been compared, though they may never have interacted.

To test the competition hypothesis, I explore the niches of creodont and carnivoramorphan species using a combination of dietary and locomotor indicators (Van Valkenburgh and Koepfli 1993; Hemmer 2004; Friscia et al. 2007; Hertler and Volmer 2008; Friscia and Van Valkenburgh 2010; Polly 2010; Volmer et al. 2016; Slater and Friscia 2019). The dietary niches of extinct species can be inferred by examining their tooth and cranial morphology, then making comparisons to extant species whose diets are well-understood (Van Valkenburgh and Koepfli 1993; Meachen and Van Valkenburgh 2009). Teeth, for example, preserve well in the fossil record (Abler 1985), and can provide dietary information, including whether species were consumers primarily of meat or other materials (Holliday and Steppan 2004; Van Valkenburgh 2007). The carnassial teeth are the primary functional teeth among carnivorous mammals because they perform much of the slicing and grinding involved in chewing (Mellett 1981; Greaves 1983; Van Valkenburgh and Koepfli 1993). Carnassial tooth morphology can therefore tell us information such as how much meat animals evolved to eat (Van Valkenburgh and Koepfli 1993). Simple, blade-like carnassial teeth are capable of effectively processing meat using slicing action but are not ideal for grinding tough vegetation. Complexly shaped teeth function like a mortar and pestle but are less efficient at slicing flesh (Greaves 1983; Van Valkenburgh and Koepfli 1993; Evans and Pineda-Munoz 2018). In some species, the post-carnassial molars provide additional grinding action during chewing (Van Valkenburgh and Koepfli 1993; Sacco and Van Valkenburgh 2004). By examining the morphology of the upper and lower carnassial teeth, as well as the post-carnassial molars (if

present), we can infer the likely diets of the fossil mammals that possessed them (Van Valkenburgh and Koepfli 1993; Friscia and Van Valkenburgh 2010).

Locomotor posture and body mass are essential factors in determining the dietary niche and lifestyle of mammals. While two species may consume identical proportions of meat, they may exhibit niche partitioning along the body mass and locomotor axes. For example, of two coexisting species, one may be large-bodied with a plantigrade gait (e.g. *Ursus horribilis*) and the other small-bodied with a digitigrade gait (e.g. *Canis lupus*). Locomotor posture is an important determinant of the ways in which mammals move in their environment and, in the case of carnivorous species, pursue their prey (Polly 2010). Digitigrady is associated with being able to walk or run for long distances, while plantigrady is associated with living in enclosed woodland areas or having an arboreal lifestyle. Protodigitigrady is an unspecialized posture intermediate between digitigrady and plantigrady (Polly 2010). Plantigrade and digitigrade species therefore tend to use different parts of the environment and exploit different types of foods (Polly 2010). Similarly, body mass sets the size of the prey that species are capable of feeding on but also that maximize caloric intake while minimizing hunting effort (the Prey-Focus Mass; PFM) (Van Valkenburgh 2007). For example, extant carnivorans above ~21kg have been documented as having a markedly higher PFM than smaller carnivorans, due to the negative caloric return they would receive when expending energy by hunting smaller prey (Van Valkenburgh 2007). By combining tooth-based estimates of diet with locomotor mode and body mass, I can estimate the main niche axes of extinct carnivorous mammals.

Herein, I test the competition hypothesis by examining niche overlap during the beginning of the Eocene (55.4–50.3 Ma; Wasatchian NALMA) and the end of the epoch (38–

33.9 Ma; Chadronian NALMA) at localities that are relatively near each other geographically (Fig. 3.4). This will allow me to determine the degree of niche overlap that occurred during the early and late Eocene and how carnivoramorphans and creodonts ecologies did or did not change in response. Niche overlap, as estimated by similarity in one or more niche axes, is interpreted as potential for resource competition. Stasis or increases in the degree of niche overlap among creodonts and carnivoramorphans from the early to late Eocene would support the competition hypothesis. Decreases in niche overlap might indicate other factors played more important roles in the ultimate extinction of creodonts in North America.

3.2 Methods

The fossil material used in this study belong to species that have been reported at four localities: Elk Creek, SC-67, Peanut Peak, and Flagstaff Rim IV. Elk Creek and SC-67 are Wasatchian (55.5 – 50.3 MA) in age. Peanut Peak and Flagstaff Rim IV are Chadronian (38 – 33.9 MA). All four of these localities are well-sampled and relatively close geographically (Fig. 3.4; Table 3.1). The fossil localities examined in this study are located on Cession 517, 632, and 700 land, which are the territories of the Crow Tribe of Montana, Cheyenne, Assiniboine, Oohenumpa, and Lakota peoples. The fossil materials used in this study (Appendix B) are housed in the collections of the American Museum of Natural History (AMNH), the Canadian Museum of Nature (CMN), the Royal Ontario Museum (ROM), the Smithsonian Institution (USNM), the University of Michigan Museum of Paleontology (UM), and the Yale Peabody Museum of Natural History (YPM). The majority of the specimens sampled were not collected at the study localities; the material from the sites themselves is often fragmentary and thus

unusable in this study. To account for this, I sampled as many specimens as possible from the species list and took averages of the various measurements to account for slight morphological differences within each species, with a focus on the most complete specimens. A full list of specimens used in this study is in Appendix B.

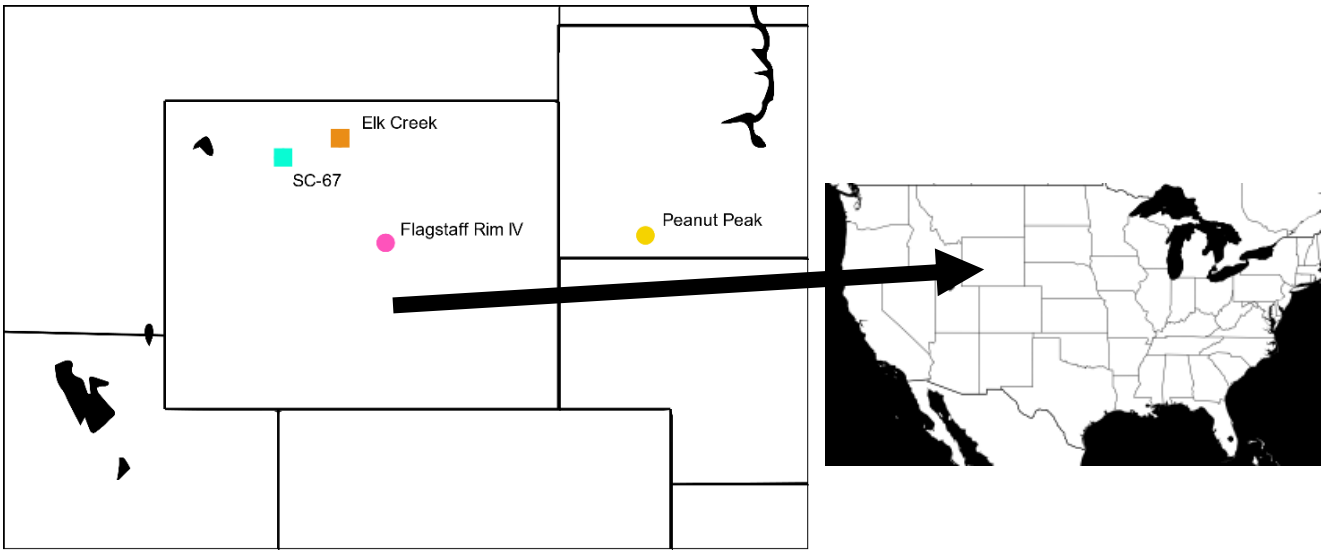

Figure 3.4. Fossil localities used in this study. Early Eocene (Wasatchian) localities are indicated by a square, late Eocene (Chadronian) localities are indicated by a circle. These localities are situated on Cession 517, 632, and 700 land, which include the traditional territories of the Crow Tribe of Montana, Cheyenne, Assiniboine, Oohenumpa, and Lakota peoples (Wyoming and South Dakota, USA). Figures modified from the Paleontological Database.

Table 3.1. Species occurrence at four Eocene fossil localities examined in this study (Clark and Beerbower 1967; Clark and Guensburg 1972; Gingerich 1989; Emry 1992; Gunnell 1998).

Species	**Code for figures**	**Group**	**Family**	**NALMA**	**Locality**
Acarictis ryani	Acr	Creodont	Hyaenodontida	Wasatchian	SC-67
Arfia junnei	Aj	Creodont	Hyaenodontida	Wasatchian	SC-67
Arfia opisthotoma	Ao	Creodont	Hyaenodontida	Wasatchian	Elk Creek
Arfia shoshoniensis	As	Creodont	Hyaenodontida	Wasatchian	Elk Creek
Brachyrhynchocyon dodgei	Bd	Carnivora	Amphicyonidae	Chadronian	Peanut Peak
Brachyrhynchocyon sp.	Bsp.	Carnivora	Amphicyonidae	Chadronian	Flagstaff Rim IV
Daphoenictis sp.	Dasp.	Carnivora	Amphicyonidae	Chadronian	Flagstaff Rim IV
Didelphodus absarokae	Da	Creodont	Hyaenodontida	Wasatchian	Elk Creek
Didymictis leptomylus	Dl	Carnivora	Viverravidae	Wasatchian	Elk Creek
Didymictis protenus	Dp	Carnivora	Viverravidae	Wasatchian	SC-67
Dinictis felina	Finf	Carnivora	Nimravidae	Chadronian	Peanut Peak
Dinictis sp.	Dinsp	Carnivora	Nimravidae	Chadronian	Flagstaff Rim IV
Dipsalidictis platypus	Dip	Creodont	Oxyaenida	Wasatchian	SC-67
Dipsalidictis transiens	Dit	Creodont	Oxyaenida	Wasatchian	SC-67
Gracilocyon winkleri	Gw	Carnivora	Miacidae	Wasatchian	SC-67
Hesperocyon gregarius	Heg	Carnivora	Canidae	Chadronian	Flagstaff Rim IV Peanut Peak
Hoplophoneus mentalis	Hmen	Carnivora	Nimravidae	Chadronian	Flagstaff Rim IV Peanut Peak
Hyaenodon cf. cruentus	Hcrue	Creodont	Hyaenodontida	Chadronian	Peanut Peak
Hyaenodon cf. montanus	Hmo	Creodont	Hyaenodontida	Chadronian	Peanut Peak
Hyaenodon crucians	Hcruc	Creodont	Hyaenodontida	Chadronian	Flagstaff Rim IV
Hyaenodon horridus	Hh	Creodont	Hyaenodontida	Chadronian	Peanut Peak
Hyaenodon megaloides	Hmeg	Creodont	Hyaenodontida	Chadronian	Flagstaff Rim IV

Hyaenodon microdon	Hmi	Creodont	Hyaenodontida	Chadronian	Flagstaff Rim IV
Hyaenodon montanus	Hmo	Creodont	Hyaenodontida	Chadronian	Flagstaff Rim IV
Miacis exiguus	Me	Carnivora	Miacidae	Wasatchian	Elk Creek
Mustelavus priscus	Mup	Carnivora	Mustelidae	Chadronian	Peanut Peak
Oodectes herpestoides	Oh	Carnivora	Miacidae	Wasatchian	Elk Creek
Oxyaena forcipita	Of	Creodont	Oxyaenida	Wasatchian	Elk Creek
Oxyaena gulo	Og	Creodont	Oxyaenida	Wasatchian	Elk Creek
Oxyaena intermedia	Oi	Creodont	Oxyaenida	Wasatchian	Elk Creek
Palaeonicits sp.	Pasp.	Creodont	Oxyaenida	Wasatchian	SC-67
Palaeonictis occidentalis	Pao	Creodont	Oxyaenida	Wasatchian	Elk Creek
Parictis dakotensis	Pad	Carnivora	Ursidae	Chadronian	Peanut Peak
Parictis sp.	Pasp.	Carnivora	Ursidae	Chadronian	Flagstaff Rim IV
Prolimnocyon atavus	Pa	Creodont	Hyaenodontida	Wasatchian	Elk Creek
Prolimnocyon eerius	Pe	Creodont	Hyaenodontida	Wasatchian	SC-67
Prototomus deimos	Pd	Creodont	Hyaenodontida	Wasatchian	SC-67
Tritemnodon sp.	Tsp.	Creodont	Hyaenodontida	Wasatchian	Elk Creek
Uintacyon massetericus	Um	Carnivora	Miacidae	Wasatchian	Elk Creek
Vassacyon promicrodon	Vap	Carnivora	Miacidae	Wasatchian	Elk Creek
Viverravus acutus	Va	Carnivora	Miacidae	Wasatchian	SC-67
Viverravus laytoni	Gl	Carnivora	Viverravidae	Wasatchian	SC-67
Viverravus politus	Vp	Carnivora	Viverravidae	Wasatchian	SC-67
Viverravus sp.	Vsp.	Carnivora	Viverravidae	Wasatchian	Elk Creek

I took dental measurements from each fossil specimen following the methods of Van Valkenburgh and Koepfli (1993), Friscia et al. (2007), and Slater and Friscia (2019). These measurements are described in Table 3.2 and illustrated in Figure 3.5. To obtain these measurements, I used iGaging EZ Cal digital calipers to take three of each measurement, then used the average calculated in excel to the nearest 0.01mm for each species to use in my

analyses. When a specimen was too large for calipers (e.g. the skull length of *Hyaenodon horridus*), I used a standard meter stick, again taking three measurements then using the average. I took as many measurements as possible, depending on the quality and completeness of each specimen. I adjusted the measurements to account for the different positions of the carnassial teeth in creodonts. To do this, I changed each measurement involving the m1 or P4 (the carnassials in carnivorans) to the carnassial teeth (m2/M1 in Oxyaenids, m3/M2 in Hyaenodontids). Similarly, I changed each measurement involving the m2 or M1 to be the "post-carnassial." This allowed measurements to be comparable among taxa. I used averages for each species for all downstream analyses (specimen list in Appendix I), supplemented with published data when possible, to calculate three ratios: relative blade length (RBL), relative lower grinding area (RLGA), and relative upper grinding area (RUGA). By using ratios instead of raw measurements, these dietary metrics can be used independent of body size. These ratios were selected because they reflect the relative sizes of the parts of the teeth that perform the cutting and grinding functions. RBL, RLGA, and RUGA were also selected based on being the most complete data that could be obtained from the focus species. The full descriptions and illustrations for these measurements can be found in Table 3.2 and Figure 3.5, respectively.

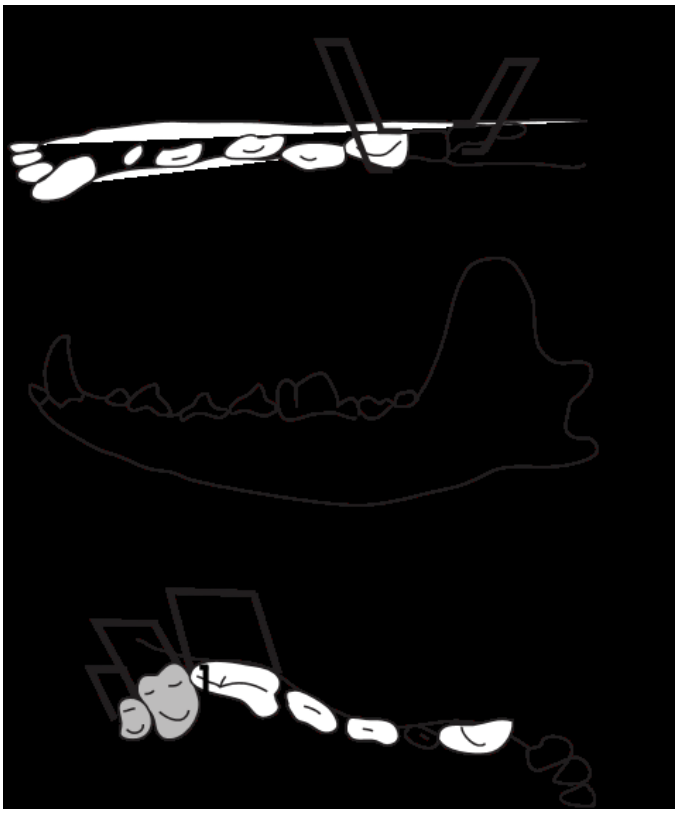

Figure 3.5. Dental measurements used to determine diet. Top: occlusal view of lower jaw, middle: labial view of lower dentition, bottom: occlusal view of upper dentition. Abbreviation descriptions are in Table 3.2. Figure modified from Slater and Friscia (2019).

I created regressions using extant carnivores to determine the percentage of meat consumption of each species (% carnivory), based on the RBL, RLGA, and RUGA of extant carnivorans published in Friscia et al. (2007), and Slater and Friscia (2019) and percent vertebrate meat consumption as published in Elton Traits 1.0 (Wilman et al. 2014). When no grinding area was present on the talonid of the lower carnassial, RLGA was listed as zero, and when no molars were present after the carnassial on the upper tooth row RUGA was also listed as zero.

Table 3.2. Jaw and dental measurements used to determine diet in Van Valkenburgh and Koepfli (1993), Friscia et al. (2007), Slater and Friscia (2019). Referenced measurements appear in bold and are illustrated in Figure 3.5. Note that these measurements are specifically designed for carnivoramorphan dentition, and thus treat "m1" as a stand-in for "lower carnassial," "m2" as "lower post-carnassial molar" etc. Descriptions modified from Slater and Friscia (2019).

Acronym	Measurement description	How it was obtained
bL	Length of the lower carnassial trigonid	See Fig. 3.5
mtr	Length of the lower carnassial talonid	See Fig. 3.5
m1L	Anteroposterior length of the lower carnassial tooth	See Fig. 3.5
m1W	Width of the lower carnassial tooth	See Fig. 3.5
m2L	Length of the lower post-carnassial tooth	See Fig. 3.5
m2W	Width of the lower post-carnassial tooth	See Fig. 3.5
P4L	Anteroposterior length of the upper carnassial tooth	See Fig. 3.5
M1L	Length of the first upper post-carnassial tooth	See Fig. 3.5
M1W	Width of the first upper post-carnassial tooth	See Fig. 3.5
M2L	Length of the second upper post-carnassial tooth	See Fig. 3.5
M2W	Width of the second upper post-carnassial tooth	See Fig. 3.5
RBL	Relative blade length of lower first molar: measured as the ratio of trigonid length **(bL)** to total anteroposterior length of m1 **(m1L)**	bl / m1L
RLGA	Relative lower grinding area: measured as the square root of the summed areas of the lower carnassial talonid and post-carnassial molar (if present) divided by the length of the m1 trigonid **(bl)**. Area was estimated as the product of maximum width **(m1W; m2W)** and length of the talonid of m1 **(mtr)** and m2 **(m2L)**, respectively	(√((mtr*m1W) + (m2L*m2W))) / BL
RUGA	Relative upper grinding area: measured as the square root of the summed areas of the post-carnassial molars (if present) divided by the anteroposterior length of P4 (or upper carnassial). Area was estimated by the product of width and length of M1 and M2, respectively	(√((M1L*M1W) + (M2L*M2W))) / P4L

I estimated the body mass for each specimen by using the average of several different methods, depending on the availability of mass estimates from the literature and the completeness of each specimen. This was to ensure that the body masses were comparable to each other by accounting for the use of different methods. When possible I included the body mass estimates by Alroy et al. (2000) in the average. The first method I used was a regression calculation developed by Van Valkenburgh (1990) using the lower carnassial length. The equation is as follows:

$$\log 10\,(body\ mass) = 2.97\,(carnassial\ length) - 2.27$$

The second method we used was a regression based on skull length developed by Van Valkenburgh (1990). The equation is as follows:

$$\log 10\,(body\ mass) = 3.13\,(skull\ length) - 5.$$

To determine the Prey-Focus Mass (PFM) for each species, I created a regression of PFM to body mass using the datasets of Tucker et al. (2016) and De Cuyper et al. (2019). I chose these datasets because of the range of extant carnivoran body masses with their associated PFMs included. I plotted the predator masses and PFMs from these datasets in Excel to determine the regression equation (Figure 3.6). The equation is as follows:

$$log_{10}PFM = 1.7008\,(log_{10}body\ mass) - 1.7511$$

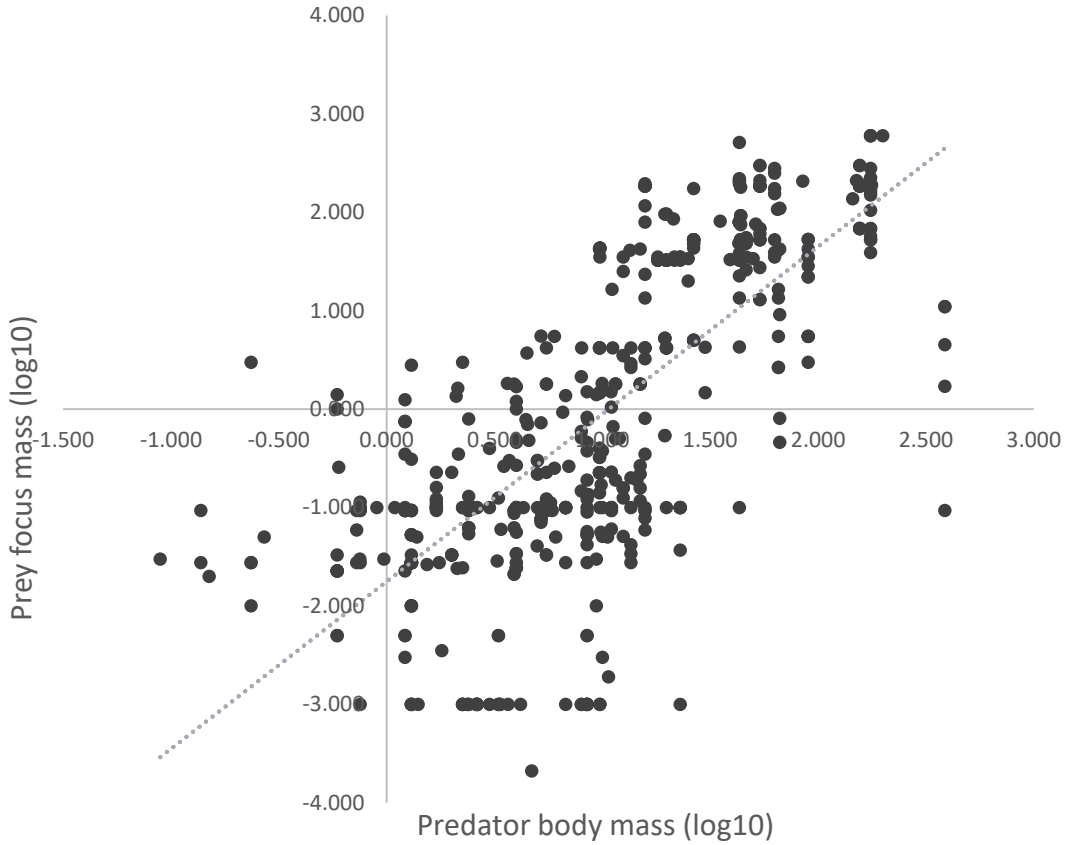

Figure 3.6. Body mass of extant carnivorans and the average body masses of their preferred prey. Data from combined datasets by Tucker et al. (2016) and De Cuyper et al. (2019).

PFMs for each species were then grouped into size categories following the methods of Hemmer (2004), Hertler and Volmer (2008), and Volmer et al. (2016), with the assumption being that the PFM of a carnivorous species, combined with their foraging strategy (e.g. group hunting, scavenging) will determine which prey-mass category the species will focus on. The prey mass categories are: <0.1, 0.2–0.5, 0.5–1, 0.5–1, 1–2, 2–5, 5–10, 10–20, 20–50, 50–100, 100–200, 200–500, 500–1000, and 1000–2000 kg, as used in Hemmer (2004). The only difference in the diet categories being that I added two new prey-mass bin categories (<0.1 and 0.2–0.5) to account for the relatively small body masses of the early Eocene species. Similarity in feeding habit was interpreted as potential for resource competition (Volmer et al. 2016).

The locomotory postures from a dataset by Lovegrove and Mowoe (2013). If a species from one of the study localities was not listed in the Lovegrove and Mowoe (2013) dataset, but other members of the genus were and all possessed the same posture, I used that posture for the species in question. For example, all 5 members of the genus *Hyaenodon* in the Lovegrove and Mowoe (2013) dataset are listed as protodigitigrade, so for the purposes of this study *H. cruentus* and *H. megaloides* were classified as protodigitigrade as well. As well, when no posture was known for a genus (e.g. *Didelphodus*), I inferred the posture based on the most common posture assigned to members their taxonomic group (Hyaenodontida).

Using percent carnivory, log body mass, and posture, I created 3D graphs for each locality to compare the niches of each species. This was done using the plot3D package in R (Soetaert 2019; Team 2020). I inferred niche overlap as clustering of species along the three axes and determined changes in niche overlap by comparing plots from Wasatchian to those of the Chadronian. Support for the competition hypothesis was interpreted as increasing niche overlap at the end of the Eocene, while support for the overspecialization hypothesis was interpreted as creodont specialization along with decreased niche overlap between the two periods.

3.4 Results

RBL, RLGA, and RUGA (see Table 3.2 for descriptions) were each correlated with the percentage of vertebrate flesh (% carnivory) in the diet of extant carnivorans (Figs. 3.7–3.9; Table 3.2), with RLGA and RUGA having a higher correlation than RBL. RLGA and RLGA (Figs. 8, 9, respectively) were negatively correlated with % carnivory, and RBL (Fig. 3.7) was positively

correlated with % carnivory. At the early Eocene (Wasatchian) localities, carnivoramorphans ranged in carnivory from 45–91%, hyaenodontids ranged from 38–100%, and oxyaenids ranged from 62–91%. At the late Eocene (Chadronian) localities carnivoramorphans ranged in carnivory from 60–100%, and hyaenodontids ranged from 94–100%.

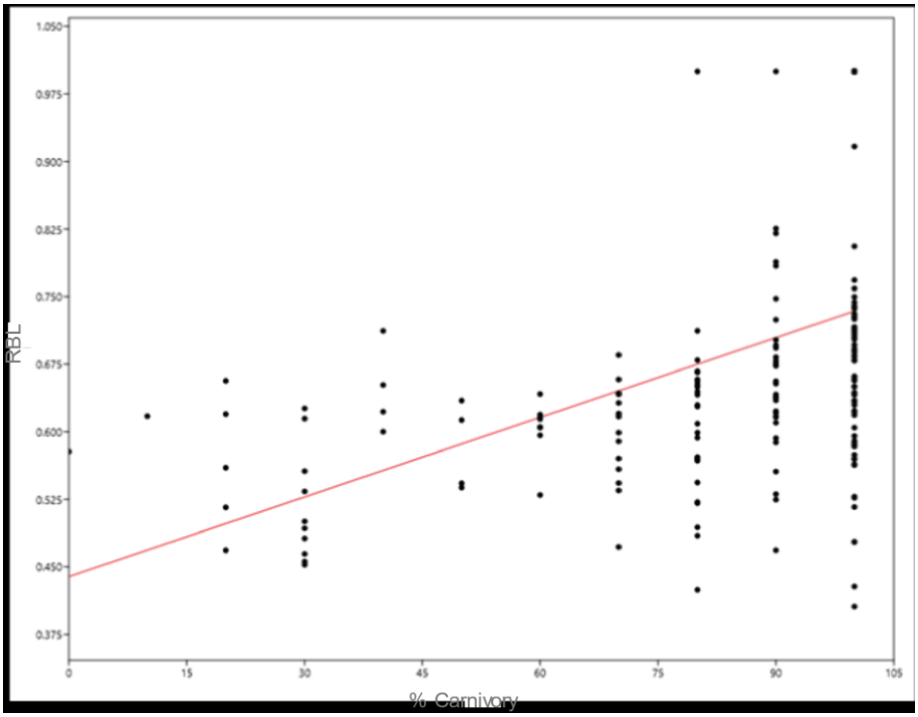

Figure 3.7. Relative blade length (RBL; see Table 3.2 for full description) and percent carnivory based on extant dental measurements from Friscia et al. (2007), and Slater and Friscia (2019) and percent carnivory as published in Elton Traits 1.0 (Wilman et al. 2014).

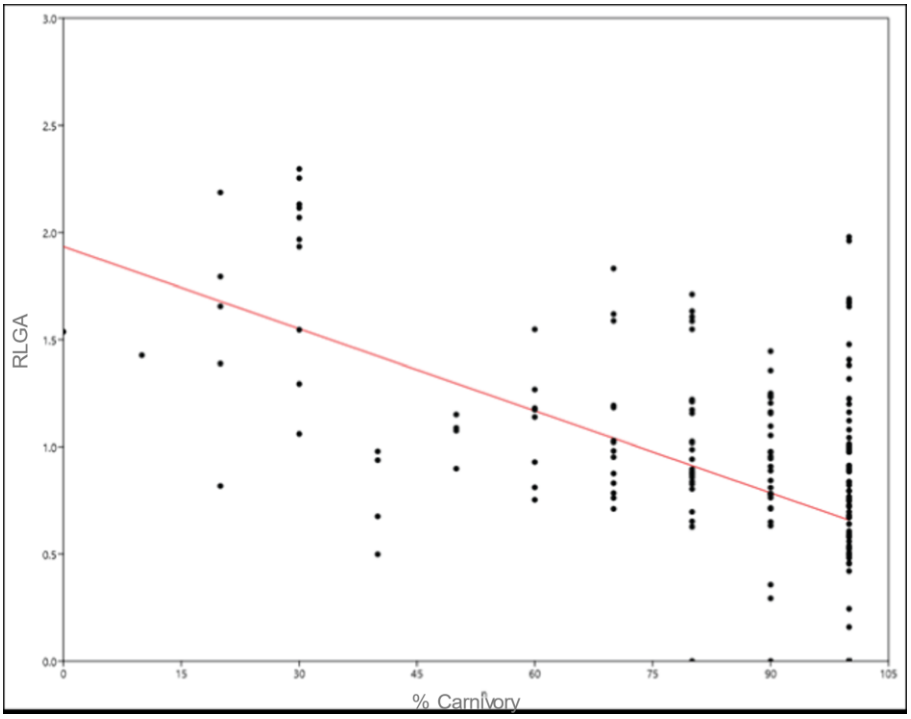

Figure 3.8. Relative lower grinding area (RLGA; see Table 3.2 for full description) and percent carnivory based on extant dental measurements from Friscia et al. (2007), and Slater and Friscia (2019) and percent carnivory as published in Elton Traits 1.0 (Wilman et al. 2014).

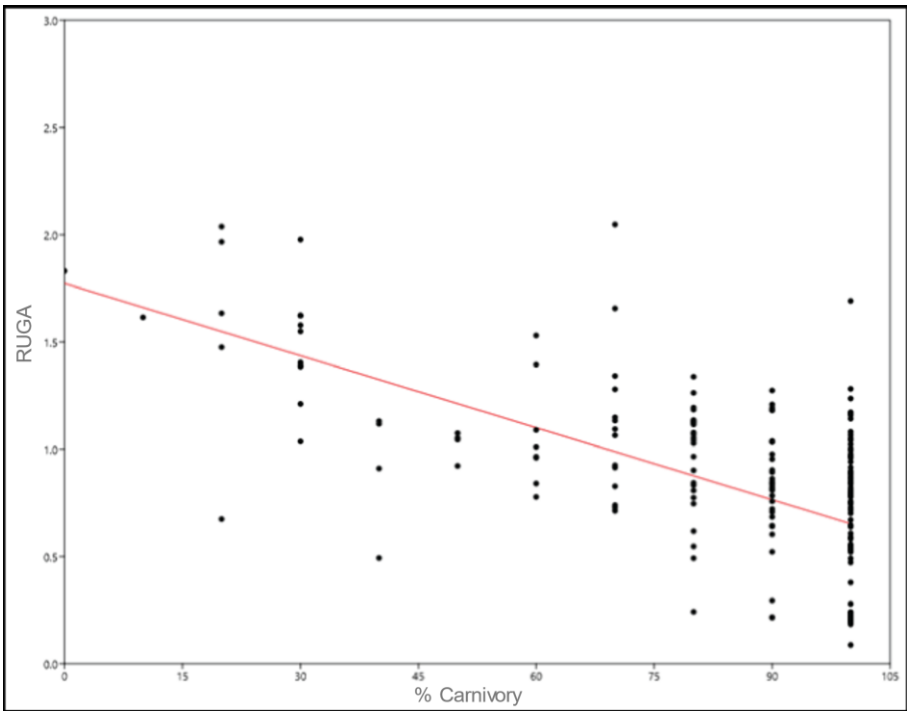

Figure 3.9. Relative lower grinding area (RUGA; see Table 3.2 for full description) and percent carnivory based on extant dental measurements from Friscia et al. (2007), and Slater and Friscia (2019) and percent carnivory as published in Elton Traits 1.0 (Wilman et al. 2014).

Table 3.3. Regression statistics based on extant dental measurements from Friscia et al. (2007), and Slater and Friscia (2019) and percent carnivory as published in Elton Traits 1.0 (Wilman et al. 2014).

Variable	Slope	Error	Intercept	Error	r	p
RBL	0.0029473	0.00043484	0.43916	0.03781	0.43046	1.3095E-10
RLGA	-0.012768	0.0013877	1.9341	0.12066	-0.54345	4.5153E-17
RUGA	-0.011212	0.00099277	1.7729	0.086324	-0.62211	3.043E-23

The PFM diagrams show that at the early Eocene localities, all species focused on prey that is relatively small (<5kg; Figs. 3.10, 3.11). Carnivoramorphans mainly focused on prey between 0.2–0.5 kg (or 0.5–1 kg, if we assume group hunting or scavenging behaviours), with some species focusing on smaller prey. This range overlaps entirely with that of the hyaenodontids at Elk Creek, which mainly focused on prey that was 1kg or smaller, with the potential exception of *Tritemnodon* sp. if we assume group hunting or scavenging behaviours (Fig. 3.10). At SC-67 the hyaenodontid species focused mainly on prey that was smaller than that of the carnivoramorphans, except for *Arfia junnei*, which focused on prey between 0.2–0.5 kg or 0.5–1 kg (Fig. 3.11). At both localities, oxyaenids overlap in prey-mass preference with the larger carnivoramorphans and hyaenodontids, mainly focusing on prey between 1–2 or 2–5 kg, which are the two largest prey-focus masses at either locality. If we assume that the largest oxyaenids (*Palaeonictis occidentalis, P.* sp., *Oxyaena intermedia*, and *O. forcipita*) participated in group hunting or scavenging behaviours (and thus focused on prey between 2–5 kg), then we can safely say that there was no PFM overlap between the oxyaenids and carnivoramorphans or hyaenodontids at SC-67 or Elk Creek.

Figure 3.10. Prey-focus mass (PFM) categories of carnivorous mammals at the Elk Creek locality (Wasatchian NALMA). Thick black bars represent the calculated PFM. Silhouettes represent concurrent potential prey species. All species codes can be found in Table 3.1.

Figure 3.11. Prey-focus mass (PFM) categories of carnivorous mammals at the SC-67 locality (Wasatchian NALMA). Thick black bars represent the calculated PFM. Silhouettes represent concurrent potential prey species. All species codes can be found in Table 3.1

At the late Eocene localities, viverravids, miacids, and oxyaenids had gone extinct, leaving only carnivorans and species of the genus *Hyaenodon*. Carnivorans generally focused on PFM categories between >0.1–10 kg, with the majority of species focusing on prey in the 2–5 kg or 5–10 kg range depending on if they participated in scavenging or group hunting behaviours or not (Figs. 3.12, 3.13). Both localities had *Hyaenodon* species that overlapped with the mid-high carnivoran PFMs (*H. microdon, H. crucians,* and *H. montanus* at Flagstaff Rim IV and *H. montanus* at Peanut Peak), and both had species that focused on prey much larger than those of any other species. At Peanut Peak, *H. cruentus* had a PFM of the 10–20 kg or 20–50 kg and *H.*

horridus had a PFM of 50–100 kg or 100–200 kg. At Flagstaff Rim IV, *H. megaloides* focused on prey in the 200–500 kg or 500–1000 kg range. These large *Hyeanodon* species had PFMs much larger than any of the carnivorans and did not overlap with any other species.

Figure 3.12. Prey-focus mass (PFM) categories of carnivorous mammals at the Flagstaff Rim IV locality (Chadronian NALMA). Thick black bars represent the calculated PFM. Silhouettes represent concurrent potential prey species. All species codes can be found in Table 3.1.

Figure 3.13. Prey-focus mass (PFM) categories of carnivorous mammals at the Peanut Peak locality (Chadronian NALMA). Thick black bars represent the calculated PFM. Silhouettes represent concurrent potential prey species. All species codes can be found in Table 3.1.

During the early Eocene, carnivore guilds showed a high degree of overlap between carnivoramorphans and creodonts (Fig. 3.14). At the Elk Creek locality, all four oxyaenids had similar body mass to each other and to some carnivoramorphans, though *Oxyaena gulo* was more carnivorous (higher % vertebrate meat in their diet) than the others (Fig. 3.14a). There were only two species of hyaenodontid, both relatively small in body mass and high in carnivory. All creodonts and most of the carnivoramorphans had a protodigitigrade posture, except for the digitigrade carnivoramorphan *Didymictis leptomylus*. The carnivoramorphans at Elk Creek were highly varied in body mass and carnivory; some overlapped with creodont species on all three axes while some exhibited no overlap (Fig. 3.14a). The SC-67 locality had only two oxyaenids, *Dipsalydictis transiens* and *D. platypus*, which both possessed similar body masses but different levels of carnivory (Fig. 3.14b). The six species of hyaenodontid at SC-67

were highly variable in carnivory levels, ranging from 47–83%, possessing body masses like the two *Dipsalidictis* species or lower (Fig. 3.14b). The four species of carnivoramorphan at SC-67 were highly similar to each other in all 3 axes, overlapping slightly with the creodonts *D. transiens* and *Prototomus deimos*, however all creodonts at SC-67 were protodigitigrade and all carnivoramorphans were digitigrade (Fig. 3.14b).

Elk Creek and SC-67 are both Wasatchian localities that are relatively close together geographically, so for the purposes of determining niche overlap it is useful to investigate the combined localities (Fig. 3.14c). In the combined Wasatchian figure (Fig. 3.14c), overlap between creodonts and carnivoramorphans is more apparent; particularly between creodonts and the smaller-bodied carnivoramorphans. The largest carnivoramorphans were all digitigrade, so even though they overlapped with oxyaenids in terms of body mass and carnivory they did not necessarily overlap in their niches. The two most carnivorous oxyaenids are only slightly larger than a carnivoramorphan and a hyaenodontid (*Miacis exiguus* and *Didelphodus absarokae*, respectively) with protodigitigrade postures and similar carnivory levels, which likely would have led to niche overlap. Hyaenodontids in the Wasatchian localities were all protodigitigrade and were highly variable in terms of carnivory levels (Fig. 3.14c). The smaller-bodied carnivoramorphans all overlapped with creodonts on all three axes, with the exception of *Oodectes herpestoides*, which was much smaller than any other species with similar carnivory levels to it.

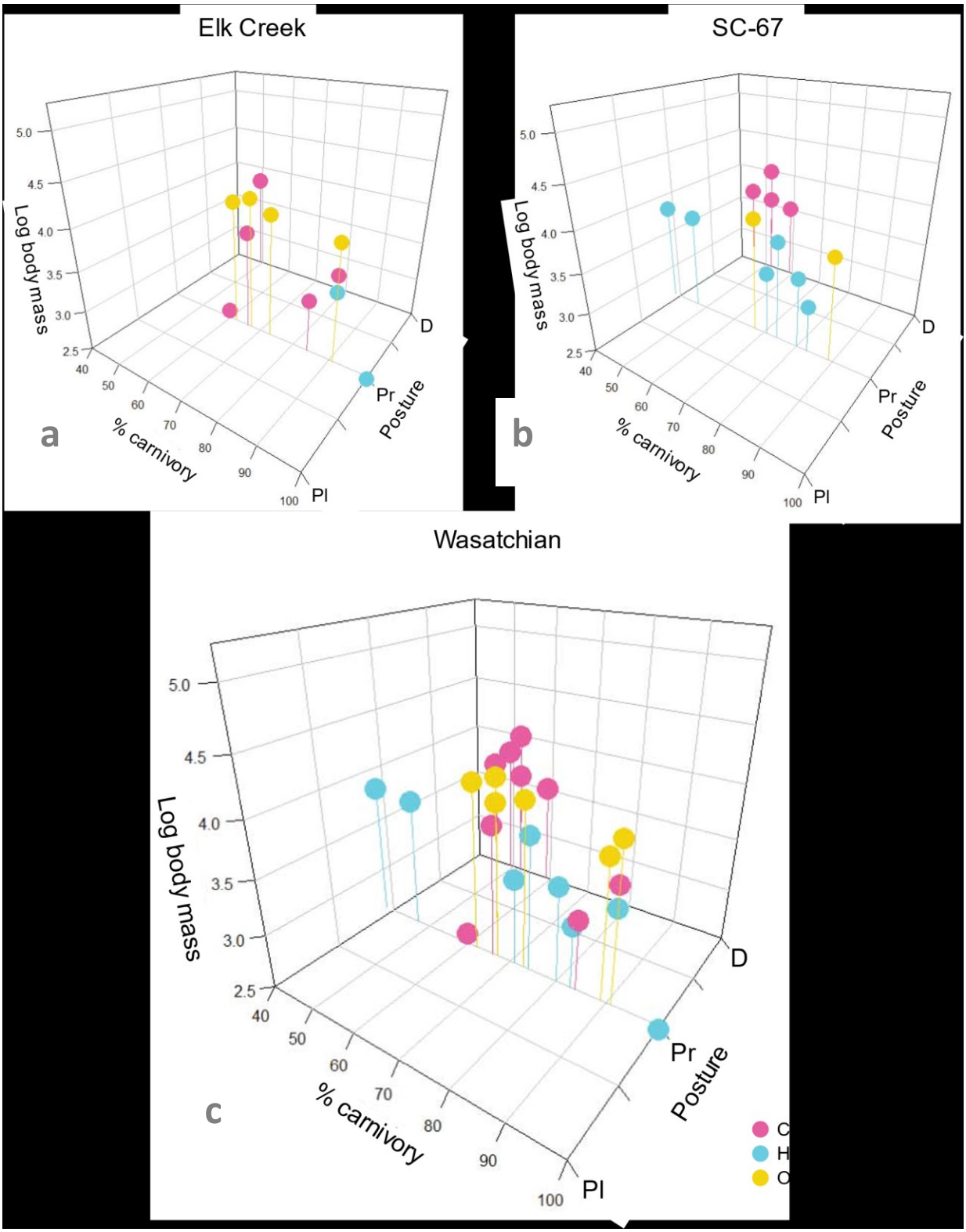

Figure 3.14. Guild structures of early Eocene (Wasatchian) localities based on % carnivory, body mass, and posture. a = Elk Creek locality; b = SC-67 locality; c = Elk Creek and SC-67 localities combined. Pl = plantigrade; Pr = protodigitigrade; D = digitigrade.

At the late Eocene (Chadronian) localities, there are fewer species at each locality. The only creodonts at these localities were of the genus *Hyaenodon*, and miacids and viverravids went extinct during the mid-Eocene leaving only carnivorans at the end (Fig. 3.15). Peanut Peak had four carnivorans and hyaenodontids, all of which were relatively large and highly carnivorous with the exception of the smaller, less carnivorous *Mustelavus priscus* (Fig. 3.15a). These large carnivorans and hyaenodontids likely avoided niche overlap through locomotory mode however; all of the large carnivorans were digitigrade while all hyaenodontids were protodigitigrade (Fig. 3.15a). At the Flagstaff Rim IV locality there is a similar distribution; two of the three carnivorans were large, digitigrade, hypercarnivores, while both hyaenodontids were large, plantigrade hypercarnivores (Fig. 3.15b). *Hyaenodon megaloides* was exceptionally large, and likely would not have overlapped with any of the species at Flagstaff Rim IV. The only exception at this locality was *Parictis dakotensis*, which was relatively small in body mass, plantigrade, and only consumed 70% meat (Fig. 3.15b).

In the combined guild structure figure for both Chadronian localities (Fig. 3.15c), the same trends are more apparent; carnivorans and creodonts were both highly carnivorous and much larger than they were during the Wasatchian, however the larger carnivorans were digitigrade and the creodonts were protodigitigrade. Some carnivorans were relatively small in the Chadronian, but no creodonts had body masses less than 14kg. Carnivorans also exhibited diversity in their posture, but all creodonts were protodigitigrade (Fig. 3.15c).

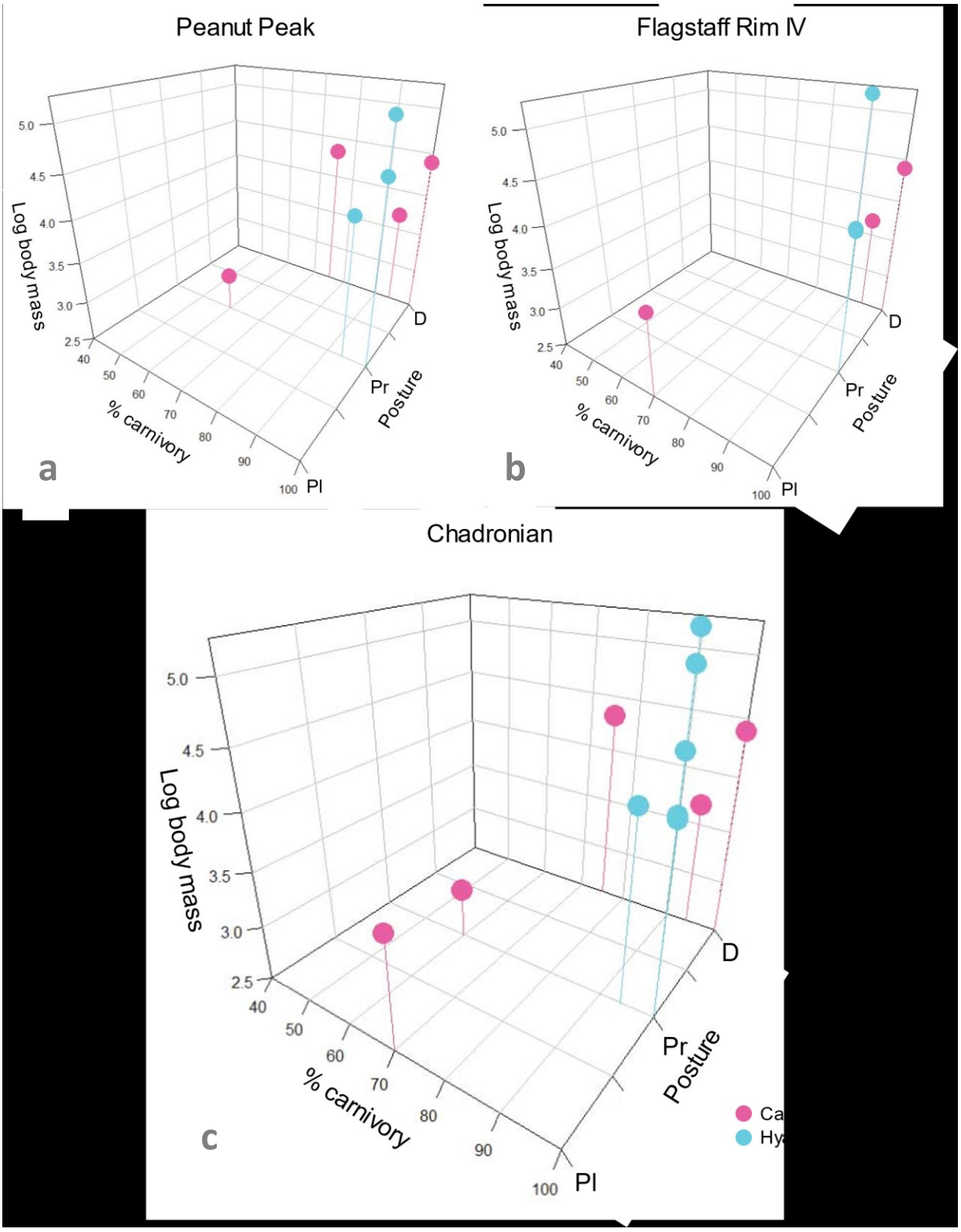

Figure 3.15. Guild structures of late Eocene (Chadronian) localities based on % carnivory, body mass, and posture. a = Elk Creek locality; b = SC-67 locality; c = Elk Creek and SC-67 localities combined. Pl = plantigrade; Pr = protodigitigrade; D = digitigrade.

3.5 Discussion

The dental metrics Relative Blade Length (RBL), Relative Lower Grinding Area (RLGA), and Relative Upper Grinding Area (RUGA) were all highly correlated with % carnivory (Figs. 3.7–3.9; Table 3.3). RBL was positively correlated with carnivory (Fig. 3.7; Table 3.3) because high relative blade length means that the main component of the carnassial tooth is the cutting blade. The blade is what allows carnivorous mammals to slice through vertebrate flesh, meaning the longer it is the more effectively the animal is able to slice through meat (Van Valkenburgh and Koepfli 1993; Friscia et al. 2007; Slater and Friscia 2019). RLGA and RUGA are both negatively correlated with % carnivory because high lower and upper grinding areas are consistent with an animal that consumes more fibrous material that must be ground down rather than sliced (Van Valkenburgh and Koepfli 1993; Friscia et al. 2007; Slater and Friscia 2019). During the Wasatchian (55.4–50.3 Ma), all groups (carnivoramorphans, hyaenodontids, and oxyaenids) had much higher variation in % carnivory than during the Chadronian (38–33.9 Ma; carnivorans and hyaenodontids). During the Wasatchian, all species ranged in carnivory from roughly 40–60% to 90–100% meat consumption. In the Chadronian, carnivoramorphans ranged from 60–100% meat consumption and hyaenodontids were nearly all 100% carnivorous (*Hyaenodon montanus* was the exception at 94%). Therefore, niche overlap, as measured using percentage of meat consumption, generally declined through the Eocene.

During the Wasatchian, coexisting oxyaenids, hyaenodontids, and carnivoramorphans all focused on prey that were <5kg. The majority focused on prey within the 0.2–0.5, 0.5–1, and 1–2 kg size ranges (Figs. 3.10, 3.11). Prey focus masses (PFMs) alone therefore suggest that every species of creodont and carnivoramorphan at the Elk Creek and SC-67 had the potential to

compete for prey resources. By the end of the Eocene epoch (Chadronian), all oxyaenids and carnivoramorphans outside of the crown group Carnivora were extinct (Goswami 2010). PFMs were much more distributed in the late Eocene, and, in general, were higher than the PFMs of the Wasatchian (Figs. 3.10, 3.11). Thus, overlap in prey focus masses decreased among carnivorans and creodonts, with most of the overlap taking place among carnivoran species (Figs. 3.10, 3.11). Unlike the Wasatchian, there were no hyaenodontids that focused on prey less than 0.5 kg. Carnivorans, however, continued to focus on smaller prey, including prey up to 10kg (Figs. 3.10–3.13). The largest hyaenodontids (*Hyaenodon cruentus, H. horridus,* and *H. megaloides*) focused on prey that were at least one PFM category higher than the largest carnivorans (two categories if the carnivorans were not scavenging or group hunting), and thus there appears to have been significant niche partitioning along the prey size axis by the late Eocene.

All creodonts in this study had a protodigitigrade posture, while carnivoramorphans exhibited all three posture types. During the Wasatchian, just over half of the carnivoramorphans were digitigrade and the rest were protodigitigrade, while, in the Chadronian, all carnivorans were digitigrade, excepting the plantigrade *Parictis dakotensis*. Differences in posture, specifically digitigrady among carnivorans, ensured some degree of niche partitioning during the late Eocene (Fig. 3.15). Digitigrady involves both limb lengthening and concentration of limb muscle mass proximal to the body. It is therefore associated with travelling long distances in open spaces, because it enhances step length and the efficiency with which limbs are swung (Christiansen 1999; Polly 2010). This may have been a major reason carnivorans survived the transition from tropical to more open, mixed woodland and grassland

ecosystems. In more open environments and combined with a transition among herbivorous species toward more unguligrade locomotion (a more extreme lengthening of the limbs than digitigrady) (Levering et al. 2017), the short limbs and protodigitigrade postures of hyaenodontids may have been disadvantageous.

When combining body mass, carnivory, and posture, it is apparent that there was a high degree of niche overlap among carnivoramorphans and creodonts during the Wasatchian (Fig. 3.14). The majority of niche overlap occurred among species with plantigrade postures, 60–75% carnivory, and of body mass ranging from 1–5 kg (Fig. 3.14). The species that occupied this niche space were primarily oxyaenids and carnivoramorphans, but also included one hyaenodontid (*Arfia opisthotoma*). By the end of the Eocene, during the Chadronian, the majority of carnivorans and creodonts were large (14–45 kg) and hypercarnivorous (70–100% carnivory; Van Valkenburgh 1991) (Fig. 3.15). Only hypercarnivorous hyaenodontid creodonts remained by the Chadronian. Smaller carnivorans (0.9–3.2 kg) with slightly lower degrees of meat consumption (60–70%) existed, but none of the species were small (1–5kg) or protodigitigrade, a niche that was occupied by a number of carnivoramorphans during the Wasatchian (Figs. 3.14, 3.15). It therefore appears that the small bodied, highly carnivorous, protodigitigrade niche was eliminated sometime during the mid-Eocene, facilitated primarily by increases in body mass and the prevalence of digitigrady among carnivorans.

Why did carnivorans and creodonts become large hypercarnivores at the end of the Eocene? Bergmann's rule states that body size increases with decreasing temperature (Bergmann 1847), and it was much cooler at the end of the Eocene than at the start (Zachos et al. 2001, 2008; Smith et al. 2010; Lovegrove and Mowoe 2013). The loss of near tropical

ecosystems in North America throughout the Eocene and consequent reduction in primary productivity are likely drivers of increases in body mass among mammals and apparent decreases in species richness (Alroy 1998; Hawkins et al. 2003; Smith et al. 2010; Lovegrove and Mowoe 2013; Fraser et al. 2015). The drivers of enhanced hypercarnivory are less clear, but may relate to retention of hypercarnivorous traits among species that survived to the late Eocene (hyaenodontids and not oxyaenids) or selection away from including vegetation of lower nutritional value (e.g. grasses) in the diet, given the comparatively short digestive systems of carnivorans (Reilly et al. 2001) and, potentially, hyaenodontids.

Whatever the drivers, hyaenodontids were the largest, most carnivorous mammals by the end of the Eocene and were extinct in North America soon after (Gunnell 1998). Once a carnivorous taxon begins to take on characteristics associated with hypercarnivory (i.e. loss of molar grinding areas), it is difficult to reverse their evolutionary course (Van Valkenburgh 1999, 2007). This is known as the "macroevolutionary ratchet" (Van Valkenburgh 2007) and can result in enhanced risk of extinction (Van Valkenburgh 2007; Smits and Evans 2012). Hypercarnivory is advantageous at the individual level because meat is an efficient source of calories for large-bodied carnivorous species (Van Valkenburgh et al. 2004; Van Valkenburgh 2007). However, at a species level, specialization is associated with greater extinction risk (Smits 2015); elimination of that specialized niche via climate change or other extrinsic changes may lead to extinction. Similarly, large body size is correlated with a host of traits that are also associated with increased extinction risk, including low population size and density as well as slow life histories (e.g. small numbers of young) (Smith et al. 2004; Van Valkenburgh 2007). Together, occupation of the large, hypercarnivorous, subdigitigrade niche by hyaenodontids at the end of the Eocene

may have ultimately pushed them to extinction. In contrast, the retention of smaller, less carnivorous species (*Mustelavus priscus* and *Parictis parvus*) may have allowed the carnivorans to diversify during the Oligo-Miocene (Fig. 3.2; Van Valkenburgh 1994; Janis et al. 1998a; Goswami 2010)

3.5 Conclusions

The results of this study do not support the competition hypothesis. I found that niche overlap was high at the start of the Eocene, but that the niches that were most occupied by carnivoramorphans and creodonts during the Wasatchian were unoccupied during the Chadronian. Creodonts (hyaendontids) became increasingly specialized during the Eocene, filling the large-bodied, hypercarnivorous niche. Though some carnivorans also became large hypercarnivores, they did not achieve the massive sizes of the hyaenodontids. Niche overlap was present along the body mass and carnivory axes at the end of the Eocene. However, separation along the posture axis indicates that carnivorans likely employed different hunting strategies and thus had access to different kinds of prey than the creodonts, reducing or eliminating niche overlap. The overspecialization of the creodonts, paired with their inability to adapt to the new landscapes that emerged at the end of the Eocene, was therefore the likely cause of their extinction.

Chapter 4: Conclusions

The "Competition Hypothesis" poses that carnivoramorphans out-competed creodonts during the Eocene in North America, and that this was the cause of the creodont extinction during the Oligocene (Friscia and Van Valkenburgh 2010). In this thesis, I tested this hypothesis by using dental metrics, body mass, and locomotory posture to test for niche overlap and thus resource competition between carnivoramorphans and creodonts during the earliest (Wasatchian NALMA; 55.4–50.3 Ma) and latest (Chadronian NALMA; 38–33.9 Ma) Eocene. Niche overlap, in this thesis, was interpreted as similarity along three niche axes: body mass, percent meat in a species' diet, and locomotor posture.

To test my hypothesis, I had planned to use 3D morphometrics combined with linear metrics (ratios of tooth length, width, area, etc.) of tooth shape to infer the dietary niches of my study species. Due to shutdowns and delays caused by COVID-19, however, I was unable to access the 3D scanning facilities, though I have collected a number of tooth molds for this purpose. Furthermore, the fragmentary nature of the specimens I examined did not allow for the prey-size preference analyses based on cranial metrics that I had initially planned to use (as used in Meachen and Van Valkenburgh (2009)). This led me to pursue alternate methods of quantifying diet using dental morphology, namely the methods of Van Valkenburgh and Koepfli (1993) as applied by Friscia et al. (2007) and Slater and Friscia (2019). While using these more traditional methods of determining diet (linear measurements rather than 3D scans), I noted a lack of literature on the relative efficacy of 3D to 2D methods of determining diet.

In the second chapter of my thesis, I compared the ability of 2D and 3D methods for inferring the diets of extant carnivorans. Though 3D methods are presently popular and are often used to infer the diet of extinct animals, they are relatively costly compared to linear metrics that can be taken using calipers alone. I found that linear metrics (ratios of tooth length, width, area, etc.) of tooth shape were more effective at differentiating among species with different types of diets than 3D morphometrics (Orientation Patch Count and Relief Index). Sample size was a major factor in the ability of the linear discriminant analyses to differentiate among diet types. A greater sample size, in fact, reduced the ability of tooth shape metrics to differentiate among diet types, likely due to the inclusion of species with similar morphologies but different diets. Combining different metrics of determining diet appears to be effective. However, phylogenetic autocorrelation and co-linearity of dental metrics must be taken into consideration when choosing metrics.

In the third chapter of my thesis, I examined niche overlap between carnivoramorphans and creodonts at four Eocene localities; the Early Eocene Wasatchian localities Elk Creek and SC-67, and the late Eocene Chadronian localities Peanut Peak and Flagstaff Rim IV. I selected these localities based on their age and representative species diversity. I interpreted niche overlap as similarity in diet (percent carnivory), locomotor mode, and body mass. I found that niche overlap between carnivoramorphans and creodonts was high during the Wasatchian and reduced greatly by the Chadronian. Many of the niches that had been occupied during the Wasatchian were virtually unoccupied during the Chadronian. My results therefore most resembled the hypothetical niche changes in figure 4.1, where niche overlap was high at the beginning of the Eocene and low to nonexistent at the end of the Eocene.

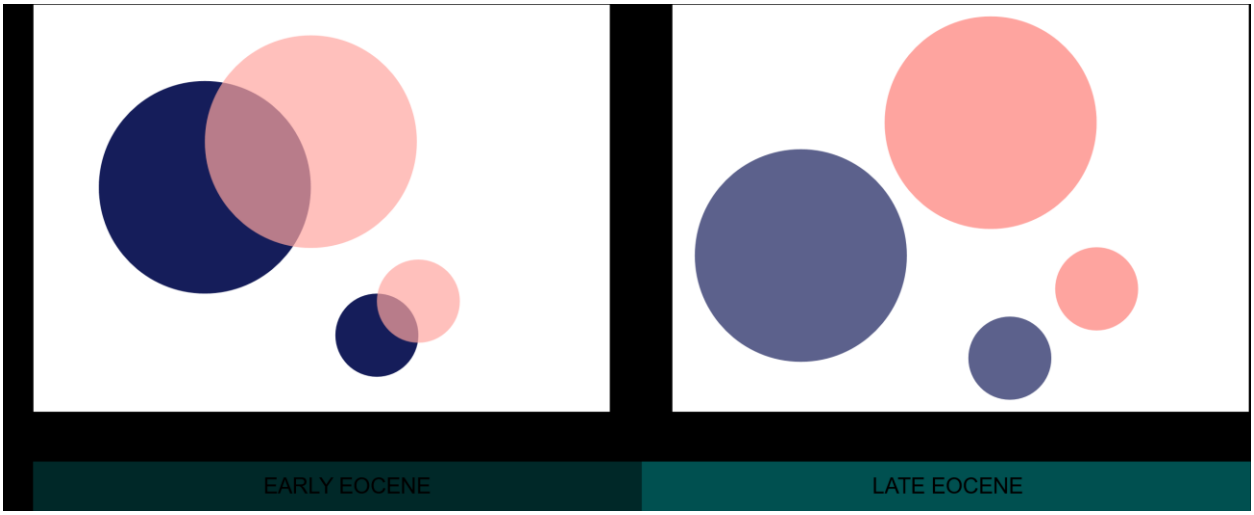

Figure 4.1. A hypothetical distribution of niche space occupied by carnivorans and creodonts. The axis titles represent different elements that comprise imaginary niche elements. In the early Eocene (left), there is overlap between the niches of carnivorans and creodonts. In the late Eocene (right), there is no niche overlap between the two groups, and the size of the creodont niches has been reduced. The dark purple circles represent hypothetical carnivoran niches and the pink circles represent hypothetical creodont niches.

Though large hypercarnivores shared dietary niches during the Chadronian they were, however, separated along the locomotor mode axis (i.e. creodonts were protodigitigrade and carnivoramorphans were digitigrade). This supports my hypothesis that hyaenodontids (the only creodonts present in the late Eocene) became specialized during the Eocene. However, the majority of carnivorans (the only carnivoramorphans present in the late Eocene) also became more specialized while still retaining some of their smaller, more generalized taxa. A more accurate representation of the changes in niche overlap that occurred is depicted in figure 4.2, which shows that niche overlap decreased at the end of the Eocene, but that the niches of both carnivorans and creodonts was reduced. Both groups became more carnivorous and greater in body mass (with the exception of some smaller, less carnivorous carnivoran species) in response to the cooling climate and changing vegetation during the Eocene.

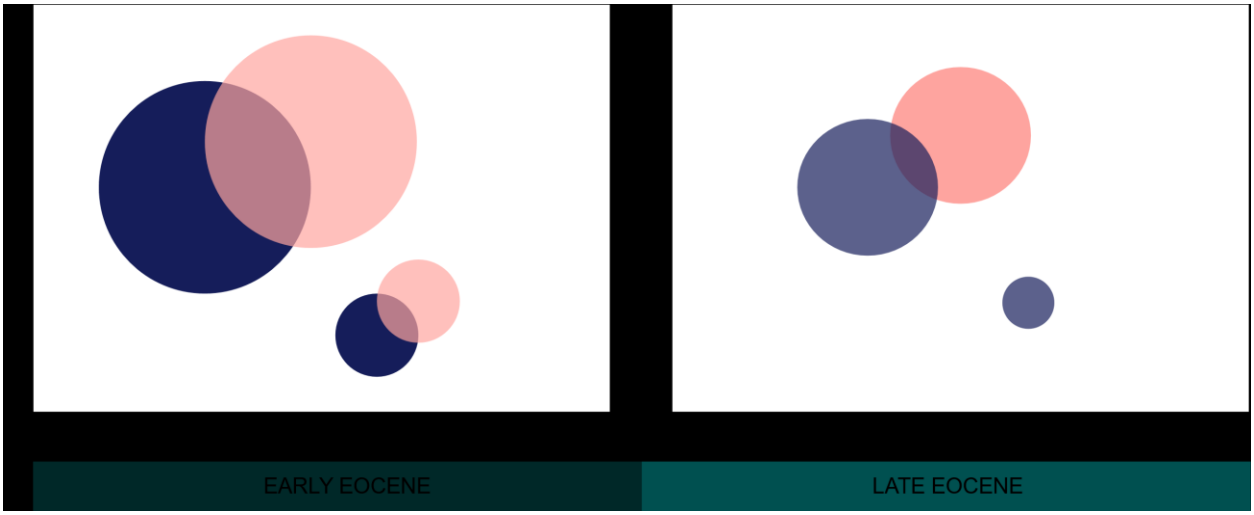

Figure 4.2. A representation of the niche space occupied by carnivorans and creodonts in this study. The axis titles represent different elements that comprise imaginary niche elements. In the early Eocene (left), there is overlap between the niches of carnivorans and creodonts. In the late Eocene (right), niche sizes have been reduced overall, and some carnivoramorphans avoid niche overlap altogether. The dark purple circles represent hypothetical carnivoran niches and the pink circles represent hypothetical creodont niches.

As herbivorous prey species adapted to the changing landscape and became more mobile grazers, the digitigrade posture of the carnivorans may have allowed them to venture out of the densely vegetated areas, which rapidly saw a decline in the populations of prey species. Hyaenodontids on the other hand, were ambush predators, reliant on large populations of large-bodied browsers. Their specialized morphology (large body size and hypercarnivory) made them vulnerable to the reduction in prey availability, while their relatively unspecialized foot posture may have limited their ability to adapt to the changes in prey lifestyles. Therefore, though competition may have been present in the early Eocene, overspecialization, not competition, appears to have been the ultimate cause of the creodont extinction.

References

Abler, J. L. 1985. Skulls in Fossil Material: One Mechanism Contributing to Their Rarity. Journal of Paleontology 59:249–250.

Adams, G. R. 2020. Description of *Calligenethlon watsoni* Based on Computed Tomography and Resulting Implications for the Phylogenetic Placement of Embolomeres. Carleton University.

Allen, K. L., S. B. Cooke, L. A. Gonzales, and R. F. Kay. 2015. Dietary Inference from Upper and Lower Molar Morphology in Platyrrhine Primates. PLoS ONE 10:1–23.

Alroy, J. 1998. Cope's Rule and the Dynamics of Body Mass Evolution in North American Fossil Mammals. Science 280:731–734.

Alroy, J., P. L. Koch, and J. C. Zachos. 2000. Global Climate Change and North American Mammalian Evolution. Paleobiology 26:259–288.

Alvarez, L. W., W. Alvarez, F. Asaro, and H. V Michel. 1980. Extraterrestrial Cause for the Experimental results and theoretical interpretation. Russell The Journal Of The Bertrand Russell Archives 208:1095–1108.

Armstrong, R. A., and R. McGehee. 1980. Competitive Exclusion. The American Naturalist 115:151–170.

Ashby, B., E. Watkins, J. Lourenço, S. Gupta, and K. R. Foster. 2017. Competing Species Leave Many Potential Niches Unfilled. Nature Ecology and Evolution 1:1495–1501.

Atkins, J. B., P. Sourges, N. B. Fröbisch, R. R. Reisz, and C. Hillary. 2020. Late Ontogeny in the Small Early Permian Amphibamiform Dissorophoid Pasawioops mayi. Journal of Vertebrate Paleontology 40:1–13.

Badgley, C., and D. L. Fox. 2000. Ecological Biogeography of North American Mammals: Species Density and Ecological Structure in Relation to Environmental Gradients. Journal of Biogeography 27:1437–1467.

Bekoff, M., J. Diamond, and J. B. Mitton. 1981. Life-History Patterns and Sociality in Canids: Body Size, Reproduction, and Behavior:386–390.

Bergmann, C. 1847. Über die Verhältnisse der Wärmeökonomie der Thiere zu ihrer Grösse. Göttinger Studien 3:595–708.

Di Bitetti, M. S., C. D. De Angelo, Y. E. Di Blanco, and A. Paviolo. 2010. Niche Partitioning and Apecies Coexistence in a Neotropical Felid Assemblage. Acta Oecologica 36:403–412.

Di Bitetti, M. S., A. Paviolo, and C. De Angelo. 2006. Density, Habitat Use and Activity Patterns of Ocelots (*Leopardus pardalis*) in the Atlantic Forest of Misiones, Argentina. Journal of Zoology 270:153–163.

Brown, W. L., and E. O. Wilson. 1956. Character Displacement. Systematic Zoology 5:49–64.

Bunn, J. M., D. M. Boyer, Y. Lipman, E. M. St. Clair, J. Jernvall, and I. Daubechies. 2011. Comparing Dirichlet Normal Surface Energy of Tooth Crowns, a New Technique of Molar Shape Quantification for Dietary Inference, with Previous Methods in Isolation and in Combination. American Journal of Physical Anthropology 145:247–261.

Burruss, D., A. Matchano, J. K. Frey, M. Andersen, and C. Sillero-Zubiri. 2017. Food Habits of the Pale Fox (*Vulpes pallida*) in Niger. African Journal of Ecology 55:664–671.

Caro, T. M., and C. J. Stoner. 2003. The Potential for Interspecific Competition Among African Carnivores. Biological Conservation 110:67–75.

Castiglione, S. et al. 2017. Diversification Rates and the Evolution of Species Range Size Frequency Distribution. Frontiers in Ecology and Evolution 5:1–10.

Christiansen, P. 1999. Scaling of the Limb Long Bones to Body Mass in Terrestrial Mammals. Journal of Morphology 239:167–190.

Christison, B. E., F. Gaidies, S. Pineda-Munoz, A. E. Evans, M. A. Gilbert, and D. Fraser. 2020. Dietary Niches of Creodonts and Carnivorans of the Late Eocene Cypress Hills Formation.

Clark, H. O., J. D. Murdoch Jr., D. P. Newman, and C. Sillero-Zubiri. 2009. *Vulpes corsac* (Carnivora: Canidae). Mammalian Species 832:1–8.

Clark, J., and J. R. Beerbower. 1967. Geology, Paleoecology, and Paleoclimatology of the Chadron Formation. Pp. 21–74 in Oligocene sedimentation, stratigraphy, paleoecology, and paleoclimatology in the Big Badlands of South Dakota (E. G. Nash & P. M. Williams, eds.). Field Museum Press, Chicago.

Clark, J., and T. E. Guensburg. 1972. Arctoid Genetic Characters as Related to the Genus *Parictis*. Field Museum of Natural History 1150.

Colbert, E. H. 1933. The skull of *Dissopsalis Carnifex* pilgrim, a Miocene Creodont from India. American Museum Novitates:265–279.

Colwell, R. K., and D. Futuyma. 1971. On the Measurement of Niche Breadth and Overlap. Ecology 52:567–576.

Condamine, F. L., J. Romieu, and G. Guinot. 2019. Climate Cooling and Clade Competition Likely Drove the Decline of Lamniform Sharks. Proceedings of the National Academy of Sciences of the United States of America 116:20584–20590.

Cossíos, E. D. 2010. *Lycalopex sechurae* (Carnivora: Canidae). Mammalian Species 42:1–6.

De Cuyper, A. et al. 2019. Predator Size and Prey Size–Gut Capacity Ratios Determine Kill Frequency and Carcass Production in Terrestrial Carnivorous Mammals. Oikos 128:13–22.

Dalponte, J. C. 2009. *Lycalopex vetulus* (Carnivora: Canidae). Mammalian Species 847:1–7.

Dayan, T., and D. Simberloff. 1998. Size Patterns Among Competitors: Ecological Character Displacement and Character Release in Mammals, with Special Reference to Island Populations. Mammal Review 28:99–124.

Dayan, T., and D. Simberloff. 2005. Ecological and Community-Wide Character Displacement: The Next Generation. Ecology Letters 8:875–894.

Elton, C. 1946. Competition and the Structure of Ecological Communities. British Ecological Society 15:54–68.

Emry, R. J. 1992. Mammalian Range Zones in the Chadronian White River Formation at Flagstaff Rim, Wyoming. Pp. 106–115 in Eocene-Oligocene Climatic and Biotic Evolution (D. R. Prothero & W. A. Berggren, eds.). Princeton University Press, Princeton, New Jersey.

Evans, A. R., and M. Fortelius. 2008. Three-Dimensional Reconstruction of Tooth Relationships

During Carnivoran Chewing. Palaeontologia Electronica 11.

Evans, A. R., M. Fortelius, J. Jernvall, and J. T. Eronen. 2005. Dental Ecomorphology of Extant European Carnivorans. Current Trends in Dental Morphology Research: 13th International Symposium on Dental Morphology 56:223–232.

Evans, A. R., and S. Pineda-Munoz. 2018. Inferring Mammal Dietary Ecology from Dental Morphology. Pp. 37–52 in Methods in Paleoecology: Reconstructing Cenozoic terrestrial environments and Ecological Communities (D. A. Croft, D. F. Su & S. W. S. Editors, eds.). Springer Nature Switzerland AG, Cham.

Evans, A. R., G. P. Wilson, M. Fortelius, and J. Jernvall. 2007. High-Level Similarity of Dentitions in Carnivorans and Rodents. Nature 445:78–81.

Faurby, S., and J. C. Svenning. 2015. A Species-Level Phylogeny of all Extant and Late Quaternary Extinct Mammals Using a Novel Heuristic-Hierarchical Bayesian Approach. Molecular Phylogenetics and Evolution 84:14–26.

Fernandez, V. et al. 2013. Synchrotron Reveals Early Triassic Odd Couple: Injured Amphibian and Aestivating Therapsid Share Burrow. PLoS ONE 8:2–8.

Figueirido, B., C. M. Janis, J. A. Pérez-Claros, M. De Renzi, and P. Palmqvist. 2011. Cenozoic Climate Change Influences Mammalian Evolutionary Dynamics. Proceedings of the National Academy of Sciences of the United States of America 109:722–727.

Flynn, J. J. 1998. Early Cenozoic Carnivora ("Miacoidea"). Pp. 112–123 in Evolution of Tertiary Mammals of North America (C. M. Janis, K. M. Scott & L. L. Jacobs, eds.). Cambridge

University Press, Cambridge.

Fraser, D. 2015. Change in North American Mammal Community Structure Under Late Cenozoic (~36 Ma-Present) Climate Change. Carleton University.

Fraser, D. et al. 2020. Investigating Biotic Interactions in Deep Time. Trends in Ecology and Evolution:1–15.

Fraser, D., R. Gorelick, and N. Rybczynski. 2015. Macroevolution and Climate Change Influence Phylogenetic Community Assembly of North American Hoofed Mammals. Biological Journal of the Linnean Society 114:485–494.

Fraser, D., R. J. Haupt, and W. Andrew Barr. 2018a. Phylogenetic Signal in Tooth Wear Dietary Niche Proxies: What it Means for Those in the Field. Ecology and Evolution 8:11363–11367.

Fraser, D., R. J. Haupt, and W. A. Barr. 2018b. Phylogenetic Signal in Tooth Wear Dietary Niche Proxies. Ecology and Evolution 8:5355–5368.

Freckleton, R. P., P. H. Harvey, and M. Pagel. 2002. Phylogenetic Analysis and Comparative Data: A Test and Review of Evidence. American Naturalist 160:712–726.

Friscia, A. R., B. Van Valkenburgh, and A. R. Biknevicius. 2007. An Ecomorphological Analysis of Extant Small Carnivorans. Journal of Zoology 272:82–100.

Friscia, A., and B. Van Valkenburgh. 2010. Ecomorphology of North American Eocene Carnivores; Evidence for Competition Between Carnivorans and Creodonts. Pp. 311–341 in Carnivoran evolution. Cambridge University Press, Cambridge.

Futuyma, D. J., and G. Moreno. 1988. The Evolution of Ecological Specialization. Annual Review of Ecology, Evolution, and Systematics 19:207–233.

Geffen, E. 1994. *Vulpes cana*. Mammalian Species:1–4.

Gingerich, P. D. 1989. New Earliest Wasatchian Mammalian Fauna from the Eocene of Northwestern Wyoming: Composition and Diversity in a Rarely Sampled High-Floodplain Assemblage. University of Michigan papers on paleontology 28.

Gompper, M. E., and A. T. Vanak. 2006. *Vulpes bengalensis*. Mammalian Species 795:1–5.

Goswami, A. 2006. Morphological Integration in the Carnivoran Skull. Evolution 60:169.

Goswami, A. 2010. Introduction to Carnivora. Pp. 1–24 in Carnivoran evolution (A. Goswami & A. Friscia, eds.). Cambridge University Press, Cambridge.

Gould, S. J., and C. Calloway. 1980. Clams and Brachiopods - Ships That Pass in the Night. Paleobiology 6:383–396.

Granger, W. 1938. A Giant Oxyaenid from the Upper Eocene of Mongolia. American Museum Novitates:1–5.

Greaves, W. S. 1983. A Functional Analysis of Carnassial Biting. Biological Journal of the Linnean Society 20:353–363.

Grossnickle, D. M., S. M. Smith, and G. P. Wilson. 2019. Untangling the Multiple Ecological Radiations of Early Mammals. Trends in Ecology and Evolution 34:936–949.

Gunnell, G. G. 1998. Creodonta. Pp. 91–109 in Evolution of Tertiary Mammals of North America

(C. M. Janis, K. M. Scott & L. L. Jacobs, eds.). Cambridge University Press, Cambridge.

Halliday, T. J. D., and A. Goswami. 2013. Testing the Inhibitory Cascade Model in Mesozoic and Cenozoic Mammaliaforms. BMC Evolutionary Biology 13.

Hammer, Ø., D. A. T. Harper, and P. D. Ryan. 2001. PAST: Paleontological Statistics Software Package for Education and Data Analysis. Palaeontologia Electronica 4:1–9.

Hardin, G. 1960. The Competitive Exclusion Principle. *Science*. .

Hawkins, B. A. et al. 2003. Energy, Water, and Broad-Scale Geographic Patterns of Species Richness. Ecology 84:3105–3117.

Hearn, A. J. et al. 2016. Predicted Distribution of the Bay Cat *Catopuma badia* (Mammalia: Carnivora: Felidae) on Borneo. Raffles Bulletin of Zoology 2016:165–172.

Hemmer, H. 2004. Notes of the Ecological Role of European Cats (Mammalia: Felidae) of the Last Two Million Years. Pp. 214–232 in iscelanea en homenaje a Emiliano Aguirre, Paleontología (E. Baquedano & S. Rubio Jara, eds.). Museo Arqueológico Regional.

Herring, S. W. 1993. Functional Morphology of Mammalian Mastication. Integrative and Comparative Biology 33:289–299.

Hertler, C., and R. Volmer. 2008. Assessing Prey Competition in Fossil Carnivore Communities - a Scenario for Prey Competition and its Evolutionary Consequences for Tigers in Pleistocene Java. Palaeogeography, Palaeoclimatology, Palaeoecology 257:67–80.

Holliday, J. A., and S. J. Steppan. 2004. Evolution of Hypercarnivory: The Effect of Specialization on Morphological and Taxonomic Diversity. Paleobiology 30:108–128.

Hutchinson, G. E. 1957. Concluding remarks. Cold Spring Harbor Symposia on Quantitative Biology 22:66–77.

Ivan, J. S., and T. M. Shenk. 2016. Winter Diet and Hunting Success of Canada Lynx in Colorado. Journal of Wildlife Management 80:1049–1058.

Jacobs, B., J. D. Kingston, and L. L. Jacobs. 1999. The Origin of Grass-Dominated Ecosystems. Annals of the Missouri Botanical Garden 86:590–643.

Janis, C. M. et al. 1998a. Carnivorous Mammals. Pp. 73–90 in Evolution of Tertiary Mammals of North America (C. M. Janis, K. M. Scott & L. L. Jacobs, eds.). Cambridge University Press, Cambridge.

Janis, C. M., K. M. Scott, and L. L. Jacobs (eds.). 1998b. Evolution of Tertiary Mammals of North America: Volume 1, Terrestrial Carnivores, Ungulates, and Ungulate Like Mammals. Cambridge University Press, Cambridge.

Jankowski, J. E., S. K. Robinson, and D. J. Levey. 2010. Squeezed at the Top: Interspecific Aggression May Constrain Elevational Ranges in Tropical Birds. Ecology 91:1877–1884.

Jiménez, J. E., and E. McMahon. 2004. Darwin's fox *Pseudalopex fulvipes* (Martin, 1837).

Kawanishi, K., and M. E. Sunquist. 2008. Food Habits and Activity Patterns of the Asiatic Golden Cat (Catopuma temminckii) and Dhole (Cuon alpinus) in a Primary Rainforest of Peninsular Malaysia. Mammal Study 33:173–177.

Laffont, R., E. Renvoisé, N. Navarro, P. Alibert, and S. Montuire. 2009. Morphological Modularity and Assessment of Developmental Processes Within the Vole Dental Row (*Microtus*

arvalis, Arvicolinae, Rodentia). Evolution and Development 11:302–311.

Laidre, K. L., J. A. Estes, M. T. Tinker, J. Bodkin, D. Monson, and K. Schneider. 2006. Patterns of Growth and Body Condition in Sea Otters from the Aleutian Archipelago Before and After the Recent Population Decline. Journal of Animal Ecology 75:978–989.

Larivière, S. 1998. Lontra felina. Mammalian Species:1–5.

Larivière, S. 1999. Mustela vison. Mammalian Species:1–9.

Larivière, S., and P. J. Seddon. 2001. *Vulpes rueppellii*. Mammalian Species:1–5.

Lavoie, M., A. Renard, and S. Larivière. 2019. *Lynx canadensis* (Carnivora: Felidae). Mammalian Species 51:136–154.

Legendre, S., and C. Roth. 2009. Correlation of Carnassial Tooth Size and Body Weight in Recent Carnivores (Mammalia). Historical Biology 1:85–98.

Levering, D., S. Hopkins, and E. Davis. 2017. Increasing Locomotor Efficiency Among North American Ungulates Across the Oligocene-Miocene Boundary. Palaeogeography, Palaeoclimatology, Palaeoecology 466:279–286.

Levins, R. 1968. Evolution in Changing Environments. Princeton University Press, Princeton, New Jersey.

Liow, L. H., T. Reitan, and P. G. Harnik. 2015. Ecological Interactions on Macroevolutionary Time Scales: Clams and Brachiopods are More Than Ships That Pass in the Night. Ecology Letters 18:1030–1039.

Liow, L. H., and N. C. Stenseth. 2007. The Rise and Fall of Species: Implications for Macroevolutionary and Macroecological Studies. Proceedings of the Royal Society B: Biological Sciences 274:2745–2752.

Livingston, S. E. 2009. The Nutrition and Natural History of the Serval (*Felis serval*) and Caracal (*Caracal caracal*). Veterinary Clinics of North America - Exotic Animal Practice 12:327–334.

López-Torres, S., K. R. Selig, K. A. Prufrock, D. Lin, and M. T. Silcox. 2018. Dental Topographic Analysis of Paromomyid (Plesiadapiformes, Primates) Cheek Teeth: More Than 15 Million Years of Changing Surfaces and Shifting Ecologies. Historical Biology 30:76–88.

Lovegrove, B. G., and M. O. Mowoe. 2013. The Evolution of Mammal Body sizes: Responses to Cenozoic Climate Change in North American Mammals. Journal of Evolutionary Biology 26:1317–1329.

Lowrey, B., L. M. Elbroch, and L. Broberg. 2016. Is Individual Prey Selection Driven by Chance or Choice? A Case Study in Cougars (Puma concolor). Mammal Research 61:353–359.

Lucas, P. W. 2004. Dental Morphology: How Teeth Work. Cambridge University Press, Cambridge.

Lucherini, M., and E. L. Vidal. 2008. Lycalopex gymnocercus (Carnivora: Canidae). Mammalian Species 820:1–9.

Lyons, S. K. et al. 2016. The Changing Role of Mammal Life Histories in Late Quaternary Extinction Vulnerability on Continents and Islands. Biology Letters 12.

Maas, M. C., M. R. L. Anthony, P. D. Gingerich, G. F. Gunnell, and D. W. Krause. 1995.

Mammalian Generic Diversity and Turnover in the Late Paleocene and Early Eocene of the Bighorn and Crazy Mountains Basins, Wyoming and Montana (USA). Palaeogeography, Palaeoclimatology, Palaeoecology 115:181–207.

Maddin, H. C., V. Màrton, J. D. Gardner, and J.-C. Rage. 2013. Micro-Computed Tomography Study of a Three-Dimensionally Preserved Neurocranium of Albanerpeton (Lissamphibia, Albanerpetontidae) from the Pliocene of Hungary. Journal of Vertebrate Paleontology 33:568–587.

Martin, L. D. 1998. Felidae. Pp. 236–242 in Evolution of Tertiary Mammals of North America (C. M. Janis, K. M. Scott & L. L. Jacobs, eds.). Cambridge University Press, Cambridge.

Mayhew, P. J., M. A. Bell, T. G. Benton, and A. J. McGowan. 2012. Biodiversity Tracks Temperature Over Time. Proceedings of the National Academy of Sciences of the United States of America 109:15141–15145.

McGill, B. J., B. J. Enquist, E. Weiher, and M. Westoby. 2006. Rebuilding Community Ecology from Functional Traits. Trends in Ecology and Evolution 21:178–185.

Mcgrew, B. J. C., V. Merriam, and K. Fox. 1979. *Vulpes macrotis*:1–6.

McInerney, F. A., and S. L. Wing. 2011. The Paleocene-Eocene Thermal Maximum: A Perturbation of Carbon Cycle, Climate, and Biosphere with Implications for the Future. Annual Review of Earth and Planetary Sciences 39:489–516.

Mckinney, M. L. 1987. Taxonomic Selectivity and Continuous Variation in Mass and Background Extinctions of Marine Taxa. *Nature*. .

Meachen, J. A., A. C. Janowicz, J. E. Avery, and R. W. Sadleir. 2014. Ecological Changes in Coyotes (*Canis latrans*) in Response to the Ice Age Megafaunal Extinctions. PLoS ONE 9:1–15.

Meachen, J., and B. Van Valkenburgh. 2009. Craniodental Indicators of Prey-Size Preference in the Felidae. Biological J 96:784–799.

Mellett, J. S. 1981. Mammalian Carnassial Function and the "Every Effect" 62:164–166.

Melstrom, K. M. 2017. The Relationship Between Diet and Tooth Complexity in Living Dentigerous Saurians. Journal of Morphology 278:500–522.

Moen, D., and H. Morlon. 2014. Why Does Diversification Slow Down? Trends in Ecology and Evolution 29:190–197.

Muñoz-Pedreros, A., J. Yáñez, H. V. Norambuena, and A. Zúñiga. 2018. Diet, Dietary Selectivity and Density of South American Grey Fox, Lycalopex griseus, in Central Chile. Integrative Zoology 13:46–57.

Novaro, A. 1997. *Pseudalopex culpaeus*. Mammalian Species:1–8.

Nowak, R. M. 2005. Aardwolf and Hyenas: Hyaenidae. Pp. 222–228 in Walker's Carnivores of the World. The Johns Hopkins University Press, Baltimore and London.

Owens, M. J., and D. D. Owens. 1978. Feeding Ecology and its Influence on Social Organization in Brown Hyenas (*Hyaena brunnae*, Thunberg) of the Central Kalahari Desert. African Journal of Ecology 16:113–135.

Pagel, M. 1999. Inferring the Historical Patterns of Biological Evolution. Nature 401:877–884.

Palmqvist, P., M. Mendoza, A. Arribas, and D. R. Gröcke. 2007. Estimating the Body Mass of Pleistocene Canids: Discussion of Some Methodological Problems and a New 'Taxon Free' Approach. Lethaia 35:358–360.

Pampush, D., J. M. Winchester, P. E. Morse, and A. Q. Vining. 2018. Package ' molaR .'

Paradis, E., and K. Schliep. 2019. Ape 5.0: an Environment for Modern Phylogenetics and Evolutionary Analyses in R. Bioinformatics 35:526–528.

Pearman, P. B., A. Guisan, O. Broennimann, and C. F. Randin. 2008. Niche Dynamics in Space and Time. Trends in Ecology and Evolution 23:149–158.

Pimm, S. L., H. L. Jones, J. Diamond, T. A. Naturalist, and N. Dec. 1988. On the Risk of Extinction. The American Naturalist 132:757–785.

Pineda-Munoz, S., J. Alroy, and A. R. Evans. 2013. Which Tooth Best Represents Whole Tooth Row Complexity in Mammals? 73rd Annual Meeting Society of Vertebrate Paleontology.

Pineda-Munoz, S., A. R. Evans, and J. Alroy. 2016. The Relationship Between Diet and Body Mass in Terrestrial Mammals. Paleobiology 42:659–669.

Pineda-Munoz, S., I. A. Lazagabaster, J. Alroy, and A. R. Evans. 2017. Inferring Diet from Dental Morphology in Terrestrial Mammals. Methods in Ecology and Evolution 8:481–491.

Pinheiro, J., S. DebRoy, D. Sarkar, and R Core Team. 2020. nlme: Linear and Nonlinear Mixed Effects Models. R package version 3:1–150.

Polly, P. D. 1993. Hyaenodontidae (Creodonta, Mammalia) and the Position of Systematics in Evolutionary Biology. University of California at Berkeley.

Polly, P. D. 2010. Tiptoeing Through the Tropics: Geographic Variation in Carnivoran Locomotor Ecomorphology in Relation to Environment. Pp. 374–410 in Carnivoran evolution (A. Friscia & B. Van Valkenburgh, eds.). Cambridge University Press, Cambridge.

Price, T. 1997. Correlated Evolution and Independent Contrasts. Philosophical Transactions of the Royal Society B: Biological Sciences 352:519–529.

Prothero, D. R. 1998a. The Chronological, Climatic, and Paleogeographic Background to North American Mammalian Evolution. Pp. 9–15 in Evolution of Tertiary Mammals of North America (C. M. Janis, K. M. Scott & L. L. Jacobs, eds.). Cambridge University Press, Cambridge.

Prothero, D. R. 1998b. Rhinocerotidae. Pp. 595–605 in Evolution of Tertiary Mammals of North America (C. M. Janis, K. M. Scott & L. L. Jacobs, eds.). Cambridge University Press, Cambridge.

Purvis, A., K. E. Jones, and G. M. Mace. 2000. Extinction. BioEssays 22:1123–1133.

Raup, D. M. 1986. Biological Extinction in Earth History. Science 231:1528–1533.

Reilly, S. M., L. D. McBrayer, and T. D. White. 2001. Prey processing in Amniotes: Biomechanical and Behavioral Patterns of Food Reduction. Comparative Biochemistry and Physiology - A Molecular and Integrative Physiology 128:397–415.

Revell, L. J. 2010. Phylogenetic Signal and Linear Regression on Species Data. Methods in Ecology and Evolution 1:319–329.

Revell, L. J. 2012. Phytools: An R package for Phylogenetic Comparative Biology (and Other

Things). Methods in Ecology and Evolution 3:217–223.

Rey, J., and S. Galeotti. 2008. Stratigraphy: Terminology and Practice. TECHNIP, Paris.

Van Rompaey, H., and M. Colyn. 2013. Central African; *Linsang Poiana* richardsonii. Pp. 253–254 in Mammals of Africa, V. Carnivores, pangolins, equids and rhinoceroses (J. Kingdon & M. Hoffman, eds.). Bloomsburt, London.

Ross, J. et al. 2016. Predicted Distribution of the Banded Civet *Hemigalus derbyanus* (Mammalia: Carnivora: Viverridae) on Borneo. Raffles Bulletin of Zoology 2016:111–117.

Russell, L. S. 1973. Erratum: Geological Evidence on the Extinction of Some Large Terrestrial Vertebrates. Canadian Journal of Earth Sciences 10:1361–1361.

Sacco, T., and B. Van Valkenburgh. 2004. Ecomorphological Indicators of Feeding Behaviour in the Bears (Carnivora: Ursidae). Journal of Zoology 263:41–54.

Sale, P. F. 1974. Overlap in Resource Use, and Interspecific Competition. Oecologia 17:245–256.

Sánchez-Barradas, A., and F. Villalobos. 2020. Species Geographical Co-occurrence and the Effect of Grinnellian and Eltonian Niche Partitioning: The Case of a Neotropical Felid Assemblage. Ecological Research 35:382–393.

Secord, R. et al. 2012. Evolution of the Earliest Horses Driven by Climate Change in the Paleocene-Eocene Thermal Maximum. Science 335:959–962.

Silva-Pereira, J. E., R. F. Moro-Rios, D. R. Bilski, and F. C. Passos. 2011. Diets of Three Sympatric Neotropical Small Cats: Food Niche Overlap and Interspecies Differences in Prey Consumption. Mammalian Biology 76:308–312.

Sinervo, B. et al. 2010. Erosion of Lizard Diversity by Climate Change and Altered Thermal Niches. Science 328:894–899.

Slater, G. J., and A. R. Friscia. 2019. Hierarchy in Adaptive radiation: A Case Study using the Carnivora (Mammalia). Evolution 73:524–539.

Smith, F. A. et al. 2004. Similarity of Mammalian Body Size Across the Taxonomic Hierarchy and Across Space and Time. American Naturalist 163:672–691.

Smith, F. A. et al. 2010. The Evolution of Maximum Body Size of Terrestrial Mammals. Science 330:1216–1219.

Smith, G. J. 2019. Coupling Paleoecological Proxies to Infer Competition, Niche Partitioning and Ecosystem Structure in Extinct Mammalian Communities. Vanderbilt University.

Smits, P. D. 2015. Expected Time-Invariant Effects of Biological Traits on Mammal Species Duration. Proceedings of the National Academy of Sciences of the United States of America 112:13015–13020.

Smits, P. D., and A. R. Evans. 2012. Functional Constraints on Tooth Morphology in Carnivorous Mammals. BMC Evolutionary Biology 12:146.

Soetaert, K. 2019. plot3D: Plotting Multi-Dimensional Data.

Spradley, J. P., J. D. Pampush, P. E. Morse, and R. F. Kay. 2017. Smooth Operator: The Effects of Different 3D Mesh Retriangulation Protocols on the Computation of Dirichlet Normal Energy. American Journal of Physical Anthropology 163:94–109.

Stanley, S. M. 1973. Effects of Competition on Rates of Evolution, with Special Reference to

Bivalve Mollusks and Mammals. Systematic Zoology 22:486–506.

Strömberg, C. A. E. 2004. Using Phytolith Assemblages to Reconstruct the Origin and Spread of Grass-Dominated Habitats in the Great Plains of North America During the Late Eocene to Early Miocene. Palaeogeography, Palaeoclimatology, Palaeoecology 207:239–275.

Strong, D. R., L. A. Szyska, and D. S. Simberloff. 1979. Test of Community-Wide Character Displacement Against Null Hypotheses. Evolution 33:897–913.

Stucky, R. K. 1992. Mammalian Faunas in North America of Bridgerian to Early Arikareean '"Ages"' (Eocene and Oligocene). Pp. 464–493 in Eocene-Oligocene Climatic and Biotic Evolution (D. R. Prothero & W. A. Berggren, eds.). Princeton University Press, Princeton, New Jersey.

Sunquist, M., and F. Sunquist. 2002. Marbled Cat. Pp. 373–376 in Wild Cats of the World. University of Chicago Press, Chicago.

Szpak, P., T. J. Orchard, I. McKechnie, and D. R. Gröcke. 2012. Historical Ecology of Late Holocene Sea Otters (*Enhydra lutris*) from Northern British Columbia: Isotopic and Zooarchaeological Perspectives. Journal of Archaeological Science 39:1553–1571.

Team, Rs. 2020. RStudio: Integrated Development for R. RStudio, PBC, Boston, MA URL http://www.rstudio.com/.

Thiel, C. 2011. Ecology and Population Status of the Serval Leptailurus serval (SCHREBER , 1776) in Zambia.

Tucker, M. A., T. J. Ord, and T. L. Rogers. 2016. Revisiting the Cost of Carnivory in Mammals.

Journal of Evolutionary Biology 29:2181–2190.

Ungar, P. S. 2010. Mammalian Teeth: Origin, Evolution, and Diversity. Baltimore.

Urban, M. C., J. J. Tewksbury, and K. S. Sheldon. 2012. On a Collision Course: Competition and Dispersal Differences Create No-Analogue Communities and Cause Extinctions During Climate Change. Proceedings of the Royal Society B: Biological Sciences 279:2072–2080.

Van Valkenburgh, B. 1990. Skeletal Predictors of Body Mass in Carnivores. Pp. 181–205 in Body size in mammalian paleobiology (J. Damuth & B. J. MacFadden, eds.). Cambridge University Press, Cambridge.

Van Valkenburgh, B. 1991. Iterative Evolution of Hypercarnivory in Canids (Mammalia: Carnivora): Evolutionary Interactions Among Sympatric Predators. Paleobiology 17:340–362.

Van Valkenburgh, B. 1994. Extinction and Replacement Among Predatory Mammals in the North American Late Eocene and Oligocene: Tracking a Paleoguild Over Twelve Million Years. Historical Biology 8:129–150.

Van Valkenburgh, B. 1999. Major Patterns in the History of Carnivorous Mammals. Annual Review of Earth and Planetary Sciences 27:463–493.

Van Valkenburgh, B. 2007. Déjà vu: The Evolution of Feeding Morphologies in the Carnivora. Integrative and Comparative Biology 47:147–163.

Van Valkenburgh, B., and I. Jenkins. 2002. Evolutionary Patterns in the History of Permo-Triassic and Cenozoic Synapsid Predators. Paleontological Society Papers 8:267–288.

Van Valkenburgh, B., and K. Koepfli. 1993. Cranial and Dental Adaptations to Predation in Canids. Symposium of the Zoological Society of London 65:15–37.

Van Valkenburgh, B., X. Wang, and J. Damuth. 2004. Cope's Rule, Hypercarnivory, and Extinction in North American Canids. Science 306:101–104.

Volmer, R., C. Hertler, and A. van der Geer. 2016. Niche Overlap and Competition Potential Among Tigers (Panthera tigris), Sabertoothed Cats (Homotherium ultimum, Hemimachairodus zwierzyckii) and Merriam's Dog (Megacyon merriami) in the Pleistocene of Java. Palaeogeography, Palaeoclimatology, Palaeoecology 441:901–911.

De Vos, J. M., L. N. Joppa, J. L. Gittleman, P. R. Stephens, and S. L. Pimm. 2015. Estimating the normal background rate of species extinction. Conservation Biology 29:452–462.

Wall, C. E., and K. K. Smith. 2001. Ingestion in Mammals. John Wiley & Sons. *Encyclopedia of Life Sciences*. .

Webb, D. S. 2006. The Great American Biotic Interchange: Patterns and Processes. Annals of the Missouri Botanical Garden 93:245–257.

Wiens, J. J. 2011. The Niche, Biogeography and Species Interactions. Philosophical Transactions of the Royal Society B: Biological Sciences 366:2336–2350.

Wiens, J. J., and C. H. Graham. 2005. Niche Conservatism: Integrating Evolution, Ecology, and Conservation Biology. Annual Review of Ecology, Evolution, and Systematics 36:519–539.

Wilman, H., J. Belmaker, J. Simpson, C. de La Rosa, M. Rivadeneira, and W. Jetz. 2014. EltonTraits 1.0 : Species-Level Foraging Attributes of the World's Birds and Mammals.

Ecology 95:2027.

Wing, S. L. 1998. Tertiary Vegetation of North America as a Context for Mammalian Evolution. Pp. 37–65 in Evolution of Tertiary Mammals of North America (C. M. Janis, K. M. Scott & L. L. Jacobs, eds.). Cambridge University Press, Cambridge.

Woodburne, M. O., G. F. Gunnell, and R. K. Stucky. 2009. Climate Directly Influences Eocene Mammal Faunal Dynamics in North America. Proceedings of the National Academy of Sciences of the United States of America 106:13399–13403.

Zachos, J. C., G. R. Dickens, and R. E. Zeebe. 2008. An Early Cenozoic Perspective on Greenhouse Warming and Carbon-Cycle Dynamics. Nature 451:279–283.

Zachos, J., H. Pagani, L. Sloan, E. Thomas, and K. Billups. 2001. Trends, Rhythms, and Aberrations in Global Climate 65 Ma to Present. Science 292:686–693.

Žliobaitė, I., M. Fortelius, and N. C. Stenseth. 2017. Reconciling Taxon Senescence with the Red Queen's Hypothesis. Nature 552:92–95.

Appendices

Appendix A: Body mass and diet categories of extant carnivorans from Friscia and Slater and Friscia (2019).

Species	Body mass (g)	Diet	Body mass source	Diet source
Acinonyx jubatus	46700	Hypercarnivore	Wilman et al. 2014	Wilman et al. 2014
Ailuropoda_melanoleuca	108400	Herbivore	Wilman et al. 2014	Wilman et al. 2014
Ailurus fulgens	4900	Herbivore	Wilman et al. 2014	Wilman et al. 2014
Amblonyx cinereus	3527.59	Insectivore	Wilman et al. 2014	Wilman et al. 2014
Aonyx capensis	18999.84	Insectivore	Wilman et al. 2014	Wilman et al. 2014
Arctictis binturong	9875	Omnivore	Wilman et al. 2014	Wilman et al. 2014
Arctogalidia trivirgata	2250	Mesocarnivore	Wilman et al. 2014	Wilman et al. 2014
Arctonyx collaris	6356	Omnivore	Wilman et al. 2014	Wilman et al. 2014
Atelocynus microtis	7749.97	Hypercarnivore	Wilman et al. 2014	Wilman et al. 2014
Atliax paludinosus	3299.97	Mesocarnivore	Wilman et al. 2014	Wilman et al. 2014
Bassaricyon alleni	1235.01	Omnivore	Wilman et al. 2014	Wilman et al. 2014
Bassaricyon gabbii	1250	Omnivore	Average for genus	Average for genus
Bassaricyon medius	1128.6275	Omnivore	Average for genus	Average for genus
Bassaricyon neblina	1128.6275	Omnivore	Wilman et al. 2014	Wilman et al. 2014
Bassariscus astutus	1129.51	Omnivore	Wilman et al. 2014	Wilman et al. 2014
Bassariscus sumichrasti	899.99	Omnivore	Wilman et al. 2014	Wilman et al. 2014
Bdeogale nigripes	2500	Insectivore	Wilman et al. 2014	Wilman et al. 2014
Bdeogale crassicauda	1549.99	Insectivore	Wilman et al. 2014	Wilman et al. 2014

Canis adustus	10249.91	Omnivore	Wilman et al. 2014	Wilman et al. 2014
Canis aureus	10345.23	Hypercarnivore	Wilman et al. 2014	Wilman et al. 2014
Canis latrans	13406.33	Hypercarnivore	Wilman et al. 2014	Wilman et al. 2014
Canis lupus	32183.33	Hypercarnivore	Wilman et al. 2014	Wilman et al. 2014
Canis mesomelas	8500.02	Mesocarnivore	Wilman et al. 2014	Wilman et al. 2014
Canis simensis	10000	Hypercarnivore	Wilman et al. 2014	Wilman et al. 2014
Caracal caracal	13749.91	Hypercarnivore	Wilman et al. 2014	Wilman et al. 2014
Catopuma badia	3500	Hypercarnivore	Hearn et al. 2016	Average for genus
Catopuma temminckii	12000	Hypercarnivore	Kawanishi and Sunquist 2008	Kawanishi and Sunquist 2008
Cerdocyon thous	5239.98	Omnivore	Wilman et al. 2014	Wilman et al. 2014
Chrotogale owstoni	3250	Insectivore	Wilman et al. 2014	Wilman et al. 2014
Chrysocyon brachyurus	23249.84	Mesocarnivore	Wilman et al. 2014	Wilman et al. 2014
Civettictis civetta	11999.97	Omnivore	Wilman et al. 2014	Wilman et al. 2014
Conepatus leuconotus	3500.02	Insectivore	Wilman et al. 2014	Wilman et al. 2014
Conepatus chinga	1917.52	Insectivore	Wilman et al. 2014	Wilman et al. 2014
Conepatus semistriatus	1200	Insectivore	Wilman et al. 2014	Wilman et al. 2014
Crocuta crocuta	66492.06	Hypercarnivore	Wilman et al. 2014	Wilman et al. 2014
Crossarchus alexandri	1500	Insectivore	Wilman et al. 2014	Wilman et al. 2014
Crossarchus obscurus		Insectivore	Wilman et al. 2014	Wilman et al. 2014
Crossarchus platycephalus	1250	Omnivore	Wilman et al. 2014	Wilman et al. 2014
Cryptoprocta ferox	9500	Hypercarnivore	Wilman et al. 2014	Wilman et al. 2014

Cuon alpinus	14173.33	Hypercarnivore	Wilman et al. 2014	Wilman et al. 2014
Cynictis penicillata	836.01	Insectivore	Wilman et al. 2014	Wilman et al. 2014
Cynogale bennettii	4500	Omnivore	Wilman et al. 2014	Wilman et al. 2014
Diplogale hosei	3124.89	Insectivore	Wilman et al. 2014	Wilman et al. 2014
Dologale dybowskii	399.9981812	Insectivore	Legendre and Roth 2009	Caro and Stoner 2003
Dusicyon australis	50003.45	Hypercarnivore	Wilman et al. 2014	Wilman et al. 2014
Eira barbara	3910.03	Hypercarnivore	Wilman et al. 2014	Wilman et al. 2014
Enhydra lutris	28350	Insectivore	Laidre et al. 2006	Szpak et al. 2012
Eupleres goudotii	3000	Insectivore	Wilman et al. 2014	Wilman et al. 2014
Felis chaus	7392.98	Hypercarnivore	Wilman et al. 2014	Wilman et al. 2014
Felis margarita	2524.99	Hypercarnivore	Wilman et al. 2014	Wilman et al. 2014
Felis nigripes	1299.99	Hypercarnivore	Wilman et al. 2014	Wilman et al. 2014
Felis silvestris	5099.99	Hypercarnivore	Wilman et al. 2014	Wilman et al. 2014
Fossa fossana	1500	Insectivore	Wilman et al. 2014	Wilman et al. 2014
Galerella sanguinea	550	Insectivore	Wilman et al. 2014	Wilman et al. 2014
Galerella pulverulenta	797	Insectivore	Wilman et al. 2014	Wilman et al. 2014
Galictis cuja	1000	Mesocarnivore	Wilman et al. 2014	Wilman et al. 2014
Galictis vittata	3200	Mesocarnivore	Wilman et al. 2014	Wilman et al. 2014
Galidia elegans	800	Hypercarnivore	Wilman et al. 2014	Wilman et al. 2014
Galidictis fasciata	550	Mesocarnivore	Wilman et al. 2014	Wilman et al. 2014
Genetta angolensis	1649.99	Hypercarnivore	Wilman et al. 2014	Wilman et al. 2014

Genetta genetta	1800	Hypercarnivore	Wilman et al. 2014	Wilman et al. 2014
Genetta maculata	2225	Hypercarnivore	Wilman et al. 2014	Wilman et al. 2014
Genetta pardina	1821.97	Mesocarnivore	Wilman et al. 2014	Wilman et al. 2014
Genetta servalina	1054.99	Hypercarnivore	Wilman et al. 2014	Wilman et al. 2014
Genetta thierryi	1400.01	Hypercarnivore	Wilman et al. 2014	Wilman et al. 2014
Genetta tigrina	2225	Hypercarnivore	Wilman et al. 2014	Wilman et al. 2014
Gulo gulo	17012.56	Hypercarnivore	Wilman et al. 2014	Wilman et al. 2014
Helarctos malayanus	289	Insectivore	Wilman et al. 2014	Wilman et al. 2014
Helogale hirtula	300	Insectivore	Wilman et al. 2014	Wilman et al. 2014
Helogale parvula	2322.5	Insectivore	Wilman et al. 2014	Wilman et al. 2014
Hemigalus derbyanus	2250	Omnivore	Ross et al. 2016	Ross et al. 2016
Herpailurus yagouaroundi	5150	Hypercarnivore	Silva-Pereira et al. 2011	Silva-Pereira et al. 2011
Herpestes brachyurus	1853.52	Mesocarnivore	Wilman et al. 2014	Wilman et al. 2014
Herpestes edwardsi	2457.431429	Mesocarnivore	Average for genus	Average for genus
Herpestes fuscus	1984.74	Mesocarnivore	Wilman et al. 2014	Wilman et al. 2014
Herpestes ichneumon	5174.98	Mesocarnivore	Wilman et al. 2014	Wilman et al. 2014
Herpestes javanicus	750	Mesocarnivore	Wilman et al. 2014	Wilman et al. 2014
Herpestes naso	2999.99	Mesocarnivore	Wilman et al. 2014	Wilman et al. 2014
Herpestes urva	1863.2	Mesocarnivore	Wilman et al. 2014	Wilman et al. 2014
Herpestes vitticollis	2575.59	Mesocarnivore	Wilman et al. 2014	Wilman et al. 2014
Hyaena brunnea	42250	Mesocarnivore	Nowak 2005	Owens and Owens 1978

Hyaena hyaena	41705.11	Hypercarnivore	Wilman et al. 2014	Wilman et al. 2014
Hydrictis maculicollis	4180.53	Hypercarnivore	Wilman et al. 2014	Wilman et al. 2014
Ichneumia albicauda	3500.02	Insectivore	Wilman et al. 2014	Wilman et al. 2014
Ictonyx libycus	2062.5	Mesocarnivore	Wilman et al. 2014	Wilman et al. 2014
Ictonyx striatus	1299.99	Mesocarnivore	Wilman et al. 2014	Wilman et al. 2014
Leopardus colocola	5157.94	Hypercarnivore	Wilman et al. 2014	Wilman et al. 2014
Leopardus geoffroyi	5157.94	Hypercarnivore	Wilman et al. 2014	Wilman et al. 2014
Leopardus guigna	5157.94	Hypercarnivore	Wilman et al. 2014	Wilman et al. 2014
Leopardus pardalis	11900.08	Hypercarnivore	Wilman et al. 2014	Wilman et al. 2014
Leopardus tigrinus	2250	Hypercarnivore	Wilman et al. 2014	Wilman et al. 2014
Leopardus wiedii	3249.97	Hypercarnivore	Wilman et al. 2014	Wilman et al. 2014
Leptailurus serval	12000	Hypercarnivore	Livingston 2009	Thiel 2011
Liberiictis kuhni	2150.01	Insectivore	Wilman et al. 2014	Wilman et al. 2014
Lontra canadensis	8087.42	Hypercarnivore	Wilman et al. 2014	Wilman et al. 2014
Lontra felina	4500	Insectivore	Larivière 1998	Larivière 1998
Lontra longicaudis	6554.96	Hypercarnivore	Wilman et al. 2014	Wilman et al. 2014
Lontra provocax	7499.98	Omnivore	Wilman et al. 2014	Wilman et al. 2014
Lutra lutra	8785.14	Mesocarnivore	Wilman et al. 2014	Wilman et al. 2014
Lutra sumatrana	5500	Mesocarnivore	Wilman et al. 2014	Wilman et al. 2014
Lutrogale perspicillata	9483.33	Mesocarnivore	Wilman et al. 2014	Wilman et al. 2014
Lycalopex culpaeus	7732.5	Hypercarnivore	Novaro 1997	Novaro 1997
Lycalopex fulvipes	2717.5	Omnivore	Jiménez and McMahon 2004	Jiménez and McMahon 2004

Lycalopex griseus	3266	Hypercarnivore	Muñoz-Pedreros et al. 2018	Muñoz-Pedreros et al. 2018
Lycalopex gymnocercus	5000	Omnivore	Lucherini and Vidal 2008	Lucherini and Vidal 2008
Lycalopex sechurae	3600	Omnivore	Cossíos 2010	Cossíos 2010
Lycalopex vetulus	3500	Insectivore	Dalponte 2009	Dalponte 2009
Lycaon pictus	22050.07	Hypercarnivore	Wilman et al. 2014	Wilman et al. 2014
Lynx canadensis	9373.25	Hypercarnivore	Wilman et al. 2014	Wilman et al. 2014
Lynx lynx	17950	Hypercarnivore	Wilman et al. 2014	Wilman et al. 2014
Lynx pardinus	9400	Hypercarnivore	Wilman et al. 2014	Wilman et al. 2014
Lynx rufus	8904.1	Hypercarnivore	Wilman et al. 2014	Wilman et al. 2014
Martes americana	1250	Mesocarnivore	Wilman et al. 2014	Wilman et al. 2014
Martes flavigula	1842.5	Hypercarnivore	Wilman et al. 2014	Wilman et al. 2014
Martes foina	1540.8	Mesocarnivore	Wilman et al. 2014	Wilman et al. 2014
Martes martes	1300	Mesocarnivore	Wilman et al. 2014	Wilman et al. 2014
Martes melampus	1000	Omnivore	Wilman et al. 2014	Wilman et al. 2014
Martes zibellina	1130	Hypercarnivore	Wilman et al. 2014	Wilman et al. 2014
Meles meles	13000	Omnivore	Wilman et al. 2014	Wilman et al. 2014
Mellivora capensis	8500	Mesocarnivore	Wilman et al. 2014	Wilman et al. 2014
Melogale moschata	805.25	Omnivore	Wilman et al. 2014	Wilman et al. 2014
Melogale personata	1702.5	Omnivore	Wilman et al. 2014	Wilman et al. 2014
Melursus ursinus	801.25	Omnivore	Wilman et al. 2014	Wilman et al. 2014
Mephitis macroura	2085.02	Omnivore	Wilman et al. 2014	Wilman et al. 2014
Mephitis mephitis	1925	Insectivore	Wilman et al. 2014	Wilman et al. 2014

Mungos mungo	650	Insectivore	Wilman et al. 2014	Wilman et al. 2014
Mungotictis decemlineata	536.99	Hypercarnivore	Wilman et al. 2014	Wilman et al. 2014
Mustela africana	171	Hypercarnivore	Wilman et al. 2014	Wilman et al. 2014
Mustela altaica	119.38	Hypercarnivore	Wilman et al. 2014	Wilman et al. 2014
Mustela erminea	464.2508333	Hypercarnivore	Average for genus	Average for genus
Mustela eversmanii	464.2508333	Hypercarnivore	Average for genus	Average for genus
Mustela felipei	211.3	Hypercarnivore	Wilman et al. 2014	Wilman et al. 2014
Mustela frenata	147	Hypercarnivore	Wilman et al. 2014	Wilman et al. 2014
Mustela kathiah	208.08	Hypercarnivore	Wilman et al. 2014	Wilman et al. 2014
Mustela lutreola	440	Hypercarnivore	Wilman et al. 2014	Wilman et al. 2014
Mustela nigripes	850	Hypercarnivore	Wilman et al. 2014	Wilman et al. 2014
Mustela nivalis	103.88	Hypercarnivore	Wilman et al. 2014	Wilman et al. 2014
Mustela nudipes	500	Hypercarnivore	Wilman et al. 2014	Wilman et al. 2014
Mustela putorius	915.37	Hypercarnivore	Wilman et al. 2014	Wilman et al. 2014
Mustela sibirica	405	Hypercarnivore	Wilman et al. 2014	Wilman et al. 2014
Mustela strigidorsa	1500	Hypercarnivore	Wilman et al. 2014	Wilman et al. 2014
Mydaus javanensis	2500	Insectivore	Wilman et al. 2014	Wilman et al. 2014
Mydaus marchei	1414.2	Insectivore	Wilman et al. 2014	Wilman et al. 2014
Nandinia binotata	2000	Herbivore	Wilman et al. 2014	Wilman et al. 2014
Nasua narica	4030.05	Omnivore	Wilman et al. 2014	Wilman et al. 2014
Nasua nasua	3793.85	Omnivore	Wilman et al. 2014	Wilman et al. 2014

Nasuella olivacea	1339.99	Omnivore	Wilman et al. 2014	Wilman et al. 2014
Neofelis nebulosa	19675.75	Hypercarnivore	Wilman et al. 2014	Wilman et al. 2014
Neovison vison	984.96	Hypercarnivore	Larivière 1999	Larivière 1999
Nyctereutes procyonoides	4040	Omnivore	Wilman et al. 2014	Wilman et al. 2014
Otocolobus manul	4000	Hypercarnivore	Ross et al 2010	Ross et al 2010
Paguma larvata	4300	Mesocarnivore	Wilman et al. 2014	Wilman et al. 2014
Panthera leo	161499.06	Hypercarnivore	Wilman et al. 2014	Wilman et al. 2014
Panthera onca	1.00E+05	Hypercarnivore	Wilman et al. 2014	Wilman et al. 2014
Panthera pardus	52038.22	Hypercarnivore	Wilman et al. 2014	Wilman et al. 2014
Panthera tigris	162564	Hypercarnivore	Wilman et al. 2014	Wilman et al. 2014
Panthera uncia	1639.99	Insectivore	Wilman et al. 2014	Wilman et al. 2014
Paracynictis selousi	3156.66	Omnivore	Wilman et al. 2014	Wilman et al. 2014
Paradoxurus hermaphroditus	2780.75	Omnivore	Wilman et al. 2014	Wilman et al. 2014
Paradoxurus zeylonensis	2854.25	Hypercarnivore	Wilman et al. 2014	Wilman et al. 2014
Pardofelis marmorata	3000	Hypercarnivore	Sunquist and Sunquist 2002	Sunquist and Sunquist 2002
Pekania pennanti	4000	Hypercarnivore	Wilman et al. 2014	Wilman et al. 2014
Poecilogale albinucha	340	Hypercarnivore	Wilman et al. 2014	Wilman et al. 2014
Poiana richardsonii	500	Mesocarnivore	Wilman et al. 2014	Van Rompaey and Colyn 2013
Potos flavus	3000	Herbivore	Wilman et al. 2014	Wilman et al. 2014
Prionailurus bengalensis	3300	Hypercarnivore	Wilman et al. 2014	Wilman et al. 2014
Prionailurus planiceps	6750	Hypercarnivore	Wilman et al. 2014	Wilman et al. 2014

Prionailurus rubiginosus	1384.38	Hypercarnivore	Wilman et al. 2014	Wilman et al. 2014
Prionailurus viverrinus	9140.33	Hypercarnivore	Wilman et al. 2014	Wilman et al. 2014
Prionodon pardicolor	512	Mesocarnivore	Wilman et al. 2014	Wilman et al. 2014
Prionodon linsang	700	Mesocarnivore	Wilman et al. 2014	Wilman et al. 2014
Procyon cancrivorus	6949.92	Omnivore	Wilman et al. 2014	Wilman et al. 2014
Procyon lotor	5524.97	Omnivore	Wilman et al. 2014	Wilman et al. 2014
Pteronura brasiliensis	23999.93	Mesocarnivore	Wilman et al. 2014	Wilman et al. 2014
Puma concolor	51600.04	Hypercarnivore	Wilman et al. 2014	Wilman et al. 2014
Rhynchogale melleri	2500	Omnivore	Wilman et al. 2014	Wilman et al. 2014
Salanoia concolor	650	Omnivore	Wilman et al. 2014	Wilman et al. 2014
Speothos venaticus	5999.98	Hypercarnivore	Wilman et al. 2014	Wilman et al. 2014
Spilogale gracilis	466.5	Omnivore	Wilman et al. 2014	Wilman et al. 2014
Spilogale putorius	341	Omnivore	Wilman et al. 2014	Wilman et al. 2014
Suricata suricatta	725.5	Insectivore	Wilman et al. 2014	Wilman et al. 2014
Taxidea taxus	7107.55	Hypercarnivore	Wilman et al. 2014	Wilman et al. 2014
Tremarctos ornatus	140000.63	Herbivore	Wilman et al. 2014	Wilman et al. 2014
Urocyon cinereoargenteus	3833.72	Omnivore	Wilman et al. 2014	Wilman et al. 2014
Urocyon littoralis	1896	Omnivore	Wilman et al. 2014	Wilman et al. 2014
Ursus americanus	99949.36	Omnivore	Wilman et al. 2014	Wilman et al. 2014
Ursus maritimus	388750.36	Hypercarnivore	Wilman et al. 2014	Wilman et al. 2014
Ursus thibetanus	77500	Omnivore	Wilman et al. 2014	Wilman et al. 2014

Ursus arctos	180520.42	Omnivore	Wilman et al. 2014	Wilman et al. 2014
Viverra megaspila	9250	Mesocarnivore	Wilman et al. 2014	Wilman et al. 2014
Viverra tangalunga	6885	Mesocarnivore	Wilman et al. 2014	Wilman et al. 2014
Viverra zibetha	9500	Hypercarnivore	Wilman et al. 2014	Wilman et al. 2014
Viverricula indica	2908.43	Mesocarnivore	Wilman et al. 2014	Wilman et al. 2014
Vormela peregusna	450.38	Hypercarnivore	Wilman et al. 2014	Wilman et al. 2014
Vulpes bengalensis	2700	Omnivore	Gompper and Vanak 2006	Gompper and Vanak 2006
Vulpes cana	1000	Insectivore	Geffen 1994	Geffen 1994
Vulpes chama	2955.02	Mesocarnivore	Wilman et al. 2014	Wilman et al. 2014
Vulpes corsac	2325	Mesocarnivore	Clark et al. 2009	Clark et al. 2009
Vulpes ferrilata	5000	Hypercarnivore	Wilman et al. 2014	Wilman et al. 2014
Vulpes lagopus	3584.37	Hypercarnivore	Wilman et al. 2014	Wilman et al. 2014
Vulpes macrotis	2050	Hypercarnivore	Mcgrew et al. 1979	Mcgrew et al. 1979
Vulpes pallida	2400	Insectivore	Palmqvist et al. 2007	Burruss et al. 2017
Vulpes rueppellii	2000	Omnivore	Larivière and Seddon 2001	Larivière and Seddon 2001
Vulpes vulpes	5476.17	Mesocarnivore	Wilman et al. 2014	Wilman et al. 2014
Vulpes zerda	2197.51	Omnivore	Wilman et al. 2014	Wilman et al. 2014
Vulpes velox	1100	Hypercarnivore	Wilman et al. 2014	Wilman et al. 2014

Appendix B: Specimens used in this thesis

Species	Code	Number	Element	Citations (if found in the literature)
Acarictis ryani	UM	75805	lower jaw	
Acarictis ryani	UM	86408	lower jaw	
Acarictis ryani			lower carnassial	Gingerich 1983; Polly 1993
Arfia junnei	UM	87344	lower jaw	
Arfia opisthotoma	ROM	43499	lower jaw	
Arfia opisthotoma	UM	28996	lower jaw	
Arfia opisthotoma	UM	75644	lower jaw	
Arfia opisthotoma	YPM	13145	lower jaw	
Arfia opisthotoma	YPM	23367	lower jaw	
Arfia shoshoniensis	FAM	15742	lower jaw	
Arfia shoshoniensis	FAM	15743	lower jaw	
Arfia shoshoniensis	FAM	15745	lower jaw	
Arfia shoshoniensis	FAM	15747	lower jaw	
Arfia shoshoniensis	FAM	16158	lower jaw	
Arfia shoshoniensis	FAM	16964	lower jaw	
Arfia shoshoniensis	ROM	43486	lower jaw	
Arfia shoshoniensis	UM	80487	lower jaw	
Arfia shoshoniensis			lower carnassial	Gingerich 1989
Brachyrhynchocyon dodgei	YPM	11422	lower jaw	
Brachyrhynchocyon dodgei	YPM	13601	lower jaw	
Brachyrhynchocyon dodgei	YPM	13601	calcaneum	
Brachyrhynchocyon dodgei	YPM	24612	calcaneum and skull	
Didelphodus absarokae	USNM	19458	lower jaw	
Didymictis dellensis	YPM	13937	lower jaw	
Didymictis leptomylus	FAM	4035	lower jaw	
Didymictis leptomylus	FAM	16220	lower jaw	
Didymictis leptomylus	ROM	45561	lower jaw	
Didymictis leptomylus	ROM	45577	lower jaw	
Didymictis leptomylus	UM	67017	lower jaw	
Didymictis leptomylus	UM	67446	lower jaw	
Didymictis leptomylus	UM	83661	lower jaw	
Didymictis leptomylus	UM	94898	lower jaw	
Didymictis protenus	FAM	55419	lower jaw	
Didymictis protenus	USNM	3619	partial skull	
Didymictis protenus	USNM	4739	lower jaw	
Didymictis protenus	USNM	4814	lower jaw	

Didymictis protenus	USNM	5028	partial skull	
Didymictis protenus	USNM	18331	partial skull	
Didymictis protenus	USNM	22802	skull	
Didymictis protenus	USNM	487891	lower jaw	
Didymictis protenus			lower carnassial	Zack 2012
Dinictis felina	ROM	52678	skull	
Dinictis felina	ROM	55365	skull	
Dinictis felina	USNM	15889	skull	
Dipsalidictis platypus	UM	114683	lower jaw	
Dipsalidictis platypus	YPM	21215	lower jaw	
Dipsalidictis platypus			lower carnassial	Gunnell 1991
Dipsalidictis transiens	UM	13153	lower m1	Gunnel & Gingerich 1991
Dipsalidictis transiens	UM	16118	lower m1	Gunnel & Gingerich 1991
Dipsalidictis transiens	UM	68201	lower m1	Gunnel & Gingerich 1991
Dipsalidictis transiens	UM	73777	lower m1	Gunnel & Gingerich 1991
Dipsalidictis transiens	UM	75783	partial skull	
Dipsalidictis transiens	UM	76230	lower m1	Gunnel & Gingerich 1991
Dipsalidictis transiens	UM	80063	lower m1	Gunnel & Gingerich 1991
Dipsalidictis transiens	UM	80704	lower m1	Gunnel & Gingerich 1991
Dipsalidictis transiens	UM	82460	lower m1	Gunnel & Gingerich 1991
Dipsalidictis transiens	UM	86025	lower m1	Gunnel & Gingerich 1991
Dipsalidictis transiens			lower carnassial	Gunnell 1991
Hesperocyon gregarius	ROM	1034	skull	
Hesperocyon gregarius	ROM	1415	skull	
Hesperocyon gregarius	USNM	2500	skull	
Hesperocyon gregarius	USNM	5922	skull	
Hesperocyon gregarius	USNM	19932	lower jaw	
Hesperocyon gregarius	YPM	10493	calcaneum and skull	
Hesperocyon gregarius	YPM	11012	calcaneum and skull	
Hoplophoneus mentalis	FAM	32668	partial skull	
Hoplophoneus mentalis	YPM	13635	partial skull	
Hyaenodon crucians	CMN	54017	skull	
Hyaenodon crucians	YPM	10076	skull	
Hyaenodon crucians	YPM	12540	partial skull	

Hyaenodon crucians	YPM	12769	skull	
Hyaenodon cruentus	CMN	8752	skull	
Hyaenodon cruentus	YPM	12745	lower jaw	
Hyaenodon cruentus	YPM	12764	partial skull	
Hyaenodon horridus	FAM	1381	calcaneum	
Hyaenodon horridus	FAM	1488	skull	
Hyaenodon horridus	FAM	75601	partial skull	
Hyaenodon horridus	FAM	75651	lower jaw	
Hyaenodon horridus	FAM	75703	partial skull	
Hyaenodon horridus	FAM	75704	skull	
Hyaenodon horridus	FAM	75705	skull	
Hyaenodon horridus	FAM	75706	lower jaw	
Hyaenodon horridus	USNM	2495	partial skull	
Hyaenodon horridus	USNM	618552	skull	
Hyaenodon megaloides	FAM	75671	skull	
Hyaenodon megaloides	USNM	489154	lower jaw	
Hyaenodon montanus	YPM	12767	lower jaw	
Hyaenodon montanus	YPM	12768	lower jaw	
Hyaenodon mustilenus	FAM	75670	partial skull	
Hyaenodon mustilenus	FAM	82920	partial skull	
Hyaenodon mustilenus	USNM	17878	skull	
Miacis exiguus	ROM	43424	partial skull	
Miacis exiguus	UM	65443	lower jaw	
Miacis exiguus	UM	73812	lower jaw	
Miacis exiguus	UM	85652	lower jaw	
Mustelavus priscus	YPM	13775	skull	
Mustelavus priscus	YPM	13776	lower jaw	
Oodectes herpestoides	YPM	11848	lower jaw	
Oodectes herpestoides	YPM	12845	lower jaw	
Oodectes herpestoides	YPM	14217	lower jaw	
Oodectes herpestoides			lower carnassial	Van Valkenburgh 1988
Oxyaena forcipita	ROM	00916	partial skull	
Oxyaena forcipita	ROM	43531	lower jaw	
Oxyaena forcipita	ROM	43532	lower jaw	
Oxyaena forcipita	ROM	43533	upper tooth row	
Oxyaena forcipita	UM	95201	lower jaw	
Oxyaena forcipita	YPM	13059	lower jaw	
Oxyaena gulo	FAM	15183	partial skull	
Oxyaena gulo	FAM	15191	partial skull	
Oxyaena gulo	FAM	15193	partial skull	
Oxyaena gulo	FAM	15199	partial skull	

Oxyaena gulo	FAM	15200	lower jaw	
Oxyaena gulo	FAM	15725	partial skull	
Oxyaena gulo	FAM	16118	lower jaw	
Oxyaena gulo	USNM	19359	partial skull	
Oxyaena intermedia	ROM	05461	partial skull	
Palaeonictis occidentalis	FAM	110	partial skull	
Palaeonictis occidentalis	FAM	15212	partial skull	
Palaeonictis occidentalis	FAM	15213	lower jaw	
Palaeonictis occidentalis	USNM	19325	partial skull	
Palaeonictis occidentalis	USNM	19333	lower jaw	
Palaeonictis occidentalis	YPM	16140	partial skull	
Palaeonictis occidentalis			lower carnassial	Chester et al. 2010
Parictis dakotensis	FAM	12244	lower jaw	
Parictis dakotensis	FAM	12245	lower jaw	
Parictis dakotensis	FAM	50240	lower jaw	
Parictis dakotensis	FAM	76196	lower jaw	
Parictis dakotensis	FAM	86215	lower jaw	
Parictis parvus	YPM	13775	partial skull	
Prolimnocyon atavus	UM	65622	skull	
Prolimnocyon atavus	UM	71130	lower jaw	
Prolimnocyon atavus	UM	75555	lower jaw	
Prolimnocyon atavus	UM	94084	lower jaw	
Prolimnocyon atavus	USNM	19479	lower jaw	
Prolimnocyon eerius	UM	87353	partial skull	
Prototomus deimos	UM	79612	lower jaw	
Prototomus deimos			lower carnassial	Polly 1993
Uintacyon masseterius	FAM	4520	lower jaw	
Uintacyon masseterius	FAM	15647	lower jaw	
Uintacyon masseterius	FAM	15719	partial skull	
Uintacyon masseterius	FAM	16231	lower jaw	
Uintacyon masseterius	FAM	16749	lower jaw	
Uintacyon masseterius	FAM	16750	lower jaw	
Uintacyon masseterius	USNM	19478	partial skull	
Vassacyon promicrodon	USNM	19492	lower jaw	
Vassacyon promicrodon	USNM	19499	lower jaw	
Viverravus acutus	FAM	90	lower jaw	
Viverravus acutus	FAM	16110	lower jaw	
Viverravus acutus	UM	9934	lower jaw	
Viverravus acutus	UM	9935	lower jaw	
Viverravus acutus	USNM	19480	lower jaw	
Viverravus acutus	USNM	22465	lower jaw	
Viverravus gracilis	YPM	11814	partial skull	

Viverravus gracilis	YPM	11836	partial skull	
Viverravus politus	FAM	15180	lower jaw	
Viverravus politus	FAM	128528	lower jaw	
Viverravus politus	ROM	45562	lower jaw	
Viverravus politus	ROM	45563	lower jaw	
Viverravus politus	UM	64636	lower jaw	
Viverravus politus	UM	72889	lower jaw	
Viverravus sp.	CMN	9212	lower carnassial	
Viverravus sp.	CMN	9776	lower carnassial	